Quarterly Reviews of Biophysics **44**, 3 (2011), pp. 311–356. © Cambridge University Press 2011
doi:10.1017/S0033583510000338 Printed in the United States of America

Structural divergence of the rotary ATPases

Stephen P. Muench[1], John Trinick[2] and Michael A. Harrison[1]*

[1] Institute of Membrane and Systems Biology, Faculty of Biological Sciences, The University of Leeds, Leeds, West Yorks, LS2 9JT, UK
[2] Institute of Cellular and Molecular Biology, Faculty of Biological Sciences, The University of Leeds, Leeds, West Yorks, LS2 9JT, UK

Abstract. The rotary ATPase family of membrane protein complexes may have only three members, but each one plays a fundamental role in biological energy conversion. The F_1F_o-ATPase (F-ATPase) couples ATP synthesis to the electrochemical membrane potential in bacteria, mitochondria and chloroplasts, while the vacuolar H^+-ATPase (V-ATPase) operates as an ATP-driven proton pump in eukaryotic membranes. In different species of archaea and bacteria, the A_1A_o-ATPase (A-ATPase) can function as either an ATP synthase or an ion pump. All three of these multi-subunit complexes are rotary molecular motors, sharing a fundamentally similar mechanism in which rotational movement drives the energy conversion process. By analogy to macroscopic systems, individual subunits can be assigned to rotor, axle or stator functions. Recently, three-dimensional reconstructions from electron microscopy and single particle image processing have led to a significant step forward in understanding of the overall architecture of all three forms of these complexes and have allowed the organisation of subunits within the rotor and stator parts of the motors to be more clearly mapped out. This review describes the emerging consensus regarding the organisation of the rotor and stator components of V-, A- and F-ATPases, examining core similarities that point to a common evolutionary origin, and highlighting key differences. In particular, it discusses how newly revealed variation in the complexity of the inter-domain connections may impact on the mechanics and regulation of these molecular machines.

1. Introduction 312

2. Physiological roles of the rotary ATPases 313

3. Domain organisation and subunit composition 314
3.1. Rotary ATPase domains contain separate motor functions 314
3.2. Subunit composition 316
3.3. Organisation of the F_1-ATPases 318
3.4. Organisation of the F_o membrane domain 320
3.5. The F-ATPase stator is different in bacteria and eukaryotes 321
3.6. Core subunits of the rotary ATPases are related 322
3.7. Subunit organisation in the rotors of A- and V-ATPases 324
3.8. Peripheral stator components of the rotary ATPases share common features 325
3.9. V/A-ATPase stator subunit *a* is a polytopic protein with two domains 327

* Author for Correspondence: Dr M. Harrison, Institute of Membrane and Systems Biology, Faculty of Biological Sciences, The University of Leeds, Leeds, West Yorks LS2 9JT, UK.
Tel.: (+44) (0)113 3437766; Email: m.a.harrison@leeds.ac.uk

https://doi.org/10.1017/S0033583510000338 Published online by Cambridge University Press

4. Rotary ATPase mechanics 328
4.1. Torque generation 328
4.2. Mechanical properties 330

5. Structural analysis of the rotary ATPases by EM 331
5.1. A brief history 331
5.2. Current EM-derived models: motors with 1-, 2- or 3-part stators 332
5.2.1. The F-ATPase – the single stalk stator model 332
5.2.2. The A-ATPase – a stator model with two stalks and a collar 334
5.2.3. The V-ATPase – a stator model with three stalks and a collar 335
5.3. Do the rotary ATPase membrane domains contain 'half channels'? 335

6. Fitting the pieces together – mosaic structures of the rotary ATPases 336
6.1. The structural model of the F-ATPase is almost complete 336
6.2. Mosaic models of the A- and V-ATPases 337

7. Unexplained features and unresolved questions 338
7.1. Is the isolated V-ATPase in a 'ground state' conformation? 338
7.2. Is stator complexity linked to regulation? 340
7.3. The motor asymmetry question 342
7.3.1. Power transmission in the F-ATPase 342
7.3.2. Power transmission in the V- and A-ATPases 343

8. Future directions 343

9. Acknowledgements 345

10. References 345

1. Introduction

The link between membrane electrochemical potential and the synthesis (or hydrolysis) of ATP was encapsulated nearly half a century ago in Mitchell's Chemiosmotic Theory, central to which is the function of a reversible 'ATP synthase' integrated into the bioenergetic membrane (Mitchell, 1961). This complex, the F_1F_o-ATPase (or F-ATPase for short) uses the transmembrane movement of protons (or, in some cases, Na^+), driven by the electrochemical membrane potential, the proton motive force (PMF) to energise the endothermic phosphorylation of ADP. We now know that this energy conversion is catalysed by the F-ATPase operating as a nano-scale machine with a rotary action (Duncan *et al.* 1995; Kinosita *et al.* 1998; Noji *et al.* 1997; Sabbert *et al.* 1996). The F-ATPase belongs to a small family of membrane complexes that originated from a common evolutionary ancestor (Grüber *et al.* 2001b; Yoshida *et al.* 2001) that includes the vacuolar H^+-translocating V_1V_o-ATPase (V-ATPase) and A_1A_o-ATPase (A-ATPase). *In vivo*, the V-ATPase operates as an ATP-powered ion pump, whereas the A-ATPases are ATP synthases in the archaea and some bacteria (Forgac, 2007; Müller & Grüber, 2003). These rotary motors are mechanical marvels, running at speeds in excess of 100 revolutions per minute, generating torque of $\sim$50 pN·nm (on a molecular scale, an enormous force) and performing energy transformation processes at close to 100% efficiency. Although crystal structures have revealed much about the organisation and connectivity of components of these rotary motors, complete atomic resolution models are not yet available. This limits understanding of the mechanism linking transmembrane ion movement to rotational movement. However, recent three-dimensional (3D) reconstructions from electron microscopy (EM) have provided new insights into the architecture of the rotary

https://doi.org/10.1017/S0033583510000338 Published online by Cambridge University Press

ATPases. This review explores current knowledge about rotary ATPase structure, mechanism and regulation. In particular, we highlight differences that have now emerged between the rotary ATPases that probably impact on the way they operate as molecular motors.

2. Physiological roles of the rotary ATPases

The F-ATPase is reversible, capable of operating either as an ATP synthase powered by the electrochemical membrane potential, or as an ATP-driven ion pump. Under aerobic conditions in mitochondria it operates in synthase mode, but a decrease in membrane potential under anaerobic conditions can cause it to operate in reverse mode, hydrolysing ATP in order to re-establish the membrane potential. The associated drop in matrix pH to $<6{\cdot}5$ promotes binding of a natural inhibitor protein IF_1 that blocks the catalytic cycle (Cabezón *et al.* 2003; Campanella *et al.* 2009; Pullman & Monroy, 1963). A similar ATP synthase operates in the thylakoid membranes of chloroplasts (the CF_1F_o-ATPase), energised by a PMF with only a proton gradient (ΔpH) component. In prokaryotes, formation of a membrane potential by aerobic respiration supports ATP synthesis by the F-ATPase as it does in mitochondria. Under conditions where ATP is produced by substrate-level phosphorylation, the bacterial F-ATPase can reverse to pump protons. In this mode, it extrudes ions from the cell to support a PMF and contribute to maintenance of cytoplasmic pH. Bacterial F-ATPases can also be Na^+-powered, for example in *Propionigenium modestum* where a Na^+-linked methylmalonyl-CoA decarboxylase establishes the necessary primary Na^+ potential (Dimroth *et al.* 2006; von Ballmoos *et al.* 2008). A Na^+-specific F-ATPase also operates in *Acetobacterium woodii*, exploiting the primary Na^+ potential set up by its Na^+-translocating ferredoxin:NAD^+ oxidoreductase (Biegel & Müller, 2010).

Although the V-ATPase may synthesise ATP *in vitro* (Hirata *et al.* 2000), its role in eukaryotes appears to be exclusively as a proton pump. V-ATPases associated with vacuolar compartments of fungi and plants maintain low pH and energise secondary active transport. In higher eukaryotes, the V-ATPase maintains the acidic pH of compartments such as clathrin-coated vesicles, early and late endosomes and lysosomes, and energises solute uptake into secretory vesicles (Forgac, 2007; Marshansky & Futai, 2008; Morel, 2003). In general, V-ATPase activity can maintain $\sim$100-fold difference in proton concentration between the cytosol and intracellular compartment. However, substantially greater differences are maintained in some systems such as citrus fruit cells. The free energy input from ATP into proton transport by the V-ATPase (a function of the cytosolic ATP/ADP/inorganic phosphate ratio) is essentially fixed, but the energy per transported proton varies with the magnitude of the pH gradient against which it is being pumped. Consequently, the lower the pH of the compartment into which the proton is being transported, the smaller the number of protons that can be transported per catalytic cycle of the V-ATPase. This is analogous to the motor operating in different gears: low gear (expressed functionally as a low H^+/ATP ratio) allows proton transport even into compartments with internal pH as low as pH 2–3. The plant tonoplast V-ATPase exhibits a H^+/ATP ratio that varies with the pH of the cytoplasm and tonoplast lumen (Davies *et al.* 1994), implying a pH-sensing function that has also been proposed for at least one mammalian V-ATPase isoform (discussed in Marshansky & Futai, 2008). Alternatively, H^+/ATP ratios could be controlled by varying the stoichiometry of membrane subunits responsible for proton translocation (discussed in Section 3).

V-ATPases are not exclusively endomembrane proteins, being also found in the plasma membranes of many polarised cells (Wieczorek *et al.* 1999). Hence, for instance, regulated translocation of the V-ATPase to the apical membranes of epididymal clear cells results in a drop

https://doi.org/10.1017/S0033583510000338 Published online by Cambridge University Press

in pH in the lumen of the reproductive tract, a crucial step in sperm maturation and activation (Breton *et al.* 1996). A second example is the plasma membrane V-ATPase from the lepidopteran larval midgut that energises secondary active transport processes as well as the alkalinisation of the gut lumen up to a pH of 12 (Wieczorek *et al.* 1991). Almost all mammalian V-ATPase subunits exist as two or more isoforms that display tissue-specific expression or differential membrane targeting (Lee *et al.* 2010b; Toei *et al.* 2010). These play key roles in, for example, renal function (Brown *et al.* 2009; Wagner *et al.* 2004), with mutations leading to renal tubular acidosis (Smith *et al.* 2000). Naturally occurring V-ATPase mutations also cause osteopetrosis (Frattini *et al.* 2000; Li *et al.* 1999) because affected osteoclasts are unable to perform the acid extrusion required for bone resorption (Blair *et al.* 1989; Väänänen *et al.* 2000). There is also evidence that differential expression of V-ATPase isoforms at the surface of cultured tumour cells correlates with cell invasiveness, linking it to metastatic potential in cancer (Hinton *et al.* 2009; Sennoune *et al.* 2004; Sennoune & Martinez-Zaguilan, 2007).

In archaea, A-ATPases can act as ATP synthases (reviewed in Müller & Grüber, 2003), with either H^+ (e.g. *Sulfolobus* and *Methanosarcina* species; Hochstein & Stan-Lotter, 1992; Inatomi, 1986; Pisa *et al.* 2007b) or Na^+ (e.g. *Pyrococcus* species; Coskun *et al.* 2004; Lingl *et al.* 2003; Pisa *et al.* 2007a) as the coupling ion. In archaeal species suggested to be primarily fermentative, the A-ATPase may operate as an ion pump. Some bacteria also have A-ATPases, and these enzymes have sometimes been referred to as 'bacterial V-ATPases' or 'V/A-ATPases' (Hilario & Gogarten, 1998). Sequence similarity, subunit composition and organisation confirm that these are much closer to the archaeal examples than to eukaryotic V-ATPases (Bernal & Stock, 2004; Mulkidjanian *et al.* 2008; Müller & Grüber, 2003); these aspects are discussed in detail below. In *Thermus thermophilus*, this type of ATPase operates predominantly as a H^+-driven ATP synthase (Nakano *et al.* 2008; Yokoyama *et al.* 1994), while in Gram-positive bacteria, such as the enterococci and clostridia, they function as Na^+ pumps (Boekema *et al.* 1999; Kakinuma *et al.* 1999; Speelmans *et al.* 1993). *Enterococcus hirae* assembles both A- and F-ATPases in the same membrane (Takase *et al.* 1993) and, to date, three species of archaea have been shown to carry genes for both enzymes (Müller & Grüber, 2003; Sumi *et al.* 1992), although expression of F-ATPase polypeptides has not been observed. The presence of genes for both types of rotary ATPase in the same species is most likely to have arisen through horizontal gene transfer, rather than parallel evolution from a common ancestral complex (Hilario & Gogarten, 1998; Mulkidjanian *et al.* 2007). Overall, the distinction between A-ATPases and 'bacterial V-ATPases' is blurred, reflecting the difficulties in discriminating between the enzymes solely on the basis of the cell where they occur. The classification here is based on subunit organisation rather than physiological function or occurrence in a particular organism. For consistency, we refer to all bacterial ATPases of the A/V-type as A-ATPase, reserving the term V-ATPase exclusively for the eukaryotic protein, as suggested in (Müller & Grüber, 2003). Our reasoning is based on the similarities in organisation between the archaeal/bacterial complexes and their divergence from the eukaryotic V-ATPase, which is the main focus of this review.

3. Domain organisation and subunit composition

3.1 Rotary ATPase domains contain separate motor functions

Despite the diversity of function, all rotary ATPases share many basic similarities. Each comprises a soluble ATP synthesising/hydrolysing domain, designated F_1, V_1 or A_1, coupled to a

https://doi.org/10.1017/S0033583510000338 Published online by Cambridge University Press

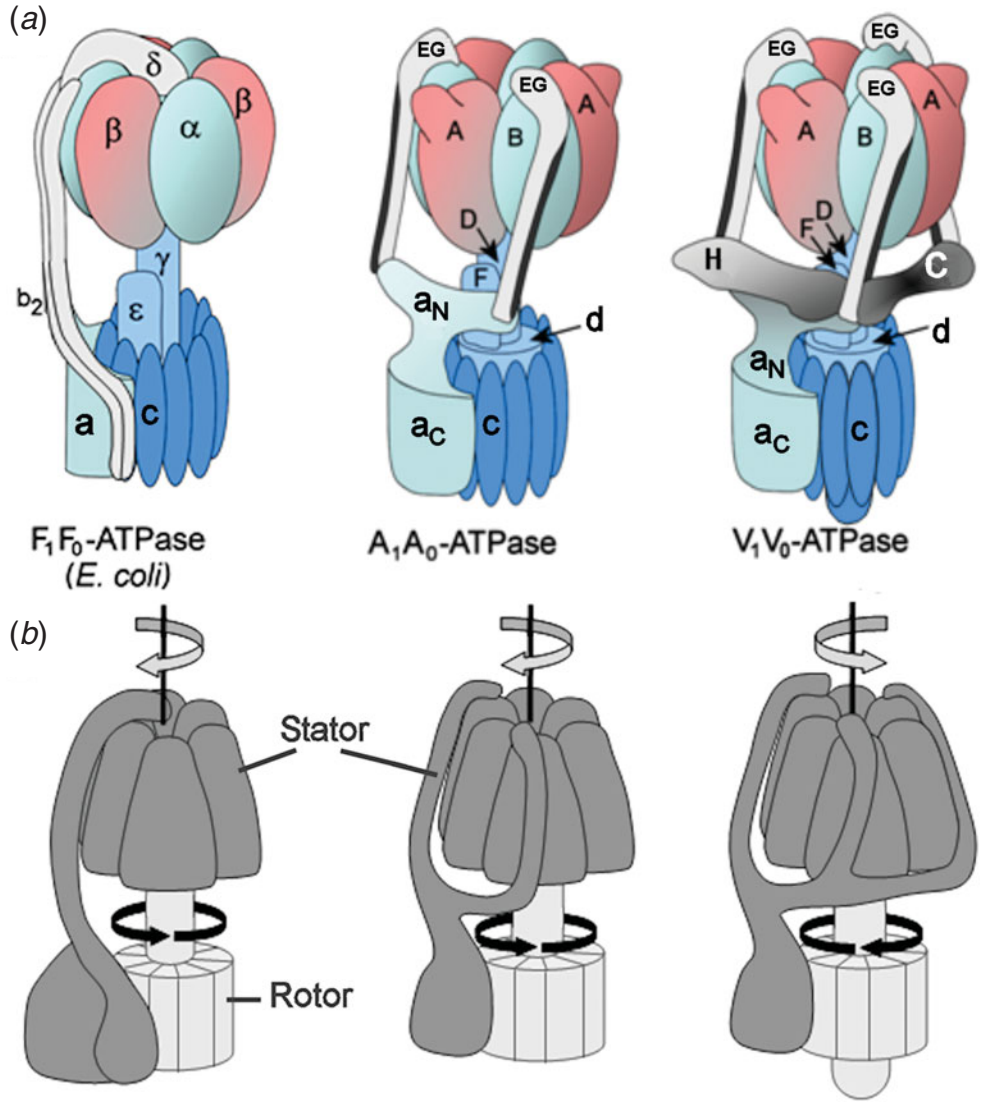


Fig. 1. Organisation of subunits in rotary ATPases. (*a*) Subunit arrangements of $(\alpha\beta)_3$:γ:ε:*c*-ring in the F-ATPase, and $(AB)_3$:D:F, E:G and *c*-ring in the A- and V-ATPases are informed by crystal structures. Other contacts are consistent with cross-linking and interaction data. Overall architecture is surmised from 3D reconstructions by EM. When viewing the external surface in this orientation, catalytic sites are at the α/β and B/A subunit interfaces where α/B is to the left of the subunit pair. In the F-ATPase, the upper part of the peripheral stalk region of the stator is aligned with a non-catalytic β-α interface. Segments a_N and a_C, respectively, correspond to the cytoplasmic N-terminal and integral membrane C-terminal domains of the A_o/V_o *a* subunits. (*b*) Organisation of rotor/stator elements. Arrows indicate relative directions of rotation of stator (grey arrow) and rotor (black arrow) during operation in synthase mode (F-ATPase and A-ATPase) or proton pump mode (V-ATPase). The *E. coli* F-ATPase rotor comprises γ:ε_b:*c*-ring, the corresponding structure in the A- and V-ATPases being D:F:*d*:*c*-ring.

membrane domain (termed F_o, V_o or A_o) that facilitates ion translocation across the membrane (Fig. 1). Each domain is essentially an independent rotary stepper motor, although the actions of these are tightly coupled and co-operative to produce a highly efficient energy conversion

https://doi.org/10.1017/S0033583510000338 Published online by Cambridge University Press

machine. The modular nature of the rotary ATPases is underlined by the observation that F_1 and A_1 domains detached from the membrane retain ATP-driven rotary movement (Imamura *et al.* 2003; Noji *et al.* 1997), and that F_1 domains from H^+- and Na^+-specific F-ATPases are to some extent interchangeable without loss of function (Laubinger *et al.* 1990). In ion pump mode, the three active sites in the soluble domain (effectively a 'three stroke motor') sequentially drive rotation of an axle that transmits energy to the membrane domain ion pump. This pump also comprises rotary and static parts, the relative movement of which is the crucial factor in transmembrane movement of ions. The static part is fixed to the soluble domain motor by means of a *stator*, preventing it from simply following the movement of the axle. ATP synthesis in the F- and A-ATPases requires the system to be powered in reverse mode, with ion movement through the membrane domain driving axle rotation. This motion is translated into sequential conformational changes in the three active sites of the soluble domain, resulting in a cycle of substrate binding, ATP synthesis, and its release. These processes are discussed below. It is worth pointing out that although the rotary ATPases are readily described in terms applied to macroscopic motors, there are limits to the analogy; the molecular motors are fundamentally different, being subject to (and dependent on) thermally driven atomic and molecular scale fluctuations (outlined in Section 4).

3.2 Subunit composition

For the non-specialist, subunit nomenclature of different rotary ATPases can appear inconsistent and confusing. Homologous subunits often have different labels and, conversely, some non-homologous subunits have acquired the same label. To clarify this, subunits from V-, A- and F-ATPases of both prokaryotes and eukaryotes are listed in Table 1. Subunits listed across the same row are functional homologues. This homology does not necessarily extend to the sequence level, and subunits that lack sequence similarity can share a common fold, as discussed below. The structure, function and mechanism of F-ATPases from bacteria and eukaryotic organelles have been comprehensively reviewed (Capaldi & Aggeler, 2002; Devenish *et al.* 2008; Dimroth *et al.* 2006; Müller & Grüber, 2003; von Ballmoos *et al.* 2008). Core components of the F-ATPases from bacteria and eukaryotes are conserved (Table 1). In the relatively simple ~530 kDa *Escherichia coli* enzyme, F_1 subunits have the stoichiometry $(\alpha\beta)_3{:}\gamma{:}\delta{:}\varepsilon$, while the membrane domain F_o comprises subunits $a{:}b_2{:}c_{10}$ (Fig. 1*a*: left). The mitochondrial F_1 and F_o have subunits $(\alpha\beta)_3{:}\gamma{:}\delta{:}\varepsilon$:OSCP:$d$:$F_6$ and $a{:}b{:}c_{10}$, respectively. Mitochondrial δ and bacterial ε are homologous, as are mitochondrial oligomycin sensitivity conferral protein (OSCP) and bacterial δ, whereas mitochondrial ε has no homologue in prokaryotes (Table 1). In this review, we have given the mitochondrial and bacterial polypeptides 'm' or 'b' designations (δ_m, δ_b, ε_m, ε_b) to help the reader distinguish between them. Defining the stator and rotor parts of these complexes integrates data from cross-linking (summarised in Capaldi *et al.* 2000; Capaldi & Aggeler, 2002), structures and single molecule fluorescence microscopy of complexes executing rotary catalysis (Kinosita *et al.* 1998; Noji *et al.* 1997; Sambongi *et al.* 1999; Ueno *et al.* 2005; Yoshida *et al.* 2001). The rotor of the mitochondrial F-ATPase comprises $\gamma{:}\delta_m{:}\varepsilon_m{:}c_{10}$, its bacterial equivalent $\gamma{:}\varepsilon_b{:}c_{10–15}$. Of these components, $\gamma{:}\delta_m{:}\varepsilon_m$ (equivalent to bacterial $\gamma{:}\varepsilon_b$) forms the axle linking the coupled motors, and $c_{10–15}$ the ring of membrane subunits that form the rotary part of the ion translocation apparatus (Fig. 1*a, b*: left). In the static part, each $\alpha\beta$ heterodimer is one catalytic unit in a trimeric assembly. The remaining subunits form the stator linkage between the $(\alpha\beta)_3$ motor and subunit *a*, which forms the static part of the ion translocator within the membrane domain.

https://doi.org/10.1017/S0033583510000338 Published online by Cambridge University Press

Table 1. *Subunits of the F-, A- and V-ATPases*

Eukaryotic V-ATPase	A_1A_o-ATPase	F_1F_o-ATPase (*E. coli*)	F_1F_o-ATPase (bovine mitochondria)	Domain	Motor component	Situation/function
A	A	β	β	$V_1/A_1/F_1$	Stator	Catalysis; torque generation
B	B	α	α	V_1/F_1	Stator	Catalysis/regulation; torque generation
C[a]	—	—	—	V_1	Stator	Stator linkage; regulatory function
D	D	γ	γ	$V_1/A_1/F_1$	Rotor	Axle of the rotary motor
E	E	δ[b]	OSCP	$V_1/A_1/F_1$	Stator	Fixing static membrane subunit *a* with respect to the $(AB)_3$ motor
F	F	—	—	V_1/A_1	Rotor	Axle of the rotor. Possible regulatory function, imposing direction of rotation?
—	—	ε[c]	δ[b]	F_1	Rotor	Rotor axle; inhibition of ATP hydrolysis when $\Delta\mu_H{}^+$ low
—	—	—	ε[c]	F_1	Rotor	Axle of the rotary motor
G	H[a]	*b*	*b*	V_1/F_o	Stator	Linkage between ATP hydrolysing and proton pumping components of the stator
H[a]	—	—	—	V_1	Stator	Inhibition of ATP turnover by membrane-detached V_1
a	I[a]	*a*	*a*	$V_o/A_o/F_o$	Stator	Static element of the membrane ion pump. Transmembrane cation movement
c[d]	*c*/K/L[d]	*c*	*c*	$V_o/A_o/F_o$	Rotor	Rotor element of the membrane ion pump. Transmembrane cation movement
d	C[a]	—	—	V_o/A_o	Rotor	Coupling between axle and ion pump elements of the rotor.
—	—	—	*d*	F_1	Stator	Linkage between ATPase and cation pump components of the stator
e	—	—	—	V_o	Stator?	Not known
—	—	—	F_6	F_1	Stator	Linkage between ATPase and cation pump components of the stator
—	—	—	A6L	F_o	Stator	Cation translocation?
—	—	—	*e, f, g, i/j*	F_o	Stator	Oligomerisation state (hence stability)?

[a]A-ATPase subunits C, H and I are, respectively, homologues of V-ATPase subunits *d*, G and *a*. V-ATPase subunits C and H have no homologues in the A-ATPase.

[b]The δ subunits of mitochondrial and bacterial F-ATPases are not homologous. We refer to them in this review as δ_m and δ_b.

[c]The ε subunits of the mitochondrial and bacterial F-ATPases are not homologous. We refer to them in this review as ε_m and ε_b.

[d]The V-ATPase subunit *c* is a 4 TMH tandem repeat of the 2-helix F-ATPase *c*. A-ATPases from different species may contain 2-, 4- or 6-helical *c* subunits. For clarity, in this review we refer to all forms as subunit *c*.

https://doi.org/10.1017/S0033583510000338 Published online by Cambridge University Press

A- and V-type ATPases are closely related, with major similarities in subunit arrangement and sequence. The A-type enzyme (Fig. 1 *a, b*: centre) is essentially a simpler version of the V-ATPase (Fig. 1 *a, b*: right), a key difference being the absence of soluble domain C and H subunits from the A-ATPase (Table 1). V_1 has subunits A–H in the stoichiometry $(AB)_3$:C:D:F:$(EG)_3$:H (Arai *et al.* 1988; Kitagawa *et al.* 2008). The equivalent structure in A_1 is $(AB)_3$:D:F:$(EG)_2$ (Esteban *et al.* 2008). Although the A-ATPase homologue of V-ATPase subunit G is referred to as H in the A-ATPase literature (Table 1), in this review we will refer to it as G for clarity. The subunits in V_o have a likely *a*:c_{10}:*d*:*e* stoichiometry, although proton pumping in *Saccharomyces* also requires two more subunit *c* isoforms designated *c′* (Vma11p) and *c″* (Vma16p) (Powell *et al.* 2000; Wang *et al.* 2007), the latter perhaps being ubiquitous. In different bacterial and archaeal A-ATPases, the *c*-subunit may be designated as K, L or *c* (Table 1), but for consistency and clarity, we refer in this review to these closely related polypeptides exclusively as *c*-subunits (see footnote to Table 1). Similarly, we refer to the A-ATPase membrane subunit I as subunit *a*, the designation of its homologues in F- and V-ATPases (Table 1). Although the A-ATPase homologue of the V-ATPase *d* subunit has historically been referred to as subunit C (Table 1), both appear to occupy similar positions within their respective enzymes (discussed below), pointing to functional homology. To help avoid confusion, we refer here to this A-ATPase subunit as subunit *d*. In line with these designations, the subunit composition of A_o is *a*:$c_{10–12}$. By analogy to V_o, subunit *d* is likely also to be part of A_o, but its co-isolation with the membrane domain has not been demonstrated biochemically.

Although the yeast V-ATPase C and H subunits have been solved (Drory *et al.* 2004; Sagermann *et al.* 2001), the majority of crystal structures are subunits or sub-complexes of bacterial enzymes assigned here as A-type. However, similarities of sequence, secondary structure and inter-subunit contacts established by cross-linking suggest that the A-ATPase subunits are good models for their V-ATPase counterparts (some exceptions to this are discussed below). As in the F-ATPase, assignment of subunits to rotor or stator integrates biochemical/structural data with single molecule rotation studies using yeast (Hirata *et al.* 2003) and *T. thermophilus* enzymes (Imamura *et al.* 2003; Yokoyama *et al.* 2003b). In V- and A-ATPases, these data assign subunits D, F, *d* and *c*-ring to the rotor (Yokoyama *et al.* 2003a) (Fig. 1 *b, c*).

3.3 Organisation of the F_1-ATPases

No complete high resolution structure for any F-ATPase complex has been solved to date. The F_1 domain is, however, more amenable to crystallography, and has been solved to 1·9 Å (Bowler *et al.* 2007). Such a high resolution is perhaps surprising, given the intrinsically dynamic and flexible nature of the complex, and is sufficient to see small but significant differences in the geometry of side chains in each active site. The F_1 $(\alpha\beta)_3$ complex has pseudo-6-fold symmetry, with each α–β interface (viewed with α to the left of the pair, as in Fig. 1 *a*) forming an active site (Abrahams *et al.* 1994). The three α–β units are in fact not equivalent; each interacts with the asymmetrical γ subunit axle and adopts a different active site conformation. In the F_1-ATPase 'reference structure' (Abrahams *et al.* 1994), two catalytic sites have similar conformations (termed β_{TP} and β_{DP}) and bind Mg^{2+} and AMP-PNP (equivalent to Mg^{2+}-ATP) and Mg^{2+}-ADP, respectively. In virtually all F_1-ATPase crystal structures, the third site has a much more open configuration and is empty (β_E). During ATP hydrolysis, each site cycles sequentially through E→TP→DP→E states, the transition to the closed β_{TP} state that is driven by ATP binding to one site having knock-on effects on the conformations of the other two. These

https://doi.org/10.1017/S0033583510000338 Published online by Cambridge University Press

changes are mediated primarily by the stepped rotation of the axle γ subunit, but are likely to also include effects transmitted through adjoining α subunits. In a crystal structure in which β_{TP} and β_{DP} are occupied by ADP-AlF_4^-, β_E is actually in a 'half-closed' conformation bound by ADP and sulphate (mimicking phosphate), and is presumed to reflect the active site state post-hydrolysis but preceding product release (Menz *et al.* 2001). ADP binding to β_{DP} is stabilised by azide that also mimics the binding of inorganic phosphate (Bowler *et al.* 2006). In the absence of azide, this site can be occupied by AMP-PNP, suggesting that it represents the 'live' site poised to hydrolyse ATP (Bowler *et al.* 2007). The active sites show differences even in the absence of bound Mg^{2+} and nucleotides (Kabaleeswaran *et al.* 2006), underlining the influence of interactions with the axle. The three conformers equate to the 'open', 'loose' and 'tight' states described by Boyer's *binding change mechanism* which reconciles the strong negative co-operativity for substrate binding shown by the three catalytic sites with the observed positive co-operativity of catalysis (reviewed in Boyer, 1997). At any point in time, the three sites display either high, medium or low affinity for substrate. By consensus, the 'open' β_E conformer is the low affinity site. However, the relative affinities of the β_{DP} and β_{TP} sites are a matter of debate: biophysical measurements and free energy difference simulations point to β_{TP} being the high affinity site (Mao & Weber, 2007; Yang *et al.* 2003), whereas greater proximity of key catalytic residues to the substrate in the β_{DP} site suggest that it is the catalytically active site and thus represents the high-affinity state (Menz *et al.* 2001).

The γ subunit forms an asymmetric axle that transmits mechanical power from the catalytic complex to the rotary *c*-ring in F_o (Stock *et al.* 1999; Watts *et al.* 1995). The first $\sim$55 and last $\sim$70 residues of this 30 kDa polypeptide fold as an α-helical coiled-coil that extends with pronounced curvature down the centre of F_1 to the surface of F_o, where it terminates in a combined α-helix/β-sheet 'foot' that includes the β-α-β-α-β topography of a Rossmann fold (Gibbons *et al.* 2000). The first short helix of this motif projects like a spur from the bottom of the concave side of the axle. In most F_1 structures, the bulge formed by the curvature of the γ subunit axle points towards the α_E/β_E site. However, crystal structures also show multiple contacts between γ and the interior surface of the $(\alpha\beta)_3$ complex, consistent with the idea that γ simultaneously influences conformations of all three catalytic subunits. Correspondingly, all three sites can simultaneously contribute to the generation of rotational movement in the γ axle during ATP hydrolysis (Ariga *et al.* 2007). Near the apex of $(\alpha\beta)_3$, the C-terminal end of γ is an α-helix that fits into a hydrophobic constriction that may act as a frictionless bearing. However, both C- and N-terminal regions of γ can be truncated with retention of at least some torque generation (Furuike *et al.* 2008; Müller *et al.* 2002). The most important contact for power transmission therefore appears to be between the convex bulge of the γ coiled-coil and a narrow band of $(\alpha\beta)_3$ close to the point at which the axle emerges (Junge *et al.* 2009; Ma *et al.* 2002). This includes a helix-loop-helix feature in the C-terminal domain of β that contains the highly conserved DELSEED sequence. This is proposed to constitute a 'lever' that transmits torque from rotor to active site in synthase mode, or applies torque to the axle in ion pump mode. This transmission may involve steric, repulsive van der Waals and electrostatic effects (Bandyopadhyay & Allison, 2004; Ma *et al.* 2002; Pu & Karplus, 2008), although the failure of mutation of negatively charged residues in the DELSEED motif to influence power transmission argues against a role for electrostatics (Hara *et al.* 2000).

Bacterial ε (ε_b) and mitochondrial δ (δ_m) are homologous polypeptides that associate with γ to form the axle (Table 1), and have distinctive N-terminal β-sandwich and C-terminal helix-loop-helix domains (Gibbons *et al.* 2000; Uhlin *et al.* 1997). The ε_b/δ_m co-rotates with γ (Aggeler *et al.*

https://doi.org/10.1017/S0033583510000338 Published online by Cambridge University Press

1997; Rondelez *et al.* 2005), with the β-sandwich region positioned at the membrane end of the axle, broadly opposite the foot of γ. The C-terminal region can exist in both compact and extended forms (Hausrath *et al.* 2001; Rodgers & Wilce, 2000), with switching between states proposed to play a role regulating catalysis (Bulygin *et al.* 2004; Kato-Yamada *et al.* 2000). ATP promotes the compact, non-inhibitory conformer by directly binding to ε_b (Kato *et al.* 2007; Kato-Yamada & Yoshida, 2003; Yagi *et al.* 2007) or via another mechanism (Feniouk *et al.* 2010) by which catalysis (in either synthetic or hydrolytic directions) can respond to fluctuations in the ATP concentration. When ATP is low, the extended form of ε_b contacts the DELSEED loop of the β 'lever' and acts as a ratchet allowing rotor movement only in the *synthetic* direction (Hara *et al.* 2001; Tsunoda *et al.* 2001). Subunit ε_m has no bacterial equivalent, and is a small polypeptide found at the foot of the axle of the mitochondrial enzyme where it couples to the *c*-ring. Its role may be to stabilise γ–*c*-ring coupling.

3.4 Organisation of the F_o membrane domain

Each *c*-ring subunit folds as a helical hairpin (Rastogi & Girvin, 1999), with the second helix forming an outer ring that interfaces with lipid (Meier *et al.* 2005a). H^+/Na^+ discrimination by bacterial *c*-rings is a function of the character and geometry of side chains arranged around a critical and highly conserved aspartate positioned mid-membrane on this outer helix (von Ballmoos *et al.* 2008). In synthase mode, the *c*-ring forms the torque generator in combination with subunit *a*, a single copy of which forms the membrane-embedded part of the F-ATPase stator. Subunit *a* and the integral membrane part of subunit *b* are the parts of the F-ATPase for which least structural data are available, and these hydrophobic components may represent the main obstacles for obtaining a complete high-resolution structure. Progress has however been made on the structures of *c*-rings from F-ATPases from both bacterial and eukaryotic sources, fuelling debate about the functional significance of variations in subunit stoichiometry and the consequent cation/ATP ratio. In the *E. coli* F-ATPase, a decameric *c*-ring may be the default size (Jiang *et al.* 2001), although the functionality of genetic fusions suggests that other stoichiometries may be tolerated (Jones & Fillingame, 1998). In contrast, crystal structures of the *c*-rings from Na^+-translocating F-ATPases of *Ilyobacter tartaricus* and *P. modestum* have c_{11} stoichiometry (Meier *et al.* 2005a, b, 2006), and AFM analyses give stoichiometries ranging between 13 and 15 for cyanobacterial enzymes (Pogoryelov *et al.* 2005, 2007). This variability extends to the *c*-rings of F-ATPases from eukaryotic organelles: the spinach chloroplast enzyme has 14 *c*-subunits (Seelert *et al.* 2000; Vollmar *et al.* 2009), whereas the yeast mitochondrial ATP synthase has only 10 (Stock *et al.* 1999). Uniquely, the bacterium *A. woodii* produces ATP using an enzyme that contains nine F-ATPase-type helical hairpin *c*-subunits associated with a single copy four transmembrane helix (TMH) *c*-subunit typically found in A- and V-ATPases (Fritz *et al.* 2008; Rahlfs *et al.* 1999). The membrane domain in *A. woodii* is essentially therefore a hybrid F_o/V_o, although the advantages conferred by this organisation remain to be determined.

Why is the *c*-subunit stoichiometry so variable? One proposal that attempts to accommodate the rather variable H^+/ATP ratios that have been reported is that an organism can adjust its *c*-ring stoichiometry such that it is optimised for particular physiological conditions (Tomashek & Brusilow, 2000). If one considers the energetic cost of making ATP to be essentially fixed, growth conditions resulting in a smaller ion motive force would demand a greater number of ion translocation events per enzyme cycle, reflected as a larger *c*-ring stoichiometry. Despite the attraction of this model, several studies have found *c*-ring stoichiometries in individual organisms

https://doi.org/10.1017/S0033583510000338 Published online by Cambridge University Press

to remain fixed irrespective of growth conditions (Ballhausen *et al.* 2009; Fritz *et al.* 2008; Meyer zu Tittingdorf *et al.* 2004). It seems therefore that each organism has one *c*-ring size customised to its specific physiology, an adaptation to the prevailing ion motive force under which its F-ATPase operates (von Ballmoos *et al.* 2008). The electrical component ($\Delta\psi$) of a PMF has been shown to be kinetically more effective at energising ATP synthesis than the ΔpH proton gradient (discussed in von Ballmoos *et al.* 2008; Dimroth *et al.* 2006). Mitochondria and some bacteria that maintain a relatively stable $\Delta\mu_X{}^+$ to which the electrical component is the main contributor may therefore be able to energise ATP synthesis with smaller *c*-rings. Larger *c*-rings (and therefore larger H^+/ATP ratios) are proposed to represent an evolutionary compromise that allows F-ATPases such as those in chloroplasts and cyanobacteria to be energised by a PMF that has only a ΔpH component. Irrespective of the overall magnitude of $\Delta\mu_X{}^+$, such systems would require a greater number of ion translocation events per ATP synthesised, hence larger *c*-rings. For a more complete discussion of this topic, see von Ballmoos *et al.* (2008, 2009). This issue is far from resolved, however: although particular cation/ATP ratios may be deduced from *c*-ring stoichiometries (*c*-ring size/3), measurements of actual operational H^+/ATP ratios often fail to match up to these numbers (Junge *et al.* 2009; Steigmiller *et al.* 2008; Tomashek & Brusilow, 2000). From a membrane protein assembly perspective, it remains unclear what organism-specific features govern assembly of similar *c*-subunits into rings of different sizes in different membranes.

Extensive mutagenesis studies have shown that stator subunit *a* is also directly involved in transmembrane ion movement (reviewed in Cain, 2000). Low-resolution models based on sequence analysis and supported by cross-linking and site-directed labelling studies suggest that this polypeptide folds with five TMHs, with TMHs 2–5 packing as a four-helical bundle (Schwem & Fillingame, 2006). Cross-linking supports a model in which TMH 4 (containing the functionally crucial Arg210 (*E. coli* residue number; Cain & Simoni, 1989; Valiyaveetil & Fillingame, 1997; Vik *et al.* 1998)) and TMH5 are adjacent to the external surface of the *c*-ring, in contact with at least two neighbouring *c*-subunits (Jiang & Fillingame, 1998; Moore & Fillingame, 2008) that step through the *a*/*c*-ring interface during rotation (Hutcheon *et al.* 2001). Topological models place the N-terminal end of TMH4 on the cytoplasmic side of the membrane (see pdb 1C17; Rastogi & Girvin, 1999). Full function requires the crucial arginine and aspartate to be at the same depth in the membrane (Langemeyer & Engelbrecht, 2007), implying close proximity between their side chains. This is consistent with a role for the positive charge of the arginine in the Brownian ratchet mechanism of the F_o motor (see section 4.1).

3.5 The F-ATPase stator is different in bacteria and eukaryotes

The part of the stator linking subunit *a* to $(\alpha\beta)_3$ varies most between bacterial and organellar F-ATPases. In *E. coli*, it comprises the δ subunit (δ_b) linked to a subunit *b* dimer (Dunn *et al.* 2000; Rodgers *et al.* 1997) (Fig. 1 *a*). The δ_b subunit associates with α at the top of F_1 (Dunn *et al.* 2000; Ogilvie *et al.* 1997; Rodgers & Capaldi, 1998) and contacts the C-terminal end of the subunit *b* dimer (McLachlin *et al.* 1998). The strength of this interaction is sufficient to resist the torque generated by the ATPase motor (Häsler *et al.* 1999; Weber *et al.* 2004). Each *b* subunit is essentially a single α-helix that extends from its contact with δ_b to an N-terminal integral membrane segment, in contact with subunit *a* and adjacent to the external surface of the *c*-ring (Jones *et al.* 2000; McLachlin *et al.* 2000). The *b* subunit remains associated with F_o when F_1 detaches from the membrane. In the mitochondrial enzyme, the δ_b subunit homologue OSCP

https://doi.org/10.1017/S0033583510000338 Published online by Cambridge University Press

(Table 1) makes very similar contacts: its N-terminal region binds with high affinity to α (Carbajo *et al.* 2007) and its C-terminal region forms strong helix–helix interactions with the C-terminal end of the single *b* α-helix (Rees *et al.* 2009). The N-terminal region of the single *b* polypeptide in the mitochondrial complex is predicted to contain two TMHs, but has only a single extramembranous α-helix reinforced by α-helices contributed by the *d* and F_6 subunits (Dickson *et al.* 2006). Several small subunits also associate with the stator in mitochondrial F_o (Table 1), with functions that may include promoting stability through dimerisation and formation of supramolecular complexes (Devenish *et al.* 2008 and references therein).

3.6 Core subunits of the rotary ATPases are related

Subunits A and B are highly conserved between A- and V-ATPases, and their sequences indicate the same common ancestor as F-ATPase β and α subunits. Comparison of crystal structures of A-ATPase A (Maegawa *et al.* 2006), B (Schäfer *et al.* 2006) and the $(AB)_3$ complex (Maher *et al.* 2009) with F_1 underlines their similarity to β and α, but also illustrates key differences (Fig. 2*a, b*). Most striking is the presence of the 'non-homologous region' (NHR) of subunit A, an $\sim$80 residue β-structure region that projects from the surface of V_1 (Fig. 2*a*). Mutations in the NHR of the *Saccharomyces* polypeptide influence coupling efficiency and the ability of the yeast enzyme to undergo controlled domain dissociation in response to physiological signals, suggesting a role in regulation (Shao *et al.* 2003; Shao & Forgac, 2004). How this might work is not clear, and similar regulatory mechanisms have not been demonstrated in A-ATPases even though the NHR is conserved. Most of the remaining fold of A is very similar to β, although the C-terminal region of A does differ in that the three α-helices closest to the membrane domain are significantly longer than in β (Fig. 2*a*) (Maher *et al.* 2009). The significance of this is unclear, although this region does contain the helix-loop-helix 'lever' structure involved in torque generation (labelled 'L' in Fig. 2*a*), with partial conservation of the F-ATPase DELSEED sequence. In the 2·8 Å structure of the $(AB)_3$ complex from *T. thermophilus*, crystallised in the absence of nucleotides, all three active sites adopt the same configuration, resembling that of the β_E site in F-ATPase (Maher *et al.* 2009). In a more complete (but lower resolution) model of the *T. thermophilus* A_1 that also includes the D and F axle subunits, the three AB units adopt different conformations and two active sites contain ADP (Numoto *et al.* 2009), mirroring the situation in the 'reference' F_1-ATPase co-crystallised with nucleotides (Abrahams *et al.* 1994). Adoption of different active site conformations therefore requires nucleotide binding, interaction with D, or both.

Overall, side chains arrangements in A_1/V_1 and F_1 active sites are remarkably conserved (Fig. 2*d*), suggesting similar reaction chemistries. In particular, this includes a glutamate residue (β-E189 and A-E257 in Fig. 2*d*) proposed to activate bound water for nucleophilic attack on the γ-phosphate of ATP during hydrolysis, and the 'arginine finger' residue (α-R375 and B-R360 in Fig. 2*d*) positioned to stabilise the penta-coordinate transition state of the γ-phosphate. Crucially, this residue changes position during the transition from 'open' to 'closed' active site states. Although the fold of B closely resembles that of F-ATPase α (Fig. 2*b*), the P-loop that contains a Walker A motif involved in nucleotide binding by A, α and β is not conserved. In line with this, but in contrast to the situation in the F_1-ATPase (Abrahams *et al.* 1994), the non-catalytic A–B interfaces in A_1 do not bind ADP (Numoto *et al.* 2009). Any possible function performed by these nucleotides in F-ATPase is therefore not conserved in the A- or V-ATPases. This difference, the presence of the NHR, or more subtle differences such as the arrangement of

https://doi.org/10.1017/S0033583510000338 Published online by Cambridge University Press

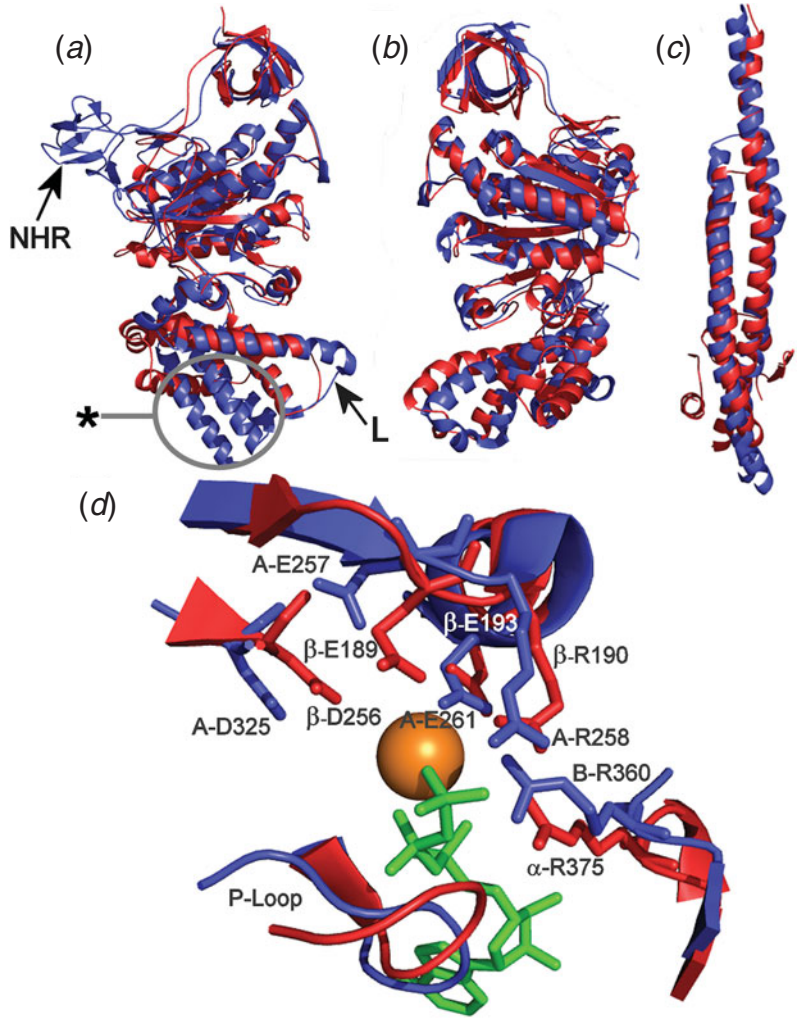


Fig. 2. Structures of rotary ATPase core subunits are conserved. (*a*) Overlay of the *T. thermophilus* A subunit (blue: pdb 3GQB) with the yeast β subunit (red: pdb 2HLD). Subunit A is presumed to be in the 'empty' state (see text for details) and is compared to the β_E conformer. There is extensive common fold, the key differences being the subunit A 'NHR' and the length of the α-helices in the C-terminal region of A (ringed). The helix-loop-helix region that in F-ATPase β contains the conserved DELSEED sequence (DALQDAE in *T. thermophilus* A) and acts as the lever that interacts with the axle is also highlighted (L). (*b*) Overlay of *T. thermophilus* B (blue) and yeast α (red) subunits shows the high degree of similarity in fold. (*c*) Despite no apparent sequence similarity, residues 1–55/132–205 of the *T. thermophilus* D subunit (blue: pdb 3A5D) fold as a coiled-coil very similar to the γ subunit that forms the axle of the F-ATPase. (*d*) Overlay of the active sites of *T. thermophilus* A-ATPase (blue) and yeast F-ATPase (red). To aid with orientation around bound nucleotide (green) and Mg^{2+} ion (orange sphere), the yeast $(\alpha\beta)_{DP}$ site is shown. β-E189 and A-E257 are equivalent to β-E188 of the bovine enzyme proposed to activate a bound water molecule for nucleophilic attack on the γ-phosphate of ATP (Abrahams *et al.* 1994). Overall similarities in active site organisation point to fundamentally similar reaction chemistries in all three ATPases.

hydrophobic residues around the A_1 active site (Maher *et al.* 2009) could account for divergence in reaction mechanisms observed as differences in the stepping characteristics of the rotor in A_1 compared with F_1 (Imamura *et al.* 2005).

https://doi.org/10.1017/S0033583510000338 Published online by Cambridge University Press

3.7 Subunit organisation in the rotors of A- and V-ATPases

Sequences of D subunits of the central stalks of the A- and V-ATPases are dissimilar to the F-ATPase γ subunit, implying no common ancestor. Comparison of D and γ structures does, however, show that they are both coiled-coils of α-helices (Numoto *et al.* 2009) (Fig. 2*c*). Subunit F is also conserved across A- and V-type complexes, albeit with somewhat lower ($\sim$28%) identity. Subunit F has been proposed to promote catalytic activity in the A_1-ATPase (Imamura *et al.* 2004), with the polypeptide able to adopt 'extended' and 'contracted' conformations in which the positions of the C-terminal $\sim$40 residues vary dramatically (Makyio *et al.* 2005). In the $(AB)_3$:D:F crystal structure, F adopts a different, possibly intermediate conformation, with its C-terminal segment extending up to contact a helix-loop-helix feature in the C-terminal domain of an A subunit (Numoto *et al.* 2009). This A subunit feature is homologous to the 'lever' of the F-ATPase β subunit that contains the conserved DELSEED sequence and is involved in energy transfer between the axle of the rotor and $(\alpha\beta)_3$ catalytic complex. The positioning of the C-terminal segment of F in the A_1 crystal structure suggests a ratchet-like function that could prevent the counter-clockwise rotation of subunit D (as viewed from the membrane) expected to result from ATP hydrolysis. This conformational flexibility of F is remarkably similar to that shown by the bacterial F-ATPase ε_b subunit that occupies a similar rotor location, although F and ε_b share no other obvious similarities. Interestingly, the fold of subunit F resembles that of CheY (Makyio *et al.* 2005), a bacterial chemotaxis response regulator that influences the directionality of flagellar rotation according to its phosphorylation state.

The 4TMH V-ATPase *c*-subunits appear to have evolved as a tandem repeat of the same 2 TMH progenitor that gave rise to F-ATPase subunit *c*, but retaining only one conserved proton-carrying glutamate on its fourth TMH. In the A-ATPases, H^+ or Na^+-specific forms of either the 2- or 4-helical forms occur in different species, perhaps as a result of exchange of genes between archaea and eubacteria (Mulkidjanian *et al.* 2008; Müller *et al.* 2005). The archaeon *Methanocaldococcus jannaschi* expresses a 6TMH *c*-subunit consisting of a triple repeat of the 2TMH helical hairpin, with the ion translocating residue deleted from the first 2TMH repeat element (Müller & Grüber, 2003). Data relating to the subunit *c* stoichiometry in A- and V-ATPase are limited, but suggest variability. The Na^+-specific *c*-ring of *E. hirae* is a decamer of 'V-ATPase type' 4TMH polypeptides (Murata *et al.* 2005), whereas the c_{12} ring from *T. thermophilus* contains 'F-ATPase type' 2TMH subunits (Toei *et al.* 2007). Uniquely, the archaeon *Methanopyrus kandleri* has a gene encoding a single *c*-type polypeptide that is a 13-mer repeat of the F-type helical hairpin polypeptide (Slesarev *et al.* 2002), but it is unclear if this is indicative of a commonly occuring stoichiometry. Superficially, the 2TMH pattern appears to be an adaptation to the ATP synthase function, whereas the 4TMH version may be an ion pump feature. However, this does not hold under scrutiny: although the A-ATPase of archaeal *Pyrococcus* species appears essentially identical to the ATP-driven Na^+ pump of the bacterium *E. hirae*, both having decameric *c*-rings of the 4TMH 'V-ATPase-type', the *Pyrococcus* enzyme can operate in either ion pump or synthase modes (Müller & Grüber, 2003). In the V-ATPase, polypeptides closely related to the 4TMH subunit *c* also assemble as hexamers (Clare *et al.* 2006), consistent with biochemical measurements of stoichiometry performed on the coated vesicle enzyme (Arai *et al.* 1988). A low H^+/ATP ratio in V-ATPases in particular could indicate a low gearing that would permit proton translocation against even a large, unfavourable pH gradient. However, the *c*-ring stoichiometry in the V-ATPase remains uncertain: the c_{10} ring from the *E. hirae* A-ATPase, rather than a

https://doi.org/10.1017/S0033583510000338 Published online by Cambridge University Press

hexameric model, proved to be the best fit to electron density maps of the *Manduca* enzyme (Muench *et al.* 2009).

The *d* subunit of the A- and V-ATPases has no homologue in the F-ATPase. It is proposed to couple the membrane end of the D/F axle to the *c*-ring (Iwata *et al.* 2004). The crystal structure of the *T. thermophilus d* subunit shows a bundle of seven long (30–39 Å) helices surrounded by a ring of shorter helical segments, giving an overall conical shape that is complementary to the cytoplasmic surface of the rotor ring (Iwata *et al.* 2004). Subunit *d* has therefore been proposed to tightly plug the socket formed by *c*-ring cylinder. Consistent with this, subunit *d* binding to the V-ATPase *c*-ring appears to be very tight, with chaotropic agents required to strip it from V_o (Bauerle *et al.* 1993). X-ray scattering analysis of the yeast *d* subunit shows a 'boxing glove' shape that is stabilised by intramolecular disulphide bonds (Thaker *et al.* 2007). The 'wrist' of this structure could be inserted into the middle of the *c*-ring. In the V-ATPase, mutations in subunit *d* can affect coupling between ATP hydrolysis and H^+ translocation (Owegi *et al.* 2006), implying that they break the coupling between axle and *c*-ring or cause it to slip under load. Alternatively, mutations could allow uncoupled leakage of protons back across the membrane ('proton slip'; Nelson *et al.* 2000).

3.8 Peripheral stator components of the rotary ATPases share common features

Structures of the mitochondrial F-ATPase stator have been solved both as a partial *b*:*d*:F_6:OSCP complex within the membrane extrinsic part of the enzyme (Rees *et al.* 2009), and as an autonomously assembling *b*:*d*:F_6 sub-complex missing only the integral membrane part of *b* (Dickson *et al.* 2006) (Fig. 3). These show that the extrinsic region of *b* is a single extended α-helix that is reinforced by shorter helical segments from *d* and F_6 (Fig. 3*c, d*). The strength of the OSCP-*b* linkage comes from extensive helical interactions.

In the A- and V-ATPases, the structure comparable to F-ATPase *b*:*d*:F_6:OSCP comprises only E and G subunits (Table 1). E:G spontaneously assembles as a highly stable 1:1 heterodimer in bacterial expression systems, although both bacterial and archaeal G polypeptides in isolation form dimers or higher order filamentous aggregates (Jones *et al.* 2010; Kish-Trier *et al.* 2008). G shares sequence similarity with the extramembranous region of the F-ATPase *b* subunit (Hunt & Bowman, 1997; Supekova *et al.* 1996), indicating a common origin. Crystal structures of the A-ATPase E:G (Lee *et al.* 2010a) and F-ATPase *b*:*d*:F_6:OSCP (Dickson *et al.* 2006) sub-complexes show that G and *b* have remarkably similar extended α-helical folds (Fig. 3). In the E:G heterodimer, a ~130 Å-long G helix runs parallel to a second helix of similar length contributed by E, with the two forming a right-handed coiled-coil (Fig. 3*a*). The C-terminal end of G interacts with the globular C-terminal domain of E (Jones *et al.* 2010; Kish-Trier & Wilkens, 2009a), which also interacts with the N-terminal region of subunit B at the apex of the soluble domain (Kish-Trier & Wilkens, 2009b), analogous to the interactions between δ_b/OSCP and α in the F-ATPase. A similar structure for the V-ATPase E:G sub-complex may be expected, given the sequence conservation between the A- and V-ATPase components. A- and V-ATPase E:G heterodimers also share similar secondary structure, and both form ~160–180 Å filaments consistent with a stator role linking the soluble and membrane domains (Féthière *et al.* 2004, 2005; Harrison *et al.* 2003; Jones *et al.* 2010; Kish-Trier *et al.* 2008; Yamamoto *et al.* 2008). In the yeast E:G heterodimer, the N-terminal regions of the two polypeptides appear quite closely aligned (Rishikesan *et al.* 2008). A key difference between the A- and V-ATPases is the stoichiometry of the E:G subunits: Mass spectrometric approaches indicate three copies of E:G

https://doi.org/10.1017/S0033583510000338 Published online by Cambridge University Press

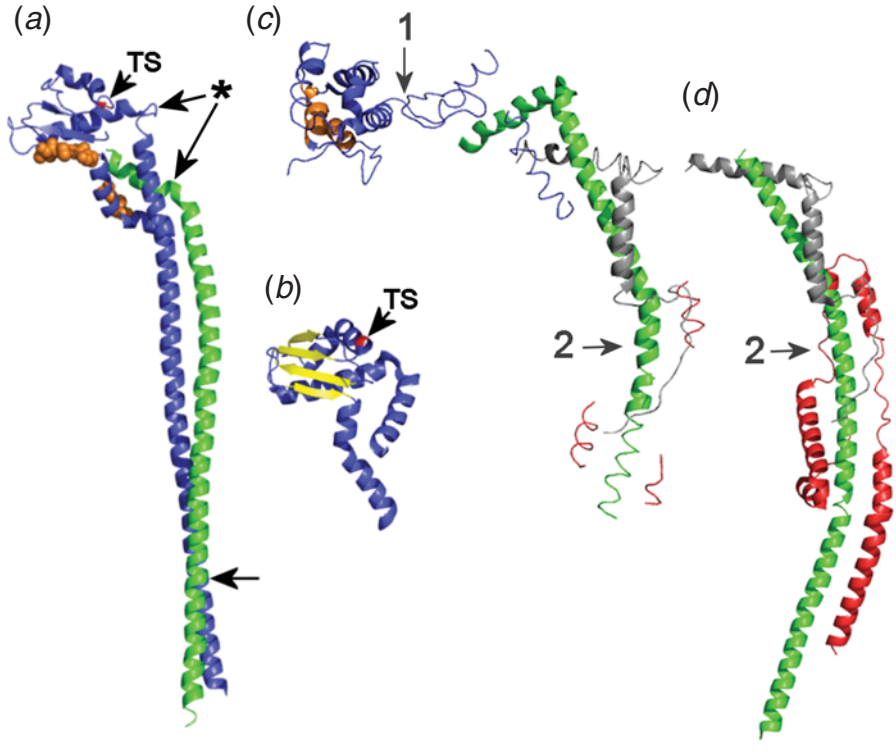


Fig. 3. Stator crystal structures. (*a*) The A-ATPase E:G sub-complex from *T. thermophilus* (pdb 3K5B) at 3·1 Å resolution comprising residues 2–188 of subunit E (blue) and 21–120 of subunit G (green). Residues in the globular domain of E involved in binding to the B subunit are orange. TS indicates the position of the temperature-sensitive mutation in the homologous *Saccharomyces* E subunit. Potentially flexible points in E and G are asterisked. The point towards the foot of the α-helical region arrowed can be cross-linked to subunit C in yeast V-ATPase (Jones *et al.* 2010). (*b*) Residues 81–198 of *Pyrococcus hirokoshii* subunit E (pdb 2DM9: Lokanath *et al.* 2007) at 1·85 Å, detailing the β-sheet structure in the globular domain. (*c*) Partial stator structure from the membrane extrinsic part of the bovine mitochondrial F-ATPase at 3·2 Å (pdb 2WSS), comprising residues 122–207 of *b* (green), 5–25/35–57 of F_6 (grey), 1–146/169–189 of OSCP (blue) and three short α-helical segments of *d* (red). Residues in OSCP involved in binding to the α subunit are orange. (*d*) Bovine F-ATPase sub-complex (pdb 2CLY) at 2·8 Å, containing subunit *b* with its transmembrane α-helical region deleted (residues 79–183: green), and residues 8–123 and 5–70 of subunits *d* (red) and F_6 (grey), respectively. The C-terminal α-helical segment of *b* apparent in (*c*) is not resolved. In (*c*) and (*d*), 1 and 2 indicate proposed points of flexibility (discussed in section 3.8).

in the V-ATPase (Kitagawa *et al.* 2008), but only two copies in the A-type complex (Esteban *et al.* 2008). This difference is discussed below in the context of the 3D models generated by EM.

Both F- and V/A-ATPase stators have been proposed to include particular points that might confer flexibility (Lee *et al.* 2010a; Rees *et al.* 2009), a property that may play a role in ATPase mechanics. In the F-ATPase, these are between the α-binding and *b*/*d*-binding domains of OSCP and at a point at which the *b* subunit bends (labelled 1 and 2 in Fig. 3*c, d*). Flexion points in E:G have been suggested near the C-terminal end of G and at the junction between N-terminal α-helical and globular domain of E (asterisk, Fig. 3*a*).

Subunits C and H are the only subunits without functional homologues in either the F- or A-type ATPases (Table 1). Subunit C has a ~110 Å-long 'dogbone' structure (Drory *et al.* 2004), and fits into the stator of the V-ATPase (Fig. 1*c*), where it contacts the N-terminal region of

https://doi.org/10.1017/S0033583510000338 Published online by Cambridge University Press

subunit E (Fig. 3*a* legend). It has been proposed to have a regulatory function, being phosphorylated in insects by protein kinase A in response to physiological signals (Voss *et al.* 2007), and by the With no K (lysine) (WNK) kinase in *Arabidopsis* (Hong-Hermesdorf *et al.* 2006). Loss of C from the V-ATPase has been shown in yeast and insects to be linked to the reversible dissociation of the V_1 from the membrane and ATPase inactivation (Kane, 1995; Merzendorfer *et al.* 2000; Parra *et al.* 2000). A similar phenomenon in yeast is also dependent on protein kinase A activity, although phosphorylation of subunit C in *Saccharomyces* has not been directly demonstrated (Bond & Forgac, 2008). Subunit H has two distinct domains assembled as an 'L-shape' (Sagermann *et al.* 2001), and is also proposed to function as a V-ATPase regulator. Domain dissociation in yeast induces a change in position of H within the V_1 complex such that its C-terminal domain comes into contact with the D:F axle (Jefferies & Forgac, 2008; Diab *et al.* 2009), presumably restricting its movement and thereby preventing ADP/ATP exchange in the active sites. The absence of homologues of these subunits from either F- or A-type ATPases presumably reflects the evolution of more sophisticated control mechanisms in eukaryotic V-ATPases, driven by the necessity to conserve ATP during periods of physiological stress.

3.9 V/A-ATPase stator subunit *a* is a polytopic protein with two domains

As in the F-ATPase, subunit *a* forms the membrane-embedded end of the stator in the A- and V-ATPases and, like its F_o equivalent, includes residues involved in H^+ translocation (Kawasaki-Nishi *et al.* 2001; Leng *et al.* 1996, 1998). Also like F-ATPase subunit *a*, it is the subunit for which we have the least structural information. Although hydropathy analysis suggests that the ~95 kDa V-ATPase *a* subunit folds with ~40 kDa N-terminal soluble (a_N) and ~55 kDa integral membrane (a_C) domains, the heterologously expressed a_N domain has also been reported to have integral membrane protein characteristics: its folding is stabilised by detergent, and it co-precipitates with synthetic liposomes (Merkulova *et al.* 2010). The a_N domain contributes to a collar structure that links together C, E, G and H subunits (see Fig. 1). Early topographic models suggested 7–9 TMHs (Kawasaki-Nishi *et al.* 2001; Leng *et al.* 1999), but a recent study (Wang *et al.* 2008) has produced a more plausible 8 TMH model, with the N-terminal domain cytoplasmically located. An even number of helices exposes the C-terminal tail to the cytoplasm, consistent with it binding to cytoplasmic phosphofructokinase-1 (Su *et al.* 2003). Secondly, it places functionally critical Arg, His and Glu residues within TMH 7 and 8 (Arg735, His743 and Glu789 in the *Saccharomyces* subunit *a*, Vph1p) in an arrangement that closely parallels that of similar residues in TMH 4 and 5 of the F-ATPase subunit *a* (Kawasaki-Nishi *et al.* 2001). The residue equivalent to the yeast Arg735 is contained within a conserved LRLWXXXXA motif, a version of which (RLXXXXXA) also persists in the F-ATPase *a* subunit. Topography with 8 TMH gives V-ATPase subunit *a* TMH7 and F-ATPase subunit *a* TMH4 the same orientation with respect to the cytoplasmic surface of the membrane. Complete traversing of the bilayer by each putative TMH is inferred, but may not be the case. Helical structures at the *c*-ring interface could be sequestered from the hydrophobic phase, allowing formation of 'helix loops' such as those found in the interiors of a number of channel proteins.

Even less is known about the topography of the 72–76 kDa A-ATPase homologue of subunit *a* (Table 1). Analysis with TMPred (Hofmann & Stoffel, 1993) suggests that A-ATPase subunit *a* has a C-terminal 6 TMH and a ~38 kDa soluble N-terminal domain (Harrison, Muench and Trinick, unpublished results), although a seven TMH model has also been proposed (Müller *et al.* 1999). As in the V-ATPase homologue, the A-ATPase a_N domain forms a collar structure that

https://doi.org/10.1017/S0033583510000338 Published online by Cambridge University Press

links together the two sets of EG heterodimeric components (Fig. 1). Limited sequence similarity between predicted helices 7/8 of V-ATPase *a* and 5/6 of its A-ATPase homologue suggests some conservation of this region across all rotary ATPases. Other regions of V-ATPase and A-ATPase *a* subunits are, however, highly divergent, with the V-ATPase polypeptide also containing a ~200-residue insert predicted to include a 60–70-residue extramembranous region on the cytoplasmic side of the membrane (Harrison, Muench and Trinick, unpublished observations). Thus, the V- and A-type subunits show some clear similarities in the organisation of helices directly involved in ion translocation, paralleling a similar structure in the F-ATPase subunit *a*, but with the V-ATPase subunit having additional complexity perhaps linked to more sophisticated regulation in eukaryotes.

V_o also contains subunit *e*, a small (8·4–9·7 kDa) and highly hydrophobic polypeptide first observed in V-ATPase preparations from bovine chromaffin granules (Ludwig *et al.* 1998) and later identified in *Manduca sexta* as an integral part of the V-ATPase (Merzendorfer *et al.* 1999). It was subsequently found to also be an essential component of the yeast enzyme (Davis-Kaplan *et al.* 2004; Sambade & Kane, 2004). Although we can presume that it is associated with subunit *a* in the membrane-embedded part of the stator, its precise function remains uncertain, and no equivalent has been found in the A-ATPases.

Further parallels can be drawn between the F- and V-ATPase membrane subunits through examination of their roles in inhibitor binding. Oligomycin resistance-conferring mutations map onto the lipid-exposed surface of the *c*-ring structures, and tributyl tin compounds also target F_o, most likely subunit *a* or the crucial *a*/*c*-ring interface (von Ballmoos *et al.* 2004). The bafilomycin-type compounds that target the V-ATPase subunit *c* (Bowman & Bowman, 2002; Huss *et al.* 2002; Whyteside *et al.* 2005) also access its membrane-embedded surface via the lipid phase (Dixon *et al.* 2004, 2008; Pali *et al.* 2004), mirroring the site and mode of action of oligomycin in the F-ATPase (Fillingame *et al.* 2002; Vik *et al.* 2000). The likely involvement of V-ATPase subunit *a* in bafilomycin binding (Wang *et al.* 2005) further implies that the effects of these compounds result directly from interference with the dynamic interface between the *a*-subunit and the *c*-ring.

4. Rotary ATPase mechanics

4.1 Torque generation

How does this assembly generate torque to power the complex in synthase mode? A model based on a Brownian ratchet mechanism has been developed (Dimroth *et al.* 2006; Junge *et al.* 1997, 2009; Vik & Antonio, 1994), supported by mechanochemical simulations and consistent with structural data (Elston *et al.* 1998; Oster & Wang, 2000a), but lacking direct experimental validation. Its key features are asymmetrically arranged and non-continuous 'half-channels' in subunit *a*, and a lipid-exposed aspartate (or glutamate) residue on each *c*-ring subunit (Fig. 4). The 'half channels' act as entry/exit portals, allowing protons to board the *c*-ring rotor, protonating the side chain of the aspartate residue. Movement of the *c*-ring, subject to thermal fluctuations but constrained by electrostatic and hydrophobic forces, can take a rotational step only if the negatively charged carboxylate side chain of the aspartate is neutralised by a proton. The probability of this occurring is increased by the prevailing membrane potential, allowing the protonated *c*-ring subunit to diffuse out of the electrostatically protective subunit *a*/*c*-ring interface. Futile stepping in the wrong direction (which could result in a proton 'short circuit')

https://doi.org/10.1017/S0033583510000338 Published online by Cambridge University Press

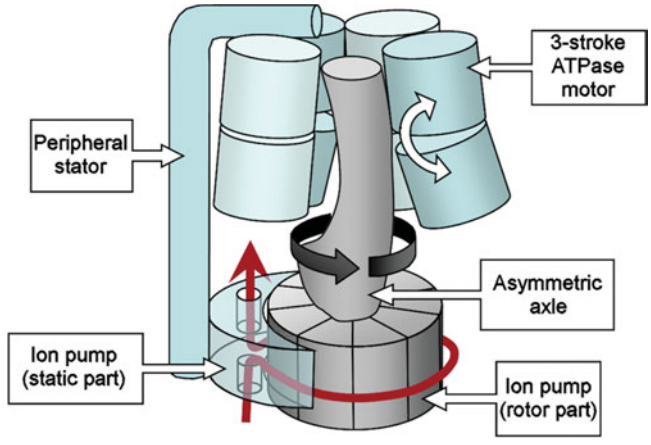


Fig. 4. Rotary ATPases – a generic model. The soluble domain of each complex houses an ATP hydrolysing/synthesising motor with three catalytic sites (*3-stroke motor*: One segment has been removed). An *asymmetric axle* connects this to an ion pump housed within the integral membrane domain. The ion pump has two parts: a rotating ring of subunits, each of which can carry one proton, and a static subunit postulated to contain two asymmetrically arranged and non-continuous 'half-channels', each accessible from only one side of the membrane. In ATP synthase mode (as in the F- and A-ATPases), the membrane potential drives a proton onto a rotor ring subunit via an 'entry' half channel. Protonation allows stepping of the ring, hence rotation (direction indicated by the grey arrow). Synchronously, a proton is lost to the 'exit' half-channel. The red arrow shows the path of proton movement. In ion pump mode (as in V-ATPase), conformational changes in the 3-stroke ATPase motor resulting from ATP turnover apply torque to the rotor, driving the rotor ring in the opposite direction. To allow relative movement of the two ion pump parts, its static component must be fixed to the 3-stroke ATPase motor by a *stator*.

may be prevented by the presence of the positively charged arginine residue on subunit *a*. The *c*-ring subunit re-entering the subunit *a*/*c*-ring interface on the other side must synchronously lose its proton to the 'exit channel', a process that may also be promoted by proximity to the subunit *a* arginine. Thus, the membrane potential biases the diffusion of the rotor *c*-ring and enforces directionality to the rotation.

The tight coupling between *c*-ring and asymmetric axle ensures their concerted movement. Given the high ATP/ADP ratio in the mitochondrial matrix, the key step requiring an input of energy is likely to be the transition to the 'open' state and the emptying of the active site of ATP (Yang *et al.* 2003). According to current models, the convex face of the rotating axle transmits this energy by working the β-subunit helix-loop-helix 'lever', forcing movement of the β C-terminal (lower) domain about a β-sheet inter-domain 'hinge' (Fig. 4). This results in opening and emptying of the active site, holding it in a state accessible for substrate binding. Simultaneously at a second site, rotational stepping induces the $\beta_{DP} \rightarrow \beta_{TP}$ transition that is presumed to include a state in which the hydrogen bonding geometry in the active site is optimal for stabilising the transition state in the phosphorylation of ADP. A similar 'rotor-lever' system is also found in the A- and V-ATPases, suggesting similar power transmission mechanisms.

In ion pump mode (as occurs in the V-ATPase), the roles of the two motors are reversed: the soluble domain ATPase is the torque generator. There is no direct experimental evidence relating to torque generation in V_1, but similarities to the F-ATPase suggest similar mechanochemical models. In F-ATPase, the driver for conformational change in the active site has been proposed to be the sequential 'zipping up' of hydrogen bonds to ATP during binding (Oster & Wang, 2000a). This results in the movement of the C-terminal domain of a β-subunit. The resulting

https://doi.org/10.1017/S0033583510000338 Published online by Cambridge University Press

lever movement applies torque to the asymmetric axle, forcing rotation (Pu & Karplus, 2008), although simultaneous contributions from all three catalytic units have been proposed (Ariga *et al.* 2007). Concerted rotation of the *c*-ring against the static *a* subunit drives proton pumping via a mechanism that may be essentially a reversal of the biased diffusion process outlined above for the synthase mode. Accordingly, a proton boarding the *c*-ring via a subunit *a* half-channel open to the cytoplasm would be carried around the full circumference of the *c*-ring before being released into an exit channel open to the lumenal side. In this instance, the torque generated by ATP hydrolysis must be sufficient to overcome the opposing load presented by the membrane potential against which the V-ATPase is operating. It can do this if the electrostatic cost of *c*-ring stepping is decreased by the acquisition of a neutralising proton on the cytoplasmic side of the membrane and by synchronous release of a proton on the lumenal side.

4.2 Mechanical properties

The robustness of purified F_1 has resulted in most of the data coming from the hydrolysing complex, with limited data available for the A_1 and V-ATPase operating in the same direction. Bulk phase measurements of ATP hydrolysis for both F_1 and the V-ATPases give turnover numbers up to $\sim 300\ s^{-1}$, which translate into rates of rotation of ~ 100 revolutions per second (r.p.s.) if ATP is not limiting. Observed rates in single molecule reporter studies are generally lower because of the limiting drag of the reporter actin filament or bead. For the F-ATPase, rotational rates too high to be compatible with bulk phase measurements have been reported, suggesting that single molecules can achieve much higher speeds between periods of inactivity (Diez *et al.* 2004; Ueno *et al.* 2005). Turnover number of $10\ s^{-1}$ for the A_1-ATPase are consistent with observed rotational rates of ~ 3 r.p.s. (Imamura *et al.* 2003). Measurements of torque generated by the F-ATPase are typically ~ 40–45 pN·nm (Futai *et al.* 2000; Noji *et al.* 1997; Sambongi *et al.* 1999), and may be as high as 56 pN·nm when corrected for surface effects (Pänke *et al.* 2001). Values for both the A_1-ATPase and *Saccharomyces* V-ATPase are lower at ~ 35 pN·nm (Hirata *et al.* 2003; Imamura *et al.* 2003). Although efficiency of energy conversion in these systems can be estimated in a number of different ways, most commonly this is a comparison of energy input, as the Gibbs free energy associated with a particular ATP/ADP/phosphate ratio under defined experimental conditions, and output as mechanical work in the form of rotation. Upper estimates suggest close to 100% efficiency (Junge, 2004; Junge *et al.* 2009; Oster & Wang, 2000b). Curiously, varying the free energy available to F_1 by manipulating the ATP/ADP ratio *in vitro* affects only the stepping frequency of the rotor, not the work done by the system. There appears to be no correlation between torque generated and the free energy available to drive the motor (Junge *et al.* 2009; Muneyuki *et al.* 2007).

Single molecule experiments performed with F_1-ATPase at high ATP concentrations show steady state catalysis resulting in apparently smooth rotational movement. However, at low-substrate concentrations distinct pauses are introduced, with each 120° catalytic cycle step made by the axle comprising $\sim 80°$ and $\sim 40°$ sub-steps (Yasuda *et al.* 2001). Correlations with substrate binding, hydrolysis and product release indicate that the longer sub-step occurs upon ATP binding, the pause preceding it being a 'binding dwell' or 'ATP waiting dwell'. Hydrolysis leads to the smaller step after a 'catalytic dwell'. Apart from the 'post-hydrolysis' structure of the F_1-ATPase bound to ADP.AlF_4^- (Menz *et al.* 2001), most crystal structures of the F_1-ATPase appear to reflect the catalytic dwell state (Okuno *et al.* 2008; Yasuda *et al.* 2003). An absence of

https://doi.org/10.1017/S0033583510000338 Published online by Cambridge University Press

observable sub-steps during catalysis by the A_1 domain suggests a somewhat different rotational mechanism, with both ATP binding and hydrolysis occurring at the same rotor angular position (Imamura *et al.* 2005). The functional significance of this difference is unclear. Correlations between F-ATPase structure and catalytic state are discussed in more detail in Okuno *et al.* (2008), Sielaff *et al.* (2008a) and Junge *et al.* (2009).

5. Structural analysis of the rotary ATPases by EM

5.1 A brief history

Early electron micrographs of mitochondrial inner membranes in negative stain showed the F_1 domain as the head of a simple 'lollipop' structure protruding ~100 Å from the membrane, connected to the bilayer via only a single central stalk (Chan *et al.* 1970). In line with current mechanistic models, this central stalk is the axle linking the coupled motor functions of the ATPase. Cryo-EM images of the *E. coli* F-ATPase *in situ* in the membrane (Lücken *et al.* 1990) revealed a second thinner, asymmetrically arranged peripheral stalk linking the two domains, which is part of the F-ATPase stator. This density is more clearly seen in images taken subsequently of the *E. coli* (Böttcher *et al.* 2000; Wilkens & Capaldi, 1998), chloroplast (Böttcher *et al.* 1998) and mitochondrial (Karrasch & Walker, 1999) enzymes.

Overall similarities in the macromolecular organisation of the F- and V-ATPases were shown by EM studies of fungal vacuoles (Bowman *et al.* 1989) and epithelia from amphibians and insects (Brown *et al.* 1987). Micrographs of heavy metal-stained membranes show a 'ball on stalk' architecture for the V-ATPase similar to that of the F-ATPase, including a globular headpiece connected to the membrane via a central stalk. EM image averages of the solubilised and purified A-ATPases from *Clostridium fervidus* (Boekema *et al.* 1997, 1999), *Methanocaldococcus jannaschii* (Coskun *et al.* 2004) and 3D reconstructions of the *T. thermophilus* enzyme (Bernal & Stock, 2004) confirmed similar architecture to the F- and V-ATPase, but revealed the existence of two peripheral stalks within the stator linking the domains. This arrangement is most clearly seen in 3D reconstructions from negative stain data (Bernal & Stock, 2004; Vonck *et al.* 2009) and most recently in the first reconstruction from data collected with frozen hydrated specimens of the *T. thermophilus* enzyme (Lau & Rubinstein, 2010). This gives an A-ATPase stator arrangement that is substantially more complicated than anything seen in the F-ATPase. Multiple stalk-like stator components have also been observed in EM images of the brain coated vesicle V-ATPase in negative stain, although their exact number cannot be determined from the image averages (Gregorini *et al.* 2007; Wilkens *et al.* 1999). The number of stalk elements in the stator of the eukaryotic V-ATPase remained a contentious issue until quite recently, with 3D reconstructions from negative stain data of the *Neurospora* (Venzke *et al.* 2005) and bovine-coated vesicle (Wilkens *et al.* 2004) enzymes suggesting two (leading to parallels with the A-ATPase), whereas the tonoplast pump of the plant *Kalanchöe* appears to have three (Domgall *et al.* 2002). V-ATPase (and A-ATPase) stators often appear incomplete in 3D reconstructions from stain data, disconnected from the membrane domain. This suggests a degree of heterogeneity in the sample, perhaps introduced during purification as a result of proteolytic degradation, or through genuine natural conformational variability with the population of ATPases on the EM grid.

Cryo-EM of detached F_1 has also revealed nucleotide-dependent changes in the position of axle subunits, providing initial evidence of rotational stepping driven by ATP turnover (Gogol *et al.* 1990; Wilkens & Capaldi, 1994). V_1 detached from V_o has also been studied: manipulation

https://doi.org/10.1017/S0033583510000338 Published online by Cambridge University Press

of energetic conditions in the larvae of the tobacco hawkmoth *M. sexta* (Sumner *et al.* 1995) or in yeast (Kane, 1995) trigger dissociation of V_1 from the membrane, allowing it to be purified in a stable, catalytically inactive form (Gräf *et al.* 1996). Small angle X-ray scattering (SAXS) analysis of *Manduca* V_1 showed an elongated structure with a headpiece of ~14·5 nm diameter and a central stalk extending ~11 nm from it (Svergun *et al.* 1998). Subsequent EM of the same complex in negative stain has revealed a 6-nm-long axle protruding from a central pore of a 13·5 nm diameter headpiece with (pseudo)6-fold symmetry (Grüber *et al.* 2000; Radermacher *et al.* 2001). At 18 Å resolution, the axle appeared to be connected asymmetrically to the surfaces of the $(AB)_3$ catalytic complex that line a central pore (Radermacher *et al.* 2001). Although at nominally lower (25 Å) resolution, EM data for V_1 from *Saccharomyces* has provided a more detailed reconstruction, with six elongated core densities surrounding an asymmetric axle (Zhang *et al.* 2003). The presence of three knob-like densities protruding at 120° intervals around the structure gives clear 3-fold symmetry to the structure. Unlike the simple extended stem seen in the *Manduca* V_1, the axle extending ~50 Å from the underside of the yeast domain has a distinctive 'L-shape', with the horizontal density being assigned to the H subunit (Zhang *et al.* 2003). Unlike V_1, but similar to the F_1-ATPase, A_1 detached from the membrane retains catalytic activity. The complex from the archaeon *Methanosarcina mazei* Gö1, for example, hydrolyses Mg.ATP at rates of ~9 μmoles/mg protein/min (equivalent to a turnover of ~25 ATP per second per active site) (Grüber *et al.* 2001a). Analysis of the active A_1 domain by SAXS coupled to *ab initio* modelling has revealed a structure similar in shape to V_1 but closer in size to F_1 (Grüber *et al.* 2001a).

Small size makes EM 3D reconstructions of isolated membrane domains difficult, with the associated detergent obscuring detail. The dominant feature of the only available V_o reconstruction is a horizontal 'arm' on the cytoplasmic side of the complex. This arm links the asymmetric part of the transmembrane region of V_o (containing the a_C integral membrane domain: Section 3.9) to the central point at which the D:F axle is proposed to link to the *d*:*c*-ring part of the rotor (Wilkens & Forgac, 2001). If, as seems likely, this arm is the subunit *a* N-terminal domain (a_N), a mechanism can be imagined in which the stator part of V_o (the subunit *a* C-terminal domain) and rotor (*d*:*c*-ring) elements of the membrane domain can become locked together. Prevention of the relative movement of these components may explain the absence of passive H^+ transport by isolated V_o (Béltran & Nelson, 1992; Zhang *et al.* 1992).

5.2 Current EM-derived models: motors with 1-, 2- or 3-part stators

5.2.1 The F-ATPase – the single stalk stator model

The only complete 3D models of the F-ATPase are of negatively stained chloroplast (Böttcher & Gräber, 2000) and *E. coli* enzymes (Böttcher *et al.* 2000), and more recently from cryo-EM of the bovine (Rubinstein *et al.* 2003) and yeast (Lau *et al.* 2008) mitochondrial enzymes. A complication with the EM approach is that F-ATPase can adopt preferred orientations on EM grids (Karrasch & Walker, 1999; Rubinstein *et al.* 2003), limiting the number of end-on and high-angle views of the complex, necessitating novel image processing (Baker & Rubinstein, 2008; Rubinstein *et al.* 2003). This approach, using asymmetric features to order a rotational series of views, has produced similar 3D reconstructions at resolutions of 32 Å (bovine) and 24 Å (yeast) showing bi-domain complexes ~250 Å along their long axes (perpendicular to the plane of the membrane) (Fig. 5*a*). The globular F_1 and F_o domains are linked by a central axle and a thinner

https://doi.org/10.1017/S0033583510000338 Published online by Cambridge University Press

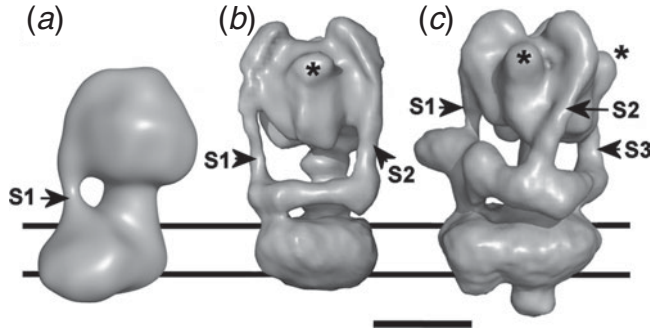


Fig. 5. 3D models from EM. (*a*) Bovine mitochondrial F-ATPase at 32 Å resolution (EBI-EMBL Electron Microscopy Database (EMDB) entry EMD-1357) by cryo-EM. (*b*) *Pyrococcus furiosus* A-ATPase at ∼23 Å resolution by negative stain EM (EMD-1542). (*c*) *Manduca sexta* V-ATPase (EMD-1590) at ∼17 Å resolution by cryo-EM. S1, s2 and s3 indicate the stator elements. For consistency, the stator nearest to the asymmetric part of the membrane domain formed by subunit *a* is designated s1. The asterisks in the A- and V-ATPase reconstructions show the locations of subunit A 'NHRs'. Parallel lines approximate the boundaries of the membrane. The scale bar represents 100 Å.

peripheral stalk forming the stator. This peripheral stalk is also visible in the negative stain reconstructions. Thus, the structure of the F-ATPase is clearly the paradigm for the rotary motor model with a single stator stalk outlined in Fig. 4. A key feature of the cryo-EM reconstructions is the left-hand curvature of the peripheral stalk as it wraps around the complex from F_o to the top of F_1. Rubinstein *et al.* have argued that this curvature is consistent with trapping the complex in ATP hydrolysing mode, stemming from dissipation of any membrane potential during purification and exposure to residual mitochondrial ATP and excess exogenous ADP (Rubinstein *et al.* 2003). However, this could equally represent the relaxed 'ground state' of the complex, since free movement of protons is always likely to accompany any ATP turnover. Curvature also suggests insertion of the *b* subunit into the membrane domain such that it is asymmetrically arranged with respect to the *a* subunit (Lau *et al.* 2008). Atomic force microscopy of the *E. coli* F_o (containing a subunit *b* dimer) suggests a similar subunit arrangement (Takeyasu *et al.* 1996).

Although relatively low resolution, a comparison of yeast and bovine F_o regions also provides insight into the positions of some of the small supernumerary subunits associated with the mitochondrial complexes (Arnold *et al.* 1998; Belogrudov *et al.* 1996). F_o of the yeast preparation lacks subunits *e* (8·2 kDa) and *g* (11·3 kDa) and therefore has a mass ∼15% smaller than its bovine counterpart. This correlates with the smaller volume of the yeast F_o (Lau *et al.* 2008). Difference maps suggest the location of these subunits in a lipid-exposed surface domain on the periphery of the integral membrane region of the F-ATPase stator. Positioning *e* and *g* adjacent to each other and to subunit *b* is consistent with co-purification, antibody labelling and cross-linking studies (Arnold *et al.* 1998; Arselin *et al.* 2003; Belogrudov *et al.* 1996; Bustos & Velours, 2005; Soubannier *et al.* 2002). This F_o location suggests how they could be involved in dimerisation of the F-ATPase as part of the process of forming supramolecular complexes in the mitochondrial inner membrane (Devenish *et al.* 2008; Minauro-Sanmiguel *et al.* 2005; Strauss *et al.* 2008; Stuart, 2008). In a recently reported 3D reconstruction of the dimeric *Saccharomyces* mitochondrial F-ATPase (Couoh-Cardel *et al.* 2010), interaction is mediated only via F_o–F_o surface contacts, with the region proposed to contain the *a*, *b* N-terminal region and the small *e/g/i* subunits interacting with the *c*-ring of the neighbouring complex. The interacting enzymes are arranged so

https://doi.org/10.1017/S0033583510000338 Published online by Cambridge University Press

that their long axes are angled at ∼45° with respect to each other, consistent with a role for F-ATPase oligomerisation in curvature of mitochondrial cristae (Couoh-Cardel *et al.* 2010).

5.2.2 The A-ATPase – a stator model with two stalks and a collar

A consistent feature of 3D reconstructions of A_1A_o-ATPases is the presence of two peripheral stalks linking the catalytic and membrane domains (Fig. 5*b*). Reconstructions of complexes from the eubacterium *T. thermophilus* (Bernal & Stock, 2004) and the hyperthermophilic archaeon *Pyrococcus furiosus* (Vonck *et al.* 2009) at ∼23 Å resolution show similar architecture. The two stators are ∼120° apart and extend ∼150 Å vertically downwards from the apex of A_1. The first stator (labelled s1 in Fig. 5*b*) joins directly to the asymmetric density in A_o corresponding to the membrane domain of subunit *a*. The second (s2 in Fig. 5*b*) extends downwards to meet a ∼100 Å long horizontal collar feature that extends at right angles from the point at which the first stalk merges with A_o. This collar is presumed to be the N-terminal domain of subunit *a*, comprising its first 330–350 residues, but has also been suggested to contain part of the A-ATPase homologue of V-ATPase subunit G (Coskun *et al.* 2004). Assuming density of 1·36 g/ml, the ∼60 000 Å^3 volume of this feature could certainly be filled by the 350 residues (42 kDa) of subunit *a*. The two stators appear equivalent in length, diameter and organisation, with both forming hooks over the apex of the A_1 domain. The central axle can also be clearly seen in the *Pyrococcus* A-ATPase reconstruction (Vonck *et al.* 2009), which has asymmetric densities that may correspond to regions of subunit D not resolved in the (partial) crystal structure, or to subunit F. Spanning ∼65 Å from the base of A_1 to the upper surface of A_o, the axle is significantly longer than the equivalent structure in the F-ATPase (∼30 Å), notwithstanding differences in the resolution of the reconstructions. A second prominent feature is the presence of 3 knob-like features projecting from the surface of the A_1 domain, spaced ∼120° apart (Fig. 5*b*). These features accommodate the 'NHRs' of subunit A.

An apparent connection between the stators across the apex of A_1 in the reconstruction of Bernal & Stock (2004) is absent from the cryo-EM reconstruction of the same *T. thermophilus* enzyme by Lau & Rubinstein (2010), and may be an image-processing problem resulting from a scarcity of end-on views of the complex on negative stain grids. Although qualitatively quite similar to the reconstructions from negative stain data, the substantially improved resolution (to approximately 16 Å) of the native *T. thermophilus* complex imaged in ice has provided the first view of the internal anatomy of the complex. As in the F-ATPase, the axle penetrates almost the full length of the A_1 domain and binds at its membrane-proximal end to a tri-lobed density that matches the A-ATPase subunit *d* homologue (Iwata *et al.* 2004). As in reconstructions from negative stain data, two peripheral stalk components of the stator, spaced 120° apart, extend down from the apex of A_1 to meet a horizontal collar. These ∼160 Å long structures appear to have only a small degree of left-hand curvature. The cryo-EM data allow organisation of the integral membrane subunits *a* and *c* to be visualised for the first time, permitting some insights into the proton translocating apparatus. Perhaps surprisingly, there is minimal contact between a bi-lobed *a* subunit membrane domain and the external surface of the subunit *c*-ring (Lau & Rubinstein, 2010), reminiscent of a gramophone needle touching a vinyl record. This contact with the *c*-ring presumably includes TMH 5 and 6 that contain residues likely to be in involved in ion translocation, based on the similarities to the V- and F-ATPase *a* subunits discussed above. We also note that the reconstructions of A-ATPases by Bernal & Stock (2004) and Vonck *et al.* (2009) display the same apparent handedness, with the horizontal collar extending clockwise

https://doi.org/10.1017/S0033583510000338 Published online by Cambridge University Press

from its contact with Stator 1 when the complex is viewed end-on to the A_1 domain. However, the absolute hand for these reconstructions was not determined. The alternative hand, shown for the *Pyrococcus* model in Fig. 5*b*, is consistent with the absolute hand determined for the *T. thermophilus* A-ATPase by Lau and Rubinstein using tilt pairs and the method of Rosenthal & Henderson (2003). We believe that this represents the correct hand for all A-ATPases, and the hand of the *Pyrococcus* A-ATPase reconstruction has been flipped in Fig. 5*b* to reflect this.

5.2.3 The V-ATPase – a stator model with three stalks and a collar

A consensus V-ATPase organisation has emerged only recently with improved 3D reconstructions. Yeast V-ATPase models generated from negative stain data (Diepholz *et al.* 2008a, b; Zhang *et al.* 2008) and for the V-ATPase from *M. sexta* larvae in vitrified ice (Muench *et al.* 2009) show three peripheral stalks (Fig. 5*c*). These form part of a stator complex that is appreciably more elaborate than that of either F- or A-ATPases, with all three stalks connecting to a horizontal collar that extends $\sim 250^\circ$ around the mid-section of the complex, substantially further than the comparable A-ATPase structure. This collar ties all three stators to the subunit *a* density in V_o. The lower region of each stalk is angled between 10° and 25°, consistent with the direction of twisting of the rotor and stators driven by ATP hydrolysis (Fig. 1*c*). In addition to the three knob-like NHR structures seen in all reconstructions of A- and V-ATPases, two other prominent features are evident in the V-ATPase. A prominent 'nose' that protrudes ~ 40 Å from the end of the collar where it meets Stator 1 (Fig. 5*c*) is proposed to be subunit H, a subunit unique to eukaryotic V-ATPases. The second feature is a ~ 35 Å protrusion from the bottom of V_o (exposed to the lumen of the endomembrane compartment, or extracellular). This feature may be peculiar to plasma membrane-localised V-ATPases, being seen in the bovine clathrin-coated vesicle (Wilkens *et al.* 1999) and *Manduca* enzymes but not in those from the yeast vacuolar membrane (Diepholz *et al.* 2008b; Zhang *et al.* 2008) or plant tonoplasts (Domgall *et al.* 2002). This density has been assigned to the glycosylated accessory subunit Ac45 (Supek *et al.* 1994; Wilkens *et al.* 1999), a polypeptide that associates with other V_o subunits in osteoclasts and appear to be involved in maintaining proton pumping activity (Feng *et al.* 2008). Although these observations support the assignment of Ac45 to this density, plasma membrane V-ATPases from epithelial cells are not recognised by antibodies to Ac45 (Supek *et al.* 1994), casting some doubt on the idea. Moreover, although genes for Ac45 homologues are present in insects, mass spectrometric analysis of the *Manduca* V-ATPase has not revealed its presence (Huss & Wieczorek, 2007).

5.3 Do the rotary ATPase membrane domains contain 'half channels'?

Is there any experimental evidence for the 'half channels' described in the Junge/Vik Brownian ratchet model (Junge *et al.* 1997; Vik & Antonio, 1994), in any class of rotary ATPase? Site-directed labelling of the *E. coli* F-ATPase subunit *a* has shown that sites predicted to be part-way down TMHs are reactive to aqueous phase reagents, suggesting the existence of water-accessible pores and consistent therefore with the presence of channels (Angevine & Fillingame, 2003; Angevine *et al.* 2007). Although no such data are available for the A- or V-ATPases, EM data do suggest the presence of pores. The reconstruction of the yeast V_o shows a pore-like depression on the lumenal/extracellular side (Wilkens & Forgac, 2001), and Diepholz *et al.* (2008a, b) have proposed that accessibility of heavy metal stain to an interior cavity in V_o of the intact yeast

https://doi.org/10.1017/S0033583510000338 Published online by Cambridge University Press

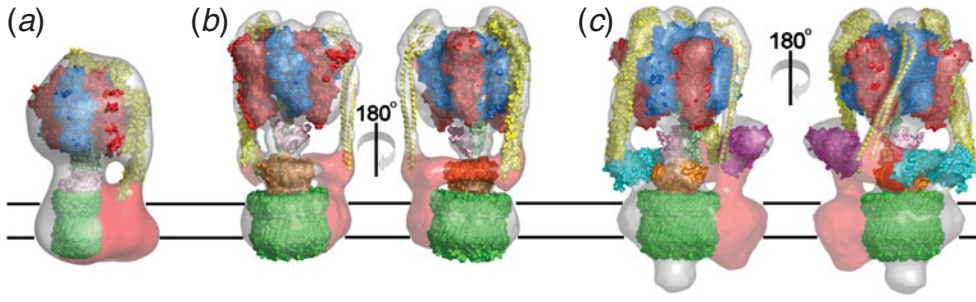


Fig. 6. Mosaic models of the rotary ATPases. Crystal structures are fitted to the 3D EM models in Fig. 5. (*a*) Mitochondrial F-ATPase with F_1-ATPase (pdb 2WSS) fitted, showing α and β subunits in blue and red, respectively. The *b*:*d*:F_6 stator sub-complex (pdb 2CLY; yellow) was fitted by superimposing it onto the backbones of the corresponding (incomplete) subunits in the 2WSS structure, with the angle of the lower stator adjusted to fit the EM density. The OSCP density from 2WSS is yellow. Fitting of the *E. coli* c_{10} ring model (pdb 1A91; green) was guided by the *c*-ring orientation in the yeast F_1-*c*10 structure (pdb 1Q01) as in Lau *et al.* (2008). (*b*) A-ATPase and (*c*) V-ATPase. Crystal structures fitted are the *T. thermophilus* $(AB)_3$:D:F complex (pdb 3A5D; A, red; B, blue; D, pale green; F, pink), E:G heterodimer in either spacefill or ribbon mode (pdb 3K5B; yellow), subunit *d* (pdb 1R5Z; orange) and *E. hirae* decameric *c*-ring (pdb 2DB4; dark green). Crystal structures of C (pdb 1U7L; cyan) and H (pdb 1HO8) are also fitted to the collar of the V-ATPase. Fitting was performed using Chimera and optimised by eye to accommodate available cross-linking data. Two views, rotated by 180°, are shown for A- and V-type complexes. Membrane domain regions coloured red are those for which no structural data are available.

V-ATPase suggests the presence of an aqueous pore. However, no pores are evident in cryo-EM models of A-ATPase or V-ATPase, and further structural and biochemical work will be needed to confirm their existence.

6. Fitting the pieces together – mosaic structures of the rotary ATPases

6.1 The structural model of the F-ATPase is almost complete

Recent 3D reconstructions from cryo-EM data and a wealth of supporting biochemical data, in particular, relating to subunit contacts, allow crystal structures of sub-complexes and individual component to be confidently fitted to give more complete models. This is particularly true of the mitochondrial F-ATPase, where there is extensive overlap between crystal structures for the yeast $(\alpha\beta)_3$:γ:δ_m:c_{10} (Stock *et al.* 1999; Dautant *et al.* 2010), the almost entirely complete membrane extrinsic part of the bovine complex (Rees *et al.* 2009) and the *b*:*d*:F_6:OSCP stator (Dickson *et al.* 2006). Optimal fitting of these structures to the cryo-EM reconstruction of the F-ATPase (Fig. 6*a*) requires removal of the inward curvature of the stator stalk which presumably occurs in the crystal structure of the membrane extrinsic region due to disconnection from the integral membrane segments of the *b* subunit (Rees *et al.* 2009). The stator tracks the non-catalytic α_{DP}/β_{TP} interface, making contacts exclusively with α at the apex of F_1, but near both α and β as it passes across the surface of F_1, consistent with cross-linking data (McLachlin *et al.* 2000). The areas of uncertainty are of course the membrane-embedded end of the stator comprising subunit *a* and the integral membrane region of subunit *b*. Crucially, lack of accurate structural models for this region limits our understanding of the organisation of the ion translocation pathway.

https://doi.org/10.1017/S0033583510000338 Published online by Cambridge University Press

6.2 Mosaic models of the A- and V-ATPases

A- and V-ATPases models are incomplete mosaics, with positioning of subunit and sub-complex crystal structures supported only by low-resolution biochemical data (Fig. 6*b, c*). However the quantity of this supporting data and quality of crystal structure fitting at least makes general positioning of subunits unambiguous, if not their precise orientations or conformations. As in the F-ATPase, the greatest uncertainty is in the *a* subunit that forms part of the stator and ion-translocation apparatus. The $(AB)_3$ and $(AB)_3$:D:F complexes fit well into both A- and V-ATPase reconstructions, facilitated by locating the three subunit A NHRs into the obvious protrusions in the EM maps (Fig. 6*b, c*). The incomplete crystal structure of the D:F axle does not reach the *d* subunit in the membrane domain, but contact in the complete A-ATPase is inferred from cross-linking between the upper rim of *d* and the F subunit (Iwata *et al.* 2004), an interaction almost certain to be conserved in the V-ATPase.

Fitting of the E:G stator sub-complex (Lee *et al.* 2010a) into A- and V-ATPase maps results in almost complete filling of the stalks linking the catalytic and membrane domains (Fig. 6*b, c*). In the A-ATPase, this places the N-terminal regions of two copies of E:G in contact with opposite ends of the ~110 Å-long horizontal arm which, by elimination, is likely to contain the soluble N-terminal domain of subunit *a* (a_N). The resulting interaction between a_N and either Stator 1 or 2 (as designated in Fig. 5) would account for the L-shaped complex formed when the *Enterococcus* homologues of E, G and a_N are co-expressed (Yamamoto *et al.* 2008). In the V-ATPase, cross-linking and protein interaction studies also indicate that both subunits E and G contact subunit *a* (Norgett *et al.* 2007; Qi & Forgac, 2008; Xu *et al.* 1999). There are clearly parallels between the A- and V-ATPases in terms of the connections between Stators 1 and 2 and the membrane domain. The contact between the C-terminal region of E and B that results from fitting of $(AB)_3$:D:F and E:G crystal structures is consistent with the contacts mapped by NMR chemical shift experiments (Kish-Trier & Wilkens, 2009b), but not with interactions with the A subunit detected fluorometrically (Biukovic *et al.* 2007).

In the A-ATPase model, the stator filaments descend from anchor points at the top of subunit B, but unlike in the F-ATPase, they do not follow the line of the non-catalytic subunit interface. Similar anchor points are evident in the V-ATPase, but the stators descend at an angle across the faces of the B subunits before crossing the lower regions of the non-catalytic A–B interfaces (Fig. 6*c*). Fitting of the E:G crystal structure suggests that the point at which the angle of each peripheral stalk changes corresponds to the flexion points suggested by Lee *et al.* (2010a). The position of E in the V-ATPase map is also consistent with chemical cross-linking to sites distributed across the surface of B (Arata *et al.* 2002). According to this arrangement of the E:G sub-complex, the C-terminal domain of E forms the primary contact with B, with the coiled coil region suspended below this but contributing little or nothing to binding to B. A temperature-sensitive mutation is sited in this region of the yeast subunit E (Fig. 3*a, b*; Zhang *et al.* 1998), indicating that thermal stability of the fold of this domain underpins its crucial role as an intermolecular linker. At current resolution, the membrane domain of the A-ATPase can accommodate either a dodecamer of 2 TMH units (Lau & Rubinstein, 2010), or a decamer of 4 TMH units (Vonck *et al.* 2009)), but the decameric complex is the best fit to V_o (Muench *et al.* 2009).

Models of the A- and V-ATPases differ at the horizontal collar, which in V-type reconstructions link the three stators (Fig. 5*c*). By analogy to the A-ATPase, part of this structure (linking Stators 1 and 2) should be the subunit *a* N-terminal domain (a_N: Fig. 1*c*), but this feature also accommodates the H and C subunits (Fig. 6*c*). The section of the collar between Stators 1 and 2

https://doi.org/10.1017/S0033583510000338 Published online by Cambridge University Press

is thicker than in the A-ATPase and has a projecting 'nose'. Positioning the H subunit crystal structure in this region, with its larger N-terminal domain within the nose, provides an excellent fit (Fig. 6*c*) and is consistent with data showing interaction with both subunit *a* (Diab *et al.* 2009; Landolt-Marticorena *et al.* 2000) and the N-terminal end of E (Lu *et al.* 2002). Thus, H lies along the cytoplasmic surface of a_N bound to Stator 1 (Fig. 8*a*). Subunit C is accommodated by the part of the horizontal collar linking Stators 2 and 3 (Fig. 6*c*), with its narrower 'head' in contact with Stator 3 and its broader 'foot' oriented towards Stator 2. Binding studies using truncated forms of C show that the 'head' region has a much greater affinity for E:G (Oot & Wilkens, 2010). Contact with the N-terminal regions of E and G at the foot of these stator elements is also consistent with cross-linking and protein interaction data (Féthière *et al.* 2005; Inoue & Forgac, 2005; Jones *et al.* 2005, 2010; Xu *et al.* 1999). A sub-complex comprising E, G and C adopts a similar L-shaped architecture to the A-ATPase E:G:a_N complex discussed above (Diepholz *et al.* 2008b), although it is unclear whether this represents a Stator 2-subunit C or Stator 3-subunit C model (or a mixture of both). Either sub-complex would have to undergo some conformational rearrangement in order to fit the corresponding stator-collar density in reconstructions of the intact enzymes (Diepholz *et al.* 2008b; Lee *et al.* 2010a). Stock and co-workers have pointed out that the V-ATPase subunit C is also an excellent fit to the horizontal arm that links the two stator stalks of the A-ATPase (Lee *et al.* 2010a). Does this mean that the two sections of the stator collar in the V-ATPase are actually broadly equivalent parts of a quasi-symmetrical 'wishbone' feature?

7. Unexplained features and unresolved questions

There are clearly major differences between the three rotary ATPases, particularly in the number and nature of the stator connections and in the coupling between the axle and *c*-ring of the rotor. If one accepts that the archaeal A-ATPase is closest to a common ancestral rotary ATPase, then several questions arise: Why did the V-ATPase evolve a triple stator connection, when it appears that mechanically two are adequate for both ATP-driven ion pumping and ATP synthesis? Similarly, why did the F-ATPase move to a single stator connection and evolve a different axle/*c*-ring coupling system? Clues to these may come from a more detailed examination of mechanics and regulation. In this section, we examine some of the questions and unexplained features arising from the EM models.

7.1 Is the isolated V-ATPase in a 'ground state' conformation?

In the improved models of A- and V-ATPases, authors have noted conformational variability between the three sectors of the A_1/V_1 domain corresponding to each A:B catalytic unit (Bernal & Stock, 2004; Diepholz *et al.* 2008a, b; Lau & Rubinstein, 2010). We have also noted this in the cryo-EM model of the *Manduca* V-ATPase. A horizontal section through the model where the D:F axle emerges from V_1 shows three densities corresponding to the bottom of each A subunit (Fig. 7*a*). The A:B interfaces closest to each of the three stators are non-catalytic. The A subunit adjacent to Stator 3 (s3) extends significantly further towards the membrane domain, suggesting that its conformation differs from that of the other two. By analogy to the F_1 and A_1 domain structures, it is likely that the two A:B units in similar conformations are those occupied by nucleotide ($(AB)_{DP}$ and $(AB)_{TP}$ in Fig. 7*a*), while the subunit extending closest to the membrane domain will be A_E, with its extended, open conformation (Diepholz *et al.* 2008a).

https://doi.org/10.1017/S0033583510000338 Published online by Cambridge University Press

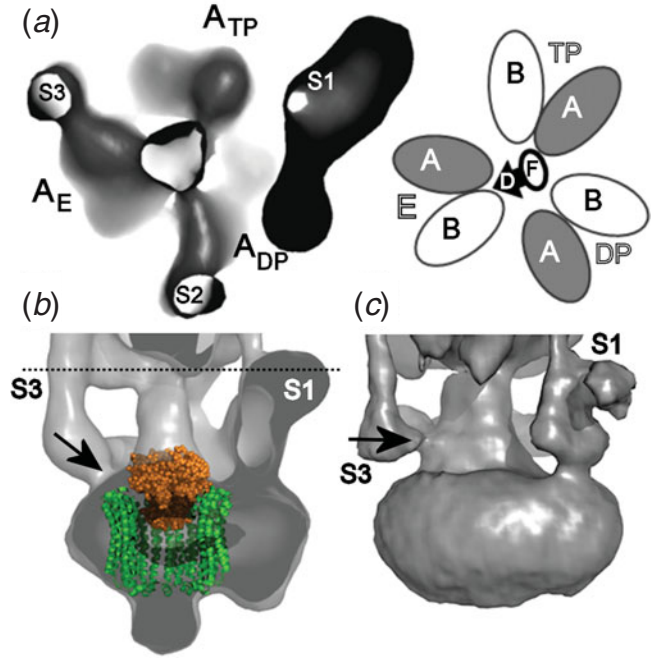


Fig. 7. Is purified V-ATPase in a homogeneous 'ground state'? (*a*) Left: lower surface of V_1 of the *Manduca* V-ATPase, viewed from the membrane. Locations of the three stator elements are indicated by s1–s3. The three densities radiating from the central axle represent the C-terminal domains of the three A subunits. The mass around s1 represents a section through part of the collar feature likely to contain the H subunit. Right: speculative arrangement of nucleotide-binding states of the active sites in V_1. Each A/B constitutes a catalytic unit, with the nucleotide-binding status of the active site at each A/B interface indicated by E ('empty'), DP (ADP and phosphate bound) or TP (ATP bound). D/F represents the axle of the V_1 motor. The convex face of the curved subunit D coiled-coil points towards the $(AB)_E$ site, indicated by the arrow, with the C-terminal domain of F closest to A_{TP}/B_{DP} (consistent with Numoto *et al.* 2009). Such a resting state ensures proximity of F to H, as discussed in the main text. ATP turnover would drive counter-clockwise rotation of the axle. 3D reconstructions of both (*b*) the *Manduca* and (*c*) *Saccharomyces* V-ATPases show apparent contact between the collar/Stator 3 (s3) junction and the *d*/*c*-ring region of the rotor (arrowed). In (*b*), a vertical section is shown to reveal fitting of the *c*-ring and subunit *d* as in Fig. 6. The dashed line represents the plane of the section shown in (*a*).

Since reconstruction involves classification and averaging of equivalent views, the presence of different A/B conformational states is indicative of two things: firstly, it is clear that the majority of particles in each EM dataset used to generate the 3D reconstructions of V-ATPases (and A-ATPases) must be in the same conformational state. Subtle differences in their catalytic domains could not be visualised without highly homogeneous specimen. The corollary of this is that, in the absence of ATP or membrane potential, the great majority of ATPases on the EM grid are in a single, stable 'ground state'. A second point is that the nucleotide occupancy of the three catalytic sites is likely to be different. In the *T. thermophilus* $(AB)_3$ crystal structure, all three active sites are in equivalent 'open' unoccupied states (Maher *et al.* 2009), but in the A_1 domain $(AB)_3$:D:F crystal structure the presence of bound nucleotide correlates with asymmetry between the catalytic units and different interactions with the D:F axle (Numoto *et al.* 2009). As in F_1-ATPase crystal structures, curvature of the lower region of the axle in the A_1 crystal structure points towards the 'empty' active site (A_E/B_E in Fig. 7*a*), with the major part of the F subunit

https://doi.org/10.1017/S0033583510000338 Published online by Cambridge University Press

sitting at the foot of the subunit D axle, below its concave surface and oriented closest to the A_{TP}/B_{DP} non-catalytic interface (Numoto *et al.* 2009) (Fig. 7*a*).

Matching the asymmetry in the A_1 (and F_1) crystal structure with that of the V-ATPase model allows us to determine the likely orientation of the D:F axle in the 'ground state' V-ATPase. From the orientation of axle subunits with respect to the A_E subunit in the A_1 structure, the concave face of D and F should face towards Stator 1 and the H subunit (Fig. 7*a*). Does this particular axle orientation have any significance? A uniform resting state may precede (and be a requirement for) the reversible domain dissociation that controls activity of some V-ATPases (Diepholz *et al.* 2008a, and discussed in the next section). In this case, the proposed axle orientation in the 'ground state' would mean that only minimal movement of subunit H would be required to bring about the contact with subunit F that occurs upon detachment and inactivation of the V_1 domain (Jefferies & Forgac, 2008). In the context of the structure of the membrane-extrinsic part of the F-ATPase, Rees *et al.* (2009) have also noted that the high degree of order in the crystals suggests a single predominant motor–stator conformation. However, fluorometric measurements of rotational movement in real time show that the F-ATPase rotor comes to rest in any one of three possible angular positions in the absence of nucleotide, or if catalytically 'frozen' by adding AMP-PNP (Zimmermann *et al.* 2005). This intrinsic heterogeneity may undermine attempts to achieve higher resolution EM reconstructions of the F-ATPase.

An anomaly of the V-ATPase models is that the region where Stator 3 joins the horizontal collar structure is apparently also in contact with the axle of the rotor, evident in both the *Manduca* (Fig. 7*b*) and *Saccharomyces* (Fig. 7*c*) enzymes from cryo-EM and negative stain data, respectively. This places the N-terminal ends of the E and G subunits of Stator 3 close to the upper rim of the *c*-ring and its subunit *d* plug (Fig. 7*b*). Although this contact is consistent with interaction between subunits G and *d in vitro* (Rishikesan *et al.* 2009), it clearly makes little sense mechanically since it ties together the rotor and stator parts of the motor. This potentially inhibitory contact may also reflect the existence of an inactive ground state in the purified V-ATPase, perhaps in response to the absence of substrate. Analysis of the complex trapped in catalytically active states may be needed to resolve this issue.

7.2 Is stator complexity linked to regulation?

A feature that distinguishes the V-ATPase from its A- and F-type cousins is sensitivity to low-energy status. In some cells, V-ATPases are major consumers of ATP, resulting in a strong need to switch off when ATP is low. This occurs via rapid and reversible detachment of V_1 from the membrane domain, a process that appears to be mediated via collar subunit C, and effected by subunit H. It is now possible to add more details to this mechanism while remaining consistent with available biochemical data. In active enzyme, H lies on top of the collar region presumed to be the N-terminal domain of subunit *a* (a_N) that links Stators 1 and 2 (Fig. 8*a*). In addition to a_N contacts, H also binds one or both of the α-helices of the E:G complex in Stator 1, perhaps via a groove that runs across its surface (Fig. 8*b*). Destabilisation of the C-subunit (as a result of, for example, phosphorylation) would in turn destabilise the a_N:C:H collar, causing the a_N domain to detach from H and the ends of Stators 1 and 2. Subunit H, no longer constrained by its association with a_N but still tethered to Stator 1, can change position such that its C-terminal domain binds to subunit F of the rotor (Diab *et al.* 2009; Jefferies & Forgac, 2008). This could involve rotation of the entire H subunit about Stator 1 by $\sim 30^\circ$ (Fig. 8*b*), which would apply

https://doi.org/10.1017/S0033583510000338 Published online by Cambridge University Press

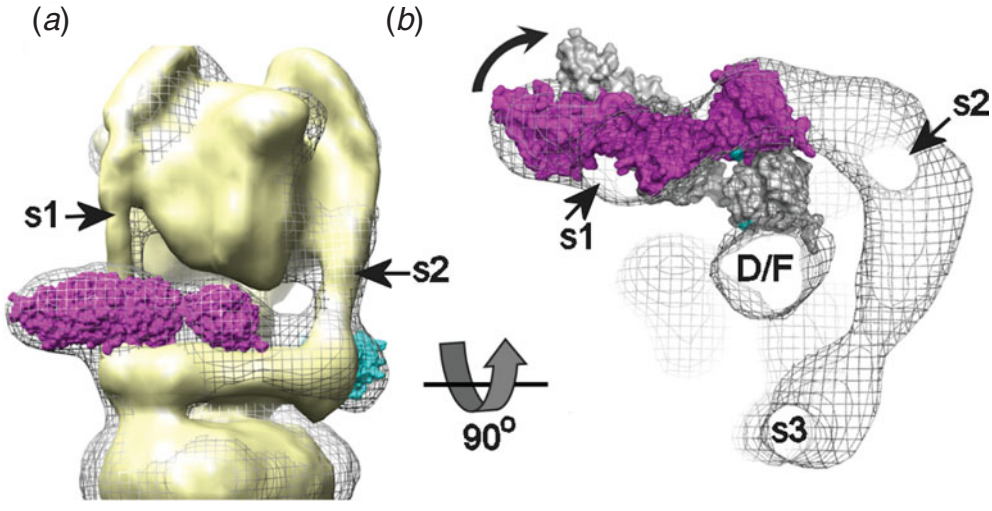


Fig. 8. Inactivation of V-ATPase by relocation of subunit H. (*a*) Superimposed models of the *Pyrococcus furiosus* A-ATPase (EMD-1542) and *Manduca* V-ATPase (EMD-1590) are shown as surface and mesh, respectively. In the V-ATPase model, additional density in the region of the horizontal collar that links Stators 1 and 2 (s1 and s2) accommodates subunit H (magenta: pdb 1ho8), with its larger N-terminal domain fitting into the projecting 'nose' of the collar and its C-terminal domain closest to Stator 2. In both A- and V-ATPases, this collar contains the N-terminal domain of subunit *a* (a_N). One end of subunit C (cyan: pdb 1u7l), fitted to the region of the collar linking Stator 2 to Stator 3, is also visible. (*b*) Model for inhibition of ATP turnover by V_1. The figure shows a horizontal section through the collar region of the *Manduca* model (grey mesh), viewed from the membrane domain. In the intact enzyme, subunit H (magenta) is constrained by contacts with a_N and is attached to Stator 1, perhaps via contacts across a groove on its surface. In the detached V_1 domain, H (grey) is no longer constrained by a_N, allowing it to rotate about its connection to Stator 1 (described by the curved arrow). Contact between the H C-terminal domain and the D:F axle prevents rotation and inhibits ATP turnover. Rotation of H by $\sim 30^\circ$ would bring it into direct contact with the axle. The residue shown in cyan is the location of the S381C mutation that cross-links to F in the detached yeast V_1.

torsion to the Stator 1 coiled-coil. Alternatively, the C-terminal domain of H alone could move, rotating about a flexible inter-domain linker. Locking the position of the rotor would have the effect of inhibiting catalytic cycling in $(AB)_3$, preventing futile ATP consumption. Relocation of a_N in V_o may also play a role in blocking the passive H^+ flow that would collapse any membrane potential, as discussed at the end of Section 5.1.

Diepholz *et al.* (2008a) argue that the complementarity needed to ensure efficient re-association of V_1 and V_o requires a uniform V_1 conformation prior to separation, or a switching mechanism that confers uniformity post-separation. According to the model in Fig. 7 and discussed above, in this conformation ATP- and ADP-occupied sites will be oriented closest to Stators 1 and 2, respectively. Controlled dissociation also requires turnover of ATP (Huss & Wieczorek, 2007), consistent with the idea that a limited number of catalytic steps is sufficient to drive all ATPases in the population into the single conformation state that permits dissociation. Such a state would ensure a uniform resting position for the D:F axle, hence the observed proximity of F to H in detached V_1 (Jefferies & Forgac, 2008) (Fig. 8*b*).

The role of subunits C and H in regulatory dissociation argues that evolution (or retention?) of three stator linkages in the eukaryotic V-ATPases is an adaptation allowing incorporation of additional regulatory features into the progenitor complex that presumably most closely

https://doi.org/10.1017/S0033583510000338 Published online by Cambridge University Press

resembled the '2-stalk stator' A-ATPase. It follows that if disconnection of Stator 3 from the network as a result of loss of subunit C is sufficient to completely destabilise V_1–V_o interaction, then the Stator 1 and Stator 2 linkages in the V-ATPase must be significantly weaker than the corresponding contacts in the A-ATPase, since the archaeal enzyme operates with only these two. The predominance of the Stator 3-subunit C contact in maintaining stator organisation in the V-ATPase fits with the high affinity between E:G and the subunit C 'head' reported by Oot & Wilkens (2010).

7.3 The motor asymmetry question

One of the most striking features of rotary ATPases is asymmetry between their ATPase and ion pump functions. Based on the stoichiometry of subunits in the catalytic domains and *c*-rings, a '3-stroke' ATPase may drive (or be energised by) 10–15 ion translocation events. Thus, the number of events linked to each 120° step (with 80°/40° sub-steps) in the catalytic domain can be non-integer. This also implies a non-integer $H^+(Na^+)$/ATP ratio for the coupled membrane that contains the ATPase, although measurements based purely on thermodynamics of ATP synthesis and its energising membrane potential suggest that this may not necessarily be the case (Steigmiller *et al.* 2008). In linear motors such as myosin, each ATP turnover is linked to a single power stroke that stems from a large conformational change, typically generating a force of magnitude $\sim$5 pN. In rotary ATPases, with non-integer H^+/ATP ratios, such a direct coupling is unlikely. Instead, a model involving some form of 'energy buffering' between the coupled motors is required which also does not compromise the extremely high efficiency of energy transfer. An elastic power transmission model has been proposed in which deformation of one or more flexible component buffers torque transmission (Cherepanov *et al.* 1999; Junge *et al.* 2009). This type of coupling is consistent with the smooth movement of the *c*-ring observed at low substrate concentrations. An advantage of this model is that it can accommodate the different *c*-ring stoichiometries. However, it does require an elastic component that presumably has a homologue in all rotary ATPases, since stoichiometry mismatch appears widespread.

7.3.1 Power transmission in the F-ATPase

Theoretical modelling and experiments on the F-ATPase have led to different proposals for this elastic element. These include the γ subunit left-handed coiled-coil (Capaldi *et al.* 2000), the peripheral stalk of the stator, and the β-sheet region of the β subunit that acts as a hinge to allow the lever movement of the C-terminal helical region (Sun *et al.* 2003). A role for winding/unwinding of γ in power transmission is supported by the shortening of F-ATPase particles observed by EM when Mg^{2+} and AMP-PNP are added (Capaldi *et al.* 2000). Flexibility of the stator stalk component is suggested by its curvature in reconstructions that appears to be compliant with the direction of rotation during ATP synthesis (Rubinstein *et al.* 2003) (Fig. 1*b*). However, several lines of evidence argue against stator elasticity. Firstly, in the mitochondrial stator, subunit *b* is reinforced by OSCP, *d* and F_6, suggesting a rigid structure (Fig. 3*d*). Potentially flexible points in the structure identified by Rees *et al.* (2009) (Fig. 3*c*) may not signify elasticity for the stator as a whole, but may instead allow flexing to accommodate catalytically driven conformational changes in the $(\alpha\beta)_3$ motor. Alternatively, applying force in a direction normal to the external surface of the *c*-ring may be important in maintaining its contact with subunit *a*.

https://doi.org/10.1017/S0033583510000338 Published online by Cambridge University Press

Even in the case of the bacterial stator, where the ability of subunit *b* to tolerate mutational additions or deletions implies flexibility (Sorgen *et al.* 1998, 1999), the implied side-to-side alignment of α-helices in the *b* dimer would restrict flexing, limiting its ability to contribute to power transmission. Secondly, compliance measurements indicate that the F-ATPase stator overall is relatively rigid, as is the γ subunit coiled-coil (Sielaff *et al.* 2008b). The region of the rotor comprising the $\gamma/\delta_m/\varepsilon_m$ 'foot' and *c*-ring extramembranous loops was identified as the most elastic and likely therefore to play a role in power transmission. An elastic power transmission model for the F-ATPase involving contributions from the β subunit hinge and rotor foot regions (but not the stator) therefore seems the most plausible.

7.3.2 Power transmission in the V- and A-ATPases

Can the same model be applied to V- and A-ATPases, or do the major differences in stator complexity and axle/*c*-ring coupling suggest a different mechanism? The currently unresolved 'foot' region of subunit D will be significantly smaller than its F-ATPase counterpart (<76 residues), and the A-ATPase homologue of *d* is a relatively compact structure, likely to be constrained by multiple contacts with the internal surface of the *c*-ring and axle. Neither is likely therefore to be functionally equivalent to the elastic components of the F-ATPase. Could the E:G stator elements contribute to power transmission? As with the F-ATPase *b* subunit, functionality of mutational insertions into subunit G implies tolerance of variations in length of this stator component (Charsky *et al.* 2000). However, molecular dynamics simulations and normal mode analysis indicate that α-helical coiled coils are very stiff for stretching, and somewhat less so for bending (Adamovic *et al.* 2008). The deformation energy associated with a $\sim$150 Å-long stator coiled coil with hendecad/quindecad repeat such as in E:G (<3·1 $k_BT\ nm^{-1}$) (Lee *et al.* 2010a) would be $\sim 2\times$ the energy associated with hydrolysis of each ATP molecule (Wolgemuth & Sun, 2006). Thus, it appears that in the A-/V-ATPase, the peripheral stalk components of the stator are relatively rigid. The structures contributing to elastic power transmission in these ATPases therefore remain unclear.

We can speculate about the evolutionary drivers for divergence in stator organisation in all three ATPases. In the eukaryotes, retention of three peripheral stalks of similar structure to those in A-ATPases facilitated incorporation of a regulatory system into the stator of the rotary motor that allowed activity to be linked to the energetic status of the cell. F-ATPases from both bacteria and organelles adapted differently, reinforcing the single remaining stator (albeit by different means). F-ATPases appear to operate with a higher average rotor torque than either the A- or V-ATPases, so this may be an adaptation in response to a need for greater mechanical robustness. This could also be the driving force for changes to the rotor/*c*-ring coupling.

8. Future directions

The last dozen years or so have revolutionised understanding of rotary ATPases. The direct demonstration of rotary motion during ATP hydrolysis has now evolved into simultaneous observation of rotation and changes in catalytic conformation or substrate/product turnover (Masaike *et al.* 2008; Nishizaka, 2004). Understanding of the structures of F_1 in different states, peripheral stator components and *c*-ring parts has also developed. Notwithstanding difficulties in correlating F_1-ATPase crystal structures with catalytic states determined biophysically

https://doi.org/10.1017/S0033583510000338 Published online by Cambridge University Press

(Okuno *et al.* 2008; Sielaff *et al.* 2008a), this has led to much more detailed models of the F_1-ATPase mechanism, although grey areas remain. Within the last year, the first A-ATPase sub-complex structures have become available. Recent history has shown that accurate, experimentally verifiable models of transport processes emerge when complete high resolution structures become available (Vinothkumar & Henderson, 2010). A key area of focus over the next few years must be the structure and function of the ion pump part of the rotary ATPases in order to understand membrane potential-powered ATP synthesis. We can anticipate that complete high resolution structures for the rotary ATPases will lead to verifiable models of proton pumping in A_o and V_o, and torque generation by the F_o electromotor. This may help reveal the basis for apparently variable H^+/ATP ratios and different gearing ratios shown by members of the rotary ATPase family.

To date, the primary role of EM in the study of the rotary ATPases has been to provide a low-resolution overview of organisation of the complexes, and to put crystal structures of sub-complexes and biochemical data into macromolecular context. However, despite enormous progress on the high resolution structures of extramembranous parts of the ATPases, EM has provided what is still the only insight into the structure of the crucial subunit *a*/*c*-ring interface (Lau & Rubinstein, 2010). In the absence of complete crystal structures, improved resolution of cryo-EM models should provide further insight into structure–function relationships in the proton pumps. Even for these relatively small, asymmetrical objects, the sub-10 Å resolution that will allow secondary structure to be seen is already feasible, although not technically trivial (Henderson, 2004). One of the most exciting applications for EM is time-resolved cryo-EM, allowing determination of natural conformations trapped $<$10 ms after introduction of substrates or inhibitors (Berriman & Unwin, 1994; White *et al.* 2003). This approach has already proved successful when applied to the analysis of conformational states of linear motors. Supported by computational methods that allow multiple conformers to be determined from single large datasets (Elad *et al.* 2008; Penczek *et al.* 2006; Scheres *et al.* 2006), this approach has the potential to demonstrate directly the structural changes that would allow discrimination between different models of power transmission. A temporal sequence of conformational states can provide constraints for mechanical simulations beyond the microsecond time domain that represents the current practical limit of molecular dynamics simulations.

The rotary ATPases are highly efficient energy conversion machines that have the remarkable ability to link the chemical and electrical energy on which life depends. The evolutionary processes that coupled together two essentially autonomous ancestral motors to give these energy converters has included revisions and adaptations that give specialisations adapted to work under particular physiological conditions and environmental pressures. With recent complete and accurate 3D models of all three rotary ATPases, we can start to draw direct comparisons between their structure/function relationships. In terms of the overall architecture of the complexes, knowledge of the A- and V-ATPases has certainly caught up with the F-ATPase, although this is not yet supported by the same wealth of functional, mechanistic and high resolution structural data. It seems clear that the additional complexity of the V-ATPase allows relatively sophisticated regulation. Where synthase and ion pump functions are represented by a single structural type, as in the A-ATPase, adaptation that maximises operational efficiency in a particular direction may be solely to do with the type of rotor ring subunit it employs. The big challenges are to see the workings of the ion translocation apparatus at atomic resolution and to characterise the mechanical changes that occur in asymmetrically coupled operation.

https://doi.org/10.1017/S0033583510000338 Published online by Cambridge University Press

9. Acknowledgements

We are grateful to Janet Vonck for providing the *Pyrococcus* A-ATPase reconstruction prior to database release, and to Helmut Wieczorek and Markus Huss for comments on the manuscript. Work in the laboratories of M. A. H. and J. T. was supported by the UK BBSRC (BB/D016142). S. P. M. has an MRC Career Development fellowship.

10. References

Abrahams, J. P., Leslie, A. G., Lutter, R. & Walker, J. E. (1994). Structure at 2·8 Å resolution of F_1-ATPase from bovine heart mitochondria. *Nature* **370**, 621–628.

Adamovic, I., Mijailovich, S. M. & Karplus, M. (2008). The elastic properties of the structurally characterized Myosin II S2 subdomain: a molecular dynamics and normal mode analysis. *Biophysical Journal* **94**, 3779–3789.

Aggeler, R., Ogilvie, I. & Capaldi, R. (1997). Rotation of the gamma-epsilon subunit domain in the *Escherichia coli* F_1F_0-ATP synthase complex. *Journal of Biological Chemistry* **272**, 19621–19624.

Angevine, C. M. & Fillingame, R. H. (2003). Aqueous access channels in subunit *a* of rotary ATP synthase. *Journal of Biological Chemistry* **278**, 6066–6074.

Angevine, C. M., Herold, K. A. G., Vincent, O. D. & Fillingame, R. H. (2007). Aqueous access pathways in ATP synthase subunit *a* - Reactivity of cysteine substituted into transmembrane helices 1, 3, and 5. *Journal of Biological Chemistry* **282**, 9001–9007.

Arai, A., Terres, G., Pink, S. & Forgac, M. (1988). Topography and subunit stoichiometry of the coated vesicle proton pump. *Journal of Biological Chemistry* **263**, 8796–8802.

Arata, Y., Baleja, J. D. & Forgac, M. (2002). Cysteine-directed cross-linking to subunit B suggests that subunit E forms part of the peripheral stalk of the vacuolar H^+-ATPase. *Journal of Biological Chemistry* **277**, 3357–3363.

Ariga, T., Muneyuki, E. & Yoshida, M. (2007). F_1-ATPase rotates by an asymmetric, sequential mechanism using all three catalytic subunits. *Nature Structural and Molecular Biology* **14**, 841–846.

Arnold, I., Pfeiffer, K., Neupert, W., Stuart, R. A. & Schägger, H. (1998). Yeast mitochondrial F_1F_0-ATP synthase exists as a dimer: identification of three dimer-specific subunits. *EMBO Journal* **17**, 7170–7178.

Arselin, G., Giraud, M. F., Dautant, A., Vaillier, J., Brethes, D., Coulary-Salin, B., Schaeffer, J. & Velours, J. (2003). The GxxxG motif of the transmembrane domain of subunit e is involved in the dimerization/oligomerization of the yeast ATP synthase complex in the mitochondrial membrane. *European Journal of Biochemistry* **270**, 1875–1884.

Baker, L. A. & Rubinstein, J. L. (2008). Angle determination for side views in single particle electron microscopy. *Journal of Structural Biology.* **162**, 468–477.

Ballhausen, B., Altendorf, K. & Deckers-Hebestreit, G. (2009). Constant c(10) ring stoichiometry in the *Escherichia coli* ATP synthase analyzed by cross-linking. *Journal of Bacteriology* **191**, 2400–2404.

Bandyopadhyay, S. & Allison, W. S. (2004). The ionic track in the F_1-ATPase from the thermophilic bacillus PS3. *Biochemistry* **43**, 2533–2540.

Bauerle, C., Ho, M. N., Lindorfer, M. A. & Stevens, T. H. (1993). The *Saccharomyces cerevisiae VMA6* gene encodes the 36-kDa subunit of the vacuolar H(+)-ATPase membrane sector. *Journal of Biological Chemistry* **268**, 12749–12757.

Belogrudov, G. I., Tomich, J. M. & Hatefi, Y. (1996). Membrane topography and near-neighbor relationships of the mitochondrial ATP synthase subunits e, f, and g. *Journal of Biological Chemistry* **271**, 20340–20345.

Béltran, C. & Nelson, N. (1992). The membrane sector of vacuolar H(+)-ATPase by itself is impermeable to protons. *Acta Physiologica Scandinavica* **607**, 41–47.

Bernal, R. A. & Stock, D. (2004). Three-dimensional structure of the intact *Thermus thermophilus* H^+-ATPase/synthase by electron microscopy. *Structure* **12**, 1789–1798.

Berriman, J. & Unwin, N. (1994). Analysis of transient structures by cryo-microscopy combined with rapid mixing of spray droplets. *Ultramicroscopy* **56**, 241–252.

Biegel, E. & Müller, V. (2010). Bacterial Na^+-translocating ferredoxin: NAD(+) oxidoreductase. *Proceedings of the National Academy of Sciences of the United States of America* **107**, 18138–18142.

Biukovic, G., Rossle, M., Gayen, S., Mu, Y. & Grüber, G. (2007). Small-angle x-ray scattering reveals the solution structure of the peripheral stalk subunit H of the A_1A_0 ATP synthase from *Methanocaldococcus jannaschii* and its binding to the catalytic A subunit. *Biochemistry* **46**, 2070–2078.

Blair, H. C., Teitelbaum, S. L., Ghiselli, R. & Gluck, S. (1989). Osteoclastic bone resorption by a polarized vacuolar proton pump. *Science* **245**, 855–857.

Boekema, E. J., Ubbink-Kok, T., Lolkema, J. S., Brisson, A. & Konings, W. N. (1997). Visualisation of a peripheral stalk in V-type ATPases: evidence for the stator structure essential to rotational catalysis. *Proceedings of the National Academy of Sciences of the United States of America* **94**, 14291–14293.

https://doi.org/10.1017/S0033583510000338 Published online by Cambridge University Press

Boekema, E. J., van Breemen, J. F. L., Brisson, A., Ubbink-Kok, T., Konings, W. N. & Lolkema, J. S. (1999). Biological motors: connecting stalks in V-type ATPase. *Nature* **401**, 37–38.

Bond, A. & Forgac, M. (2008). The Ras/cAMP/protein kinase A pathway regulates glucose-dependent assembly of the vacuolar (H+)-ATPase in yeast. *Journal of Biological Chemistry* **283**, 36513–36521.

Böttcher, B., Bertsche, I., Reuter, R. & Gräber, P. (2000). Direct visualisation of conformational changes in EF_0F_1 by electron microscopy. *Journal of Molecular Biology* **296**, 449–457.

Böttcher, B. & Gräber, P. (2000). The structure of the H+-ATP synthase from chloroplasts and its subcomplexes as revealed by electron microscopy. *Biochimica et Biophysica Acta – Bioenergetics* **1458**, 404–416.

Böttcher, B., Schwarz, L. & Gräber, P. (1998). Direct indication for the existence of a double stalk in CF_0F_1. *Journal of Molecular Biology* **281**, 757–762.

Bowler, M. W., Montgomery, M. G., Leslie, A. G. & Walker, J. E. (2006). How azide inhibits ATP hydrolysis by the F-ATPases. *Proceedings of the National Academy of Sciences of the United States of America* **103**, 8646–8649.

Bowler, M. W., Montgomery, M. G., Leslie, A. G. & Walker, J. E. (2007). Ground state structure of F_1-ATPase from bovine heart mitochondria at 1·9 A resolution. *Journal of Biological Chemistry* **282**, 14238–14242.

Bowman, B. J. & Bowman, E. J. (2002). Mutations in subunit *c* of the vacuolar ATPase confer resistance to bafilomycin and identify a conserved antibiotic binding site. *Journal of Biological Chemistry* **277**, 3965–3972.

Bowman, B. J., Dschida, W. J., Harris, T. & Bowman, E. J. (1989). The vacuolar ATPase of *Neurospora crassa* contains an F_1-like structure. *Journal of Biological Chemistry* **264**, 15606–15612.

Boyer, P. D. (1997). The ATP synthase – a splendid molecular machine. *Annual Review of Biochemistry.* **66**, 717–749.

Breton, S., Smith, P. J. S., Lui, B. & Brown, D. (1996). Acidification of the male reproductive tract by a proton pumping (H+)-ATPase. *Nature Medicine* **2**, 470–472.

Brown, D., Gluck, S. & Hartwig, J. (1987). Structure of the novel membrane-coating material in proton-secreting epithelial cells and identification as an H^+ATPase. *Journal of Cell Biology* **105**, 1637–1648.

Brown, D., Paunescu, T. G., Breton, S. & Marshansky, V. (2009). Regulation of the V-ATPase in kidney epithelial cells: dual role in acid-base homeostasis and vesicle trafficking. *Journal of Experimental Biology* **212**, 1762–1772.

Bulygin, V. V., Duncan, T. M. & Cross, R. L. (2004). Rotor/stator interactions of the epsilon subunit in *Escherichia coli* ATP synthase and implications for enzyme regulation. *Journal of Biological Chemistry* **279**, 35616–35621.

Bustos, D. M. & Velours, J. (2005). The modification of the conserved GXXXG motif of the membrane-spanning segment of subunit g destabilizes the supramolecular species of yeast ATP synthase. *Journal of Biological Chemistry* **280**, 29004–29010.

Cabezón, E., Montgomery, M. G., Leslie, A. G. & Walker, J. E. (2003). The structure of the bovine F_1-ATPase in complex with its regulatory protein IF_1. *Nature Structural Biology* **10**, 744–750.

Cain, B. D. (2000). Mutagenic analysis of the F_0 stator subunits. *Journal of Bioenergetics and Biomembranes* **32**, 365–371.

Cain, B. D. & Simoni, R. D. (1989). Proton translocation by the F_1F_0ATPase of *Escherichia coli*. Mutagenic analysis of the a subunit. *Journal of Biological Chemistry* **264**, 3292–3300.

Campanella, M., Parker, N., Tan, C. H., Hall, A. M. & Duchen, M. R. (2009). IF_1: setting the pace of the F_1F_0-ATP synthase. *Trends in Biochemical Science* **34**, 343–350.

Capaldi, R. A. & Aggeler, R. (2002). Mechanism of the F_1F_0-type ATP synthase, a biological rotary motor. *Trends in Biochemical Science* **27**, 154–160.

Capaldi, R. A., Schulenberg, B., Murray, J. & Aggeler, R. (2000). Cross-linking and electron microscopy studies of the structure and functioning of the *Escherichia coli* ATP synthase. *Journal of Experimental Biology* **203**, 29–33.

Carbajo, R. J., Kellas, F. A., Yang, J. C., Runswick, M. J., Montgomery, M. G., Walker, J. E. & Neuhaus, D. (2007). How the N-terminal domain of the OSCP subunit of bovine F_1F_0-ATP synthase interacts with the N-terminal region of an α subunit. *Journal of Molecular Biology* **368**, 310–318.

Chan, T. L., Greenawalt, J. W. & Pedersen, P. L. (1970). Biochemical and ultrastructural properties of a mitochondrial inner membrane fraction deficient in outer membrane and matrix activities. *Journal of Cell Biology* **45**, 291–305.

Charsky, C. M. H., Schumann, N. J. & Kane, P. M. (2000). Mutational analysis of subunit G (Vma10p) of the yeast vacuolar H^+-ATPase. *Journal of Biological Chemistry* **275**, 37232–37239.

Cherepanov, D. A., Mulkidjanian, A. Y. & Junge, W. (1999). Transient accumulation of elastic energy in proton translocating ATP synthase. *FEBS Letters* **449**, 1–6.

Clare, D. K., Orlova, E. V., Finbow, M. E., Harrison, M. A., Findlay, J. B. C. & Saibil, H. R. (2006). An expanded and flexible form of the vacuolar ATPase membrane sector. *Structure* **14**, 1149–1156.

Coskun, Ü., Chaban, Y. L., Lingl, A., Müller, V., Keegstra, W., Boekema, E. J. & Grüber, G. (2004). Structure and subunit arrangement of the A-type ATP synthase complex from the archaeon *Methanococcus jannaschii* visualized by electron microscopy. *Journal of Biological Chemistry* **279**, 38644–38648.

https://doi.org/10.1017/S0033583510000338 Published online by Cambridge University Press

Couoh-Cardel, S. J., Uribe-Carvajal, S., Wilkens, S. & García-Trejo, J. J. (2010). Structure of dimeric F_1F_O-ATP synthase. *Journal of Biological Chemistry* **285**, 36447–36455.

Dautant, A., Velours, J. & Giraud, M. F. (2010). Crystal structure of the Mg.ADP-inhibited state of the yeast F_1c_{10}-ATP synthase. *Journal of Biological Chemistry* **285**, 29502–29510.

Davies, J. M., Hunt, I. E. & Sanders, D. (1994). Vacuolar H(+)-pumping ATPase variable transport coupling ratio controlled by pH. *Proceedings of the National Academy of Sciences of the United States of America* **91**, 8547–8551.

Davis-Kaplan, S. R., McVey Ward, D., Shiflett, S. L. & Kaplan, J. (2004). Genome-wide analysis of iron-dependent drowth reveals a novel yeast gene required for vacuolar acidification. *Journal of Biological Chemistry* **279**, 4322–4329.

Devenish, R. J., Prescott, M. & Rodgers, A. J. W. (2008). The structure and function of mitochondrial F_1F_0-ATP synthases. *International Reviews of Cell and Molecular Biology* **267**, 1.

Diab, H., Ohira, M., Liu, M., Cobb, E. & Kane, P. M. (2009). Subunit interactions and requirements for inhibition of the yeast V_1-ATPase. *Journal of Biological Chemistry* **284**, 13316–13325.

Dickson, V. K., Silvester, J. A., Fearnley, I. M., Leslie, A. G. & Walker, J. E. (2006). On the structure of the stator of the mitochondrial ATP synthase. *EMBO Journal* **25**, 2911–2918.

Diepholz, M., Börsch, M. & Böttcher, B. (2008a). Structural organization of the V-ATPase and its implications for regulatory assembly and disassembly. *Biochemical Society Transactions* **36**, 1027–1031.

Diepholz, M., Venzke, D., Prinz, S., Batisse, C., Flörchinger, B., Rössle, M., Svergun, D. I., Böttcher, B. & Féthière, J. (2008b). A different conformation for EGC stator subcomplex in solution and in the assembled yeast V-ATPase: possible implications for regulatory disassembly. *Structure* **16**, 1789–1798.

Diez, M., Zimmermann, B., Börsch, M., Konig, M., Schweinberger, E., Steigmiller, S., Reuter, R., Felekyan, S., Kudryavtsev, V., Seidel, C. A. M. & Gräber, P. (2004). Proton-powered subunit rotation in single membrane-bound F_0F_1-ATP synthase. *Nature Structural and Molecular Biology* **11**, 135–141.

Dimroth, P., Von Ballmoos, C. & Meier, T. (2006). Catalytic and mechanical cycles in F-ATP synthases: fourth in the cycles review series. *EMBO Reports* **7**, 276–282.

Dixon, N., Pali, T., Kee, T. P., Ball, S., Harrison, M. A., Findlay, J. B. C., Nyman, J., Väänänen, K., Finbow, M. E. & Marsh, D. (2008). Interaction of spin-labeled inhibitors of the vacuolar H+-ATPase with the transmembrane V_0-sector. *Biophysical Journal* **94**, 506–514.

Dixon, N., Pali, T., Kee, T. P. & Marsh, D. (2004). Spin-labelled vacuolar-ATPase inhibitors in lipid membranes. *Biochimica et Biophysica Acta* **1665**, 177–183.

Domgall, I., Venzke, D., Luttge, U., Ratajczak, R. & Böttcher, B. (2002). Three-dimensional map of a plant V-ATPase based on electron microscopy. *Journal of Biological Chemistry* **277**, 13115–13121.

Drory, O., Frolow, F. & Nelson, N. (2004). Crystal structure of yeast V-ATPase subunit C reveals its stator function. *EMBO Reports* **5**, 1148–1152.

Duncan, T. M., Bulygin, V. V., Zhou, Y., Hutcheon, M. L. & Cross, R. L. (1995). Rotation of subunits during catalysis by *Escherichia coli* F1- ATPase. *Proceedings of the National Academy of Sciences of the United States of America* **92**, 10964–10968.

Dunn, S. D., Revington, M., Cipriano, D. J. & Shilton, B. H. (2000). The b-subunit of *Escherichia coli* ATP synthase. *Journal of Bioenergetics & Biomembranes* **32**, 347–355.

Elad, N., Clare, D. K., Saibil, H. R. & Orlova, E. V. (2008). Detection and separation of heterogeneity in molecular complexes by statistical analysis of their two-dimensional projections. *Journal of Structural Biology* **162**, 108–120.

Elston, T., Wang, H. & Oster, G. (1998). Energy transduction in ATP synthase. *Nature* **391**, 510–513.

Esteban, O., Bernal, R. A., Donohoe, M., Videler, H., Sharon, M., Robinson, C. V. & Stock, D. (2008). Stoichiometry and localization of the stator subunits E and G in *Thermus thermophilus* H^+-ATPase/synthase. *Journal of Biological Chemistry* **283**, 2595–2603.

Feng, H., Cheng, T., Pavlos, N. J., Yip, K. H. M., Carrello, A., Seeber, R., Eidne, K., Zheng, M. H. & Xu, J. (2008). Cytoplasmic terminus of vacuolar type proton pump accessory subunit Ac45 is required for proper interaction with V_0 domain subunits and efficient osteoclastic bone resorption. *Journal of Biological Chemistry* **283**, 13194–13204.

Feniouk, B. A., Kato-Yamada, Y., Yoshida, M. & Suzuki, T. (2010). Conformational transitions of subunit ε in ATP synthase from thermophilic Bacillus PS3. *Biophysical Journal* **98**, 434–442.

Féthière, J., Venzke, D., Diepholz, M., Seybert, A., Geerlof, A., Gentzel, M., Wilm, M. & Böttcher, B. (2004). Building the stator of the yeast vacuolar-ATPase: specific interaction between subunits E and G. *Journal of Biological Chemistry* **279**, 40670–40676.

Féthière, J., Venzke, D., Madden, D. R. & Böttcher, B. (2005). Peripheral stator of the yeast V-ATPase: stoichiometry and specificity of interaction between the EG complex and subunits C and H. *Biochemistry* **44**, 15906–15914.

Fillingame, R. H., Angevine, C. M. & Dmitriev, O. Y. (2002). Coupling proton movements to c-ring rotation in F_1F_0 ATP synthase: aqueous access channels and

https://doi.org/10.1017/S0033583510000338 Published online by Cambridge University Press

helix rotations at the a-c interface. *Biochimica et Biophysica Acta* **1555**, 29–36.

Forgac, M. (2007). Vacuolar ATPases: rotary proton pumps in physiology and pathophysiology. *Nature Reviews Molecular and Cellular Biology* **8**, 917–929.

Frattini, A., Orchard, P. J., Sobacchi, C., Giliani, S., Abinun, M., Mattsson, J. P., Keeling, D. J., Andersson, A. K., Wallbrandt, P., Zecca, L., Notarangelo, L. D., Vezzoni, P. & Villa, A. (2000). Defects in TCIRG1 subunit of the vacuolar proton pump are responsible for a subset of human autosomal recessive osteopetrosis. *Nature Genetics* **25**, 343–346.

Fritz, M., Klyszejko, A. L., Morgner, N., Vonck, J., Brutschy, B., Muller, D. J., Meier, T. & Müller, V. (2008). An intermediate step in the evolution of ATPases – a hybrid F_0-V_0 rotor in a bacterial Na^+ F_1F_0 ATP synthase. *FEBS Journal* **275**, 1999–2007.

Furuike, S., Hossain, M. D., Maki, Y., Adachi, K., Suzuki, T., Kohori, A., Itoh, H., Yoshida, M. & Kinosita Jr. K. (2008). Axle-less F_1-ATPase rotates in the correct direction. *Science* **319**, 955–958.

Futai, M., Omote, H., Sambongi, Y. & Wada, Y. (2000). Synthase (H+ ATPase): coupling between catalysis, mechanical work, and proton translocation. *Biochimica et Biophysica Acta – Bioenergetics* **1458**, 276–288.

Gibbons, C., Montgomery, M. G., Leslie, A. G. W. & Walker, J. E. (2000). The structure of the central stalk in bovine F_1-ATPase at 2·4 Å resolution. *Nature Structural and Molecular Biology* **7**, 1055–1061.

Gogol, E. P., Johnston, E., Aggeler, R. & Capaldi, R. A. (1990). Ligand-dependent structural variations in *Escherichia coli* F_1 ATPase revealed by cryoelectron microscopy. *Proceedings of the National Academy of Sciences of the United States of America* **87**, 9585–9589.

Gräf, R., Harvey, W. R. & Wieczorek, H. (1996). Purification and properties of a cytosolic V_1-ATPase. *Journal of Biological Chemistry* **271**, 20908–20913.

Gregorini, M., Wang, J., Xie, X. S., Milligan, R. A. & Engel, A. (2007). Three-dimensional reconstruction of bovine brain V-ATPase by cryo-electron microscopy and single particle analysis. *Journal of Structural Biology* **158**, 445–454.

Grüber, G., Radermacher, M., Ruiz, T., Godovac-Zimmermann, J., Canas, B., Kleine-Kohlbrecher, D., Huss, M., Harvery, W. R. & Wieczorek, H. (2000). Three-dimensional structure and subunit topology of the V_1 ATPase from *Manduca sexta* midgut. *Biochemistry* **39**, 8609–8616.

Grüber, G., Svergun, D. I., Coskun, Ü., Lemker, T., Koch, M. H. J., Schägger, H. & Müller, V. (2001a). Structural insights into the A_1 ATPase from the archaeon, *Methanosarcina mazei* Gö1. *Biochemistry* **40**, 1890–1896.

Grüber, G., Wieczorek, H., Harvey, W. R. & Müller, V. (2001b). Structure–function relationships of A-, F- and V-ATPases. *Journal of Experimental Biology* **204**, 2597–2605.

Hara, K. Y., Kato-Yamada, Y., Kikuchi, Y., Hisabori, T. & Yoshida, M. (2001). The Role of the β DELSEED motif of F_1-ATPase: propagation of the inhibitory effect of the ε subunit. *Journal of Biological Chemistry* **276**, 23969–23973.

Hara, K. Y., Noji, H., Bald, D., Yasuda, R., Kinosita, K. & Yoshida, M. (2000). The role of the DELSEED motif of the β subunit in rotation of F_1-ATPase. *Journal of Biological Chemistry* **275**, 14260–14263.

Harrison, M. A., Durose, L., Song, C. F., Barratt, E., Trinick, J., Jones, R. & Findlay, J. B. C. (2003). Structure and function of the vacuolar H^+-ATPase: moving from low resolution models to high resolution structures. *Journal of Bioenergetics and Biomembranes* **35**, 337–345.

Häsler, K., Pänke, O. & Junge, W. (1999). On the stator of rotary ATP synthase: the binding strength of subunit δ to $(\alpha\beta)_3$ as determined by fluorescence correlation spectroscopy. *Biochemistry* **38**, 13759–13765.

Hausrath, A. C., Capaldi, R. A. & Matthews, B. W. (2001). The conformation of the ε and g-subunits within the *Escherichia coli* F_1 ATPase. *Journal of Biological Chemistry* **276**, 47227–47232.

Henderson, R. (2004). Realizing the potential of electron cryo-microscopy. *Quarterly Reviews of Biophysics* **37**, 3–13.

Hilario, E. & Gogarten, J. P. (1998). The prokaryote-to-eukaryote transition reflected in the evolution of the V/F/A-ATPase catalytic and proteolipid subunits. *Journal of Molecular Evolution* **46**, 703–715.

Hinton, A., Sennoune, S. R., Bond, S., Fang, M., Reuveni, M., Sahagian, G. G., Jay, D., Martinez-Zaguilan, R. & Forgac, M. (2009). Function of a subunit isoforms of the V-ATPase in pH homeostasis and in vitro invasion of MDA-MB231 human breast cancer cells. *Journal of Biological Chemistry* **284**, 16400–16408.

Hirata, T., Iwamoto-Kihara, A., Sun-Wada, G. H., Okajima, T., Wada, Y. & Futai, M. (2003). Subunit rotation of vacuolar-type proton pumping ATPase: relative rotation of the G and *c* subunits. *Journal of Biological Chemistry* **278**, 23714–23719.

Hirata, T., Nakamura, N., Omote, H., Wada, Y. & Futai, M. (2000). Regulation and reversibility of vacuolar H^+-ATPase. *Journal of Biological Chemistry* **275**, 386–389.

Hochstein, L. I. & Stan-Lotter, H. (1992). Purification and properties of an ATPase from *Sulfolobus solfataricus*. *Archives of Biochemistry and Biophysics* **295**, 153–160.

Hofmann, K. & Stoffel, W. (1993). TMbase – a database of membrane spanning proteins segments. *Biological Chemistry Hoppe-Seyler* **374**, 166–173.

Hong-Hermesdorf, A., Brux, A., Grüber, A., Grüber, G. & Schumacher, K. (2006). A WNK kinase binds and phosphorylates V-ATPase subunit C. *FEBS Letters* **580**, 932–939.

https://doi.org/10.1017/S0033583510000338 Published online by Cambridge University Press

Hunt, I. E. & Bowman, B. J. (1997). The intriguing evolution of the b and G subunits in F-type and V-type ATPases: isolation of the vma-10 gene from *Neurospora crassa*. *Journal of Bioenergetics and Biomembranes* **29**, 533–540.

Huss, M., Ingenhorst, G., Konig, S., Gassel, M., Drose, S., Zeeck, A., Altendorf, K. & Wieczorek, H. (2002). Concanamycin A, the specific inhibitor of V-ATPases, binds to the V_0 subunit *c*. *Journal of Biological Chemistry* **277**, 40544–40548.

Huss, M. & Wieczorek, H. (2007). Influence of ATP and ADP on dissociation of the V-ATPase into its V_1 and V_0 complexes. *FEBS Letters* **581**, 5566–5572.

Hutcheon, M. L., Duncan, T. M., Ngai, H. & Cross, R. L. (2001). Energy-driven subunit rotation at the interface between subunit *a* and the *c* oligomer in the F_0 sector of *Escherichia coli* ATP synthase. *Proceedings of the National Academy of Sciences of the United States of America* **98**, 8519–8524.

Imamura, H., Ikeda, C., Yoshida, M. & Yokoyama, K. (2004). The F subunit of *Thermus thermophilus* V_1-ATPase promotes ATPase activity but is not necessary for rotation. *Journal of Biological Chemistry* **279**, 18085–18090.

Imamura, H., Nakano, M., Noji, H., Muneyuki, E., Ohkuma, S., Yoshida, M. & Yokoyama, K. (2003). Evidence for rotation of V_1-ATPase. *Proceedings of the National Academy of Sciences of the United States of America* **100**, 2312–2315.

Imamura, H., Takeda, M., Funamoto, S., Shimabukuro, K., Yoshida, M. & Yokoyama, K. (2005). Rotation scheme of V_1-motor is different from that of F_1-motor. *Proceedings of the National Academy of Sciences of the United States of America* **102**, 17929–17933.

Inatomi, K. (1986). Characterization and purification of the membrane-bound ATPase of the archaebacterium *Methanosarcina barkeri*. *Journal of Bacteriology* **167**, 837–841.

Inoue, T. & Forgac, M. (2005). Cysteine-mediated cross-linking indicates that subunit C of the V-ATPase is in close proximity to subunits E and G of the V_1 domain and subunit *a* of the V_0 Domain. *Journal of Biological Chemistry* **280**, 27896–27903.

Iwata, M., Imamura, H., Stambouli, E., Ikeda, C., Tamakoshi, M., Nagata, K., Makyio, H., Hankamer, B., Barber, J., Yoshida, M., Yokoyama, K. & Iwata, S. (2004). Crystal structure of a central stalk subunit C and reversible association/dissociation of vacuole-type ATPase. *Proceedings of the National Academy of Sciences of the United States of America* **101**, 59–64.

Jefferies, K. C. & Forgac, M. (2008). Subunit H of the vacuolar (H+) ATPase inhibits ATP hydrolysis by the free V_1 domain by interaction with the rotary subunit F. *Journal of Biological Chemistry* **283**, 4512–4519.

Jiang, W. & Fillingame, R. H. (1998). Interacting helical faces of subunits a and c in the F_1F_0ATP synthase of *Escherichia coli* defined by disulfide cross-linking. *Proceedings of the National Academy of Sciences of the United States of America* **95**, 6607–6612.

Jiang, W., Hermolin, J. & Fillingame, R. H. (2001). The preferred stoichiometry of c subunits in the rotary motor sector of *Escherichia coli* ATP synthase is 10. *Proceedings of the National Academy of Sciences of the United States of America* **98**, 4966–4971.

Jones, P. C. & Fillingame, R. H. (1998). Genetic fusions of subunit *c* in the F_0 sector of H^+-transporting ATP synthase. *Journal of Biological Chemistry* **273**, 29701–29705.

Jones, P. C., Hermolin, J., Jiang, W. & Fillingame, R. H. (2000). Insights into the rotary catalytic mechanism of F_0F_1 ATP synthase from the cross-linking of subunits b and c in the *Escherichia coli* enzyme. *Journal of Biological Chemistry* **275**, 31340–31346.

Jones, R. P. O., Durose, L. J., Findlay, J. B. C. & Harrison, M. A. (2005). Defined sites of interaction between subunits E (Vma4p), C (Vma5p), and G (Vma10p) within the stator structure of the vacuolar H^+-ATPase. *Biochemistry* **44**, 3933–3941.

Jones, R. P. O., Durose, L. J., Phillips, C., Keen, J. N., Findlay, J. B. C. & Harrison, M. A. (2010). A site-directed cross-linking approach to the characterization of subunit E-subunit G contacts in the vacuolar H+-ATPase stator. *Molecular Membrane Biology* **27**, 147–159.

Junge, W. (2004). Protons, proteins and ATP. *Photosynthesis Research* **80**, 197–221.

Junge, W., Lill, H. & Engelbrecht, S. (1997). ATP synthase: an electrochemical transducer with rotatory mechanics. *Trends in Biochemical Science* **22**, 420–423.

Junge, W., Sielaff, H. & Engelbrecht, S. (2009). Torque generation and elastic power transmission in the rotary F_0F_1-ATPase. *Nature* **459**, 364–370.

Kabaleeswaran, V., Puri, N., Walker, J. E., Leslie, A. G. W. & Mueller, D. M. (2006). Novel features of the rotary catalytic mechanism revealed in the structure of yeast F-1 ATPase. *EMBO Journal* **25**, 5433–5442.

Kakinuma, Y., Yamato, I. & Murata, T. (1999). Structure and function of vacuolar Na^+-translocating ATPase in *Enterococcus hirae*. *Journal of Bioenergetics and Biomembranes* **31**, 7–14.

Kane, P. M. (1995). Disassembly and reassembly of the yeast vacuolar H(+)-ATPase *in vivo*. *Journal of Biological Chemistry* **270**, 17025–17032.

Karrasch, S. & Walker, J. E. (1999). Novel features in the structure of bovine ATP synthase. *Journal of Molecular Biology* **290**, 379–384.

Kato, S., Yoshida, M. & Kato-Yamada, Y. (2007). Role of the ε subunit of thermophilic F_1-ATPase as a sensor for ATP. *Journal of Biological Chemistry* **282**, 37618–37623.

Kato-Yamada, Y. & Yoshida, M. (2003). Isolated ε subunit of thermophilic F_1-ATPase binds ATP. *Journal of Biological Chemistry* **278**, 36013–36016.

Kato-Yamada, Y., Yoshida, M. & Hisabori, T. (2000). Movement of the helical domain of the ε subunit is

https://doi.org/10.1017/S0033583510000338 Published online by Cambridge University Press

required for the activation of thermophilic F_1-ATPase. *Journal of Biological Chemistry* **275**, 35746–35750.

Kawasaki-Nishi, S., Nishi, T. & Forgac, M. (2001). Arg-735 of the 100-kDa subunit *a* of the yeast V-ATPase is essential for proton translocation. *Proceedings of the National Academy of Sciences of the United States of America* **98**, 12397–12402.

Kinosita, K., Yasuda, R., Noji, H., Ishiwata, S. & Yoshida, M. (1998). F_1-ATPase: a rotary motor made of a single molecule. *Cell* **93**, 21–24.

Kish-Trier, E., Briere, L. A., Dunn, S. D. & Wilkens, S. (2008). The stator complex of the A_1A_0-ATP synthase-structural characterization of the E and H subunits. *Journal of Molecular Biology* **375**, 673–685.

Kish-Trier, E. & Wilkens, S. (2009a). Domain architecture of the stator complex of the A_1A_0-ATP synthase from *Thermoplasma acidophilum*. *Journal of Biological Chemistry* **284**, 12031–12040.

Kish-Trier, E. & Wilkens, S. (2009b). Interaction of the *Thermoplasma acidophilum* A_1A_0-ATP synthase peripheral stalk with the catalytic domain. *FEBS Letters* **583**, 3121–3126.

Kitagawa, N., Mazon, H., Heck, A. J. R. & Wilkens, S. (2008). Stoichiometry of the peripheral stalk subunits E and G of yeast V_1-ATPase determined by mass spectrometry. *Journal of Biological Chemistry* **283**, 3329–3337.

Landolt-Marticorena, C., Williams, K. M., Correa, J., Chen, W. & Manolson, M. F. (2000). Evidence that the NH_2 terminus of Vph1p, an integral subunit of the V_0 sector of the yeast V-ATPase, interacts directly with the Vma1p and Vma13p subunits of the V_1 sector. *Journal of Biological Chemistry* **275**, 15449–15457.

Langemeyer, L. & Engelbrecht, S. (2007). Essential arginine in subunit *a* and aspartate in subunit *c* of F_0F_1 ATP synthase: effect of repositioning within Helix 4 of subunit *a* and Helix 2 of subunit *c*. *Biochimica et Biophysica Acta* **1767**, 998–1005.

Lau, W. C. Y., Baker, L. A. & Rubinstein, J. L. (2008). Cryo-EM structure of the yeast ATP synthase. *Journal of Molecular Biology* **382**, 1256–1264.

Lau, W. C. Y. & Rubinstein, J. L. (2010). Structure of intact *Thermus thermophilus* V-ATPase by cryo-EM reveals organization of the membrane-bound V_0 motor. *Proceedings of the National Academy of Sciences of the United States of America* **107**, 1367–1372.

Laubinger, G., Deckers-Hebestreit, G., Altendorf, K. & Dimroth, P. (1990). A hybrid adenosine triphosphatase composed of F_1 of Escherichia coli and F_0 of *Propionigenium modestum* is a functional sodium ion pump. *Biochemistry* **29**, 5458–5463.

Lee, L. K., Stewart, A. G., Donohoe, M., Bernal, R. A. & Stock, D. (2010a). The structure of the peripheral stalk of *Thermus thermophilus* H^+-ATPase/synthase. *Nature Structural and Molecular Biology* **17**, 373–79.

Lee, S. K., Li, W., Ryu, S. E., Rhim, T. & Ahnn, J. (2010b). Vacuolar (H+)-ATPases in *Caenorhabditis elegans*: what can we learn about giant H^+ pumps from tiny worms? *Biochimica et Biophysica Acta* **1797**, 1687–1695.

Leng, X. H., Manolson, M. F. & Forgac, M. (1998). Function of the COOH-terminal domain of Vph1p in activity and assembly of the yeast V-ATPase. *Journal of Biological Chemistry* **273**, 6717–6723.

Leng, X. H., Manolson, M. F., Liu, Q. & Forgac, M. (1996). Site-directed mutagenesis of the 100-kda subunit (Vph1p) of the yeast vacuolar (H+)-ATPase. *Journal of Biological Chemistry* **271**, 22487–22493.

Leng, X. H., Nishi, T. & Forgac, M. (1999). Transmembrane topography of the 100-kda a subunit (Vph1p) of the yeast vacuolar proton translocating ATPase. *Journal of Biological Chemistry* **274**, 14655–14661.

Li, Y. P., Chen, W., Liang, Y. Q., Li, E. & Stashenko, P. (1999). Atp6i-deficient mice exhibit severe osteopetrosis due to loss of osteoclast-mediated extracellular acidification. *Nature Genetics* **23**, 447–451.

Lingl, A., Huber, H., Stetter, K. O., Mayer, F., Kellermann, J. & Müller, V. (2003). Isolation of a complete A_1A_0 ATP synthase comprising nine subunits from the hyperthermophile *Methanococcus jannaschii*. *Extremophiles* **7**, 249–257.

Lokanath, N. K., Matsuura, Y., Kuroishi, C., Takahashi, N. & Kunishima, N. (2007). Dimeric core structure of modular stator subunit E of archaeal H+-ATPase. *Journal of Molecular Biology* **366**, 933–944.

Lu, M., Vergara, S., Zhang, L., Holliday, L. S., Aris, J. & Gluck, S. L. (2002). The amino-terminal domain of the E subunit of vacuolar H+-ATPase (V-ATPase) interacts with the H subunit and is required for V-ATPase function. *Journal of Biological Chemistry* **277**, 38409–38415.

Lücken, U., Gogol, E. P. & Capaldi, R. A. (1990). Structure of the ATP synthase complex (ECF_1F_0) of *Escherichia coli* from cryoelectron microscopy. *Biochemistry* **29**, 5339–5343.

Ludwig, J., Kerscher, S., Brandt, U., Pfeiffer, K., Getlawi, F., Apps, D. K. & Schägger, H. (1998). Identification and characterisation of a novel 9·2-kDa membrane sector-associated protein of vacuolar proton ATPase form chromaffin granules. *Journal of Biological Chemistry* **273**, 10939–10947.

Ma, J., Flynn, T. C., Cui, Q., Leslie, A. G. W., Walker, J. E. & Karplus, M. (2002). A dynamic analysis of the rotation mechanism for conformational change in F_1-ATPase. *Structure* **10**, 921–931.

Maegawa, Y., Morita, H., Iyaguchi, D., Yao, M., Watanabe, N. & Tanaka, I. (2006). Structure of the catalytic nucleotide-binding subunit A of A-type ATP synthase from *Pyrococcus horikoshii* reveals a novel domain related to the peripheral stalk. *Acta Crystallographica D* **62**, 483–488.

Maher, M. J., Akimoto, S., Iwata, M., Nagata, K., Hori, Y., Yoshida, M., Yokoyama, S., Iwata, S. & Yokoyama, K. (2009). Crystal structure of A_3B_3

https://doi.org/10.1017/S0033583510000338 Published online by Cambridge University Press

complex of V-ATPase from *Thermus thermophilus*. *EMBO Journal* **28**, 3771–3779.

Makyio, H., Iino, R., Ikeda, C., Imamura, H., Tamakoshi, M., Iwata, M., Stock, D., Bernal, R. A., Carpenter, E. P., Yoshida, M., Yokoyama, K. & Iwata, S. (2005). Structure of a central stalk subunit F of prokaryotic V-type ATPase/synthase from *Thermus thermophilus*. *EMBO Journal* **24**, 3974–3983.

Mao, H. Z. & Weber, J. (2007). Identification of the β_{TP} site in the x-ray structure of F_1-ATPase as the high-affinity catalytic site. *Proceedings of the National Academy of Sciences of the United States of America* **104**, 18478–18483.

Marshansky, V. & Futai, M. (2008). The V-type H^+-ATPase in vesicular trafficking: targeting, regulation and function. *Current Opinion in Cell Biology* **20**, 415–426.

Masaike, T., Koyama-Horibe, F., Oiwa, K., Yoshida, M. & Nishizaka, T. (2008). Cooperative three-step motions in catalytic subunits of F_1-ATPase correlate with 80° and 40° substep rotations. *Nature Structural and Molecular Biology* **15**, 1326–1333.

Mclachlin, D. T., Bestard, J. A. & Dunn, S. D. (1998). The b and δ subunits of the *Escherichia coli* ATP synthase interact via residues in their C-terminal regions. *Journal of Biological Chemistry* **273**, 15162–15168.

Mclachlin, D. T., Coveny, A. M., Clark, S. M. & Dunn, S. D. (2000). Site-directed cross-linking of b to the α, β, and a subunits of the *Escherichia coli* ATP synthase. *Journal of Biological Chemistry* **275**, 17571–17577.

Meier, T., Ferguson, S. A., Cook, G. M., Dimroth, P. & Vonck, J. (2006). Structural investigations of the membrane-embedded rotor ring of the F-ATPase from *Clostridium paradoxum*. *Journal of Bacteriology* **188**, 7759–7764.

Meier, T., Polzer, P., Diederichs, K., Welte, W. & Dimroth, P. (2005a). Structure of the rotor ring of F-type Na^+-ATPase from *Ilyobacter tartaricus*. *Science* **308**, 659–662.

Meier, T., Yu, J., Raschle, T., Henzen, F., Dimroth, P. & Muller, D. J. (2005b). Structural evidence for a constant c_{11} ring stoichiometry in the sodium F-ATP synthase. *FEBS Journal* **272**, 5474–5483.

Menz, R. I., Walker, J. E. & Leslie, A. G. W. (2001). Structure of bovine mitochondrial F_1-ATPase with nucleotide bound to all three catalytic sites: implications for the mechanism of rotary catalysis. *Cell* **106**, 331–341.

Merkulova, M., McKee, M., Dip, P. V., Grüber, G. & Marshansky, V. (2010). N-terminal domain of V-ATPase a2-subunit displays integral membrane protein properties. *Protein Science* **19**, 1850–1862.

Merzendorfer, H., Huss, M., Schmid, R., Harvey, W. R. & Wieczorek, H. (1999). A novel insect V-ATPase subunit M9·7 is glycosylated extensively. *Journal of Biological Chemistry* **274**, 17372–17378.

Merzendorfer, H., Reineke, S., Zhao, X.-F., Jacobmeier, B., Harvey, W. R. & Wieczorek, H. (2000). The multigene family of the tobacco hornworm V-ATPase: novel subunits a, C, D, H and putative isoforms. *Biochimica et Biophysica Acta* **1467**, 369–379.

Meyer zu Tittingdorf, J. M. W., Rexroth, S., Schafer, E., Schlichting, R., Giersch, C., Dencher, N. A. & Seelert, H. (2004). The stoichiometry of the chloroplast ATP synthase oligomer III in *Chlamydomonas reinhardtii* is not affected by the metabolic state. *Biochimica et Biophysica Acta* **1659**, 92–99.

Minauro-Sanmiguel, F., Wilkens, S. & García, J. J. (2005). Structure of dimeric mitochondrial ATP synthase: novel F_o bridging features and the structural basis of mitochondrial cristae biogenesis. *Proceedings of the National Academy of Sciences of the United States of America* **102**, 12356–12358.

Mitchell, P. (1961). Coupling of phosphorylation to electron and hydrogen transfer by a chemi-osmotic type of mechanism. *Nature* **191**, 144–148.

Moore, K. J. & Fillingame, R. H. (2008). Structural interactions between transmembrane helices 4 and 5 of subunit *a* and the subunit *c* ring of *Escherichia coli* ATP synthase. *Journal of Biological Chemistry* **283**, 31726–31735.

Morel, N. (2003). Neurotransmitter release: the dark side of the vacuolar-H^+-ATPase. *Biology of the Cell* **95**, 453–457.

Muench, S. P., Huss, M., Song, C. F., Phillips, C., Wieczorek, H., Trinick, J. & Harrison, M. A. (2009). Cryo-electron microscopy of the vacuolar ATPase motor reveals its mechanical and regulatory complexity. *Journal of Molecular Biology* **386**, 389–399.

Mulkidjanian, A., Galperin, M., Makarova, K., Wolf, Y. & Koonin, E. (2008). Evolutionary primacy of sodium bioenergetics. *Biology Direct* **3**, 13.

Mulkidjanian, A. Y., Makarova, K. S., Galperin, M. Y. & Koonin, E. V. (2007). Inventing the dynamo machine: the evolution of the F-type and V-type ATPases. *Nature Reviews Microbiology* **5**, 892–899.

Müller, M., Pänke, O., Junge, W. & Engelbrecht, S. (2002). F_1-ATPase, the C-terminal end of subunit γ is not required for ATP hydrolysis-driven rotation. *Journal of Biological Chemistry* **277**, 23308–23313.

Müller, V. & Grüber, G. (2003). ATP synthases: structure, function and evolution of unique energy converters. *Cellular and Molecular Life Sciences* **60**, 474–494.

Müller, V., Lingl, A., Lewalter, K. & Fritz, M. (2005). ATP synthases with novel rotor subunits: new insights into structure, function and evolution of ATPases. *Journal of Bioenergetics and Biomembranes* **37**, 455–460.

Müller, V., Ruppert, C. & Lemker, T. (1999). Structure and function of the A(1)A(0)-ATPases from methanogenic archaea. *Journal of Bioenergetics and Biomembranes* **31**, 15–27.

Muneyuki, E., Watanabe-Nakayama, T., Suzuki, T., Yoshida, M., Nishizaka, T. & Noji, H. (2007). Single molecule energetics of F_1-ATPase motor. *Biophysical Journal* **92**, 1806–1812.

https://doi.org/10.1017/S0033583510000338 Published online by Cambridge University Press

Murata, T., Yamato, I., Kakinuma, Y., Leslie, A. G. W. & Walker, J. E. (2005). Structure of the rotor of the V-type Na^+-ATPase from *Enterococcus hirae*. *Science* **308**, 654–659.

Nakano, M., Imamura, H., Toei, M., Tamakoshi, M., Yoshida, M. & Yokoyama, K. (2008). ATP hydrolysis and synthesis of a rotary motor V-ATPase from *Thermus thermophilus*. *Journal of Biological Chemistry* **283**, 20789–20796.

Nelson, N., Perzov, N., Cohen, A., Hagai, K., Padler, V. & Nelson, H. (2000). The cellular biology of proton-motive force generation by V-ATPases. *Journal of Experimental Biology* **203**, 89–95.

Nishizaka, T. (2004). Chemomechanical coupling in F_1-ATPase revealed by simultaneous observation of nucleotide kinetics and rotation. *Nature Structural and Molecular Biology* **11**, 142–148.

Noji, H., Yasuda, R., Yoshida, M. & Kinosita, K. (1997). Direct observation of the rotation of F_1-ATPase. *Nature* **386**, 299–302.

Norgett, E. E., Borthwick, K. J., Al Lamki, R. S., Su, Y., Smith, A. N. & Karet, F. E. (2007). V_1 and V_0 domains of the human H+-ATPase are linked by an interaction between the G and a subunits. *Journal of Biological Chemistry* **282**, 14421–14427.

Numoto, N., Hasegawa, Y., Takeda, K. & Miki, K. (2009). Inter-subunit interaction and quaternary rearrangement defined by the central stalk of prokaryotic V_1-ATPase. *EMBO Reports* **10**, 1228–1234.

Ogilvie, I., Aggeler, R. & Capaldi, R. A. (1997). Cross-linking of the δ subunit to one of the three α subunits has no effect on functioning, as expected if δ is a part of the stator that links the F_1 and F_0 parts of the *Escherichia coli* ATP synthase. *Journal of Biological Chemistry* **272**, 16652–16656.

Okuno, D., Fujisawa, R., Iino, R., Hirono-Hara, Y., Imamura, H. & Noji, H. (2008). Correlation between the conformational states of F_1-ATPase as determined from its crystal structure and single-molecule rotation. *Proceedings of the National Academy of Sciences of the United States of America* **105**, 20722–20727.

Oot, R. A. & Wilkens, S. (2010). Domain characterization and interaction of the yeast vacuolar ATPase subunit C with the peripheral stator stalk subunits E and G. *Journal of Biological Chemistry* **285**, 24654–24664.

Oster, G. & Wang, H. Y. (2000a). Reverse engineering a protein: the mechanochemistry of ATP synthase. *Biochimica et Biophysica Acta* **1458**, 482–510.

Oster, G. & Wang, H. Y. (2000b). Why is the mechanical efficiency of F-1-ATPase so high? *Journal of Bioenergetics and Biomembranes* **32**, 459–469.

Owegi, M. A., Pappas, D. L., Finch Jr., M. W., Bilbo, S. A., Resendiz, C. A., Jacquemin, L. J., Warrier, A., Trombley, J. D., McCulloch, K. M., Margalef, K. L. M., Mertz, M. J., Storms, J. M., Damin, C. A. & Parra, K. J. (2006). Identification of a domain in the V_0 subunit *d* that is critical for coupling of the yeast vacuolar proton-translocating ATPase. *Journal of Biological Chemistry* **281**, 30001–30014.

Pali, T., Dixon, N., Kee, T. P. & Marsh, D. (2004). Incorporation of the V-ATPase inhibitors concanamycin and indole pentadiene in lipid membranes. Spin-label EPR studies. *Biochimica et Biophysica Acta* **1663**, 14–18.

Pänke, O., Cherepanov, D. A., Gumbiowski, K., Engelbrecht, S. & Junge, W. (2001). Viscoelastic dynamics of actin filaments coupled to rotary F-ATPase: angular torque profile of the enzyme. *Biophysical Journal* **81**, 1220–1233.

Parra, K. J., Keenan, K. L. & Kane, P. M. (2000). The H subunit (Vma13p) of the yeast V-ATPase inhibits the ATPase activity of cytosolic V_1 complexes. *Journal of Biological Chemistry* **275**, 21761–21767.

Penczek, P. A., Chao, Y., Frank, J. & Spahn, C. M. T. (2006). Estimation of variance in single particle reconstruction using the bootstrap technique. *Journal of Structural Biology* **154**, 168–183.

Pisa, K. Y., Huber, H., Thom, M. & Müller, V. (2007a). A sodium ion-dependent A_1A_0 ATP synthase from the hyperthermophilic archaeon *Pyrococcus furiosus*. *FEBS Journal* **274**, 3928–3938.

Pisa, K. Y., Weidner, C., Maischak, H., Kavermann, H. & Müller, V. (2007b). The coupling ion in the methanoarchaeal ATP synthases: H^+ vs. Na^+ in the A(1)A(0) ATP synthase from the archaeon *Methanosarcina mazei* Gö1. *FEMS Microbiology Letters* **277**, 56–63.

Pogoryelov, D., Reichen, C., Klyszejko, A. L., Brunisholz, R., Muller, D. J., Dimroth, P. & Meier, T. (2007). The oligomeric state of c rings from cyanobacterial F-ATP synthases varies from 13 to 15. *Journal of Bacteriology* **189**, 5895–5902.

Pogoryelov, D., Yu, J., Meier, T., Vonck, J., Dimroth, P. & Muller, D. J. (2005). The c15 ring of the *Spirulina platensis* F-ATP synthase: F_1/F_0 symmetry mismatch is not obligatory. *EMBO Reports* **6**, 1040–1044.

Powell, B., Graham, L. A. & Stevens, T. H. (2000). Molecular characterization of the yeast vacuolar H^+-ATPase proton pore. *Journal of Biological Chemistry* **275**, 23654–23660.

Pu, J. & Karplus, M. (2008). How subunit coupling produces the γ subunit rotary motion in F_1-ATPase. *Proceedings of the National Academy of Sciences of the United States of America* **105**, 1192–1197.

Pullman, M. E. & Monroy, G. C. (1963). A naturally occurring inhibitor of mitochondrial adenosine triphosphatase. *Journal of Biological Chemistry* **238**, 3762–3769.

Qi, J. & Forgac, M. (2008). Function and subunit interactions of the N-terminal domain of subunit *a* (Vph1p) of the yeast V-ATPase. *Journal of Biological Chemistry* **283**, 19274–19282.

Radermacher, M., Ruiz, T., Wieczorek, H. & Grüber, G. (2001). The structure of the V1-ATPase by electron

https://doi.org/10.1017/S0033583510000338 Published online by Cambridge University Press

microscopy of single particles. *Journal of Structural Biology* **135**, 26–37.

Rahlfs, S., Aufurth, S. & Müller, V. (1999). The Na^+-F_1F_0-ATPase operon from *Acetobacterium woodii*. Operon structure and presence of multiple copies of atpE which encode proteolipids of 8- and 18-kDa. *Journal of Biological Chemistry* **274**, 33999–34004.

Rastogi, V. K. & Girvin, M. E. (1999). Structural changes linked to proton translocation by subunit *c* in the ATP synthase. *Nature* **402**, 263–268.

Rees, D. M., Leslie, A. G. W. & Walker, J. E. (2009). The structure of the membrane extrinsic region of bovine ATP synthase. *Proceedings of the National Academy of Sciences of the United States of America* **106**, 21597–21601.

Rishikesan, S., Gayen, S., Thaker, Y. R., Vivekanandan, S., Manimekalai, M. S. S., Yau, Y. H., Shochat, S. G. & Grüber, G. (2009). Assembly of subunit *d* (Vma6p) and G (Vma10p) and the NMR solution structure of subunit G (G(1–59)) of the *Saccharomyces cerevisiae* V_1V_0 ATPase. *Biochimica et Biophysica Acta* **1787**, 242–251.

Rishikesan, S., Thaker, Y. R., Priya, R., Gayen, S., Manimekalai, M. S. S., Hunke, C. & Grüber, G. (2008). Spectroscopical identification of residues of subunit G of the yeast V-ATPase in its connection with subunit E. *Molecular Membrane Biology* **25**, 400–410.

Rodgers, A. J. W. & Capaldi, R. A. (1998). The second stalk composed of the b- and delta-subunits connects F_0 to F_1 via and alpha-subunit in the *Escherichia coli* ATP synthase. *Journal of Biological Chemistry* **273**, 29406–29410.

Rodgers, A. J. W. & Wilce, M. C. J. (2000). Structure of the g-e complex of ATP synthase. *Nature Structural and Molecular Biology* **7**, 1051–1054.

Rodgers, A. J. W., Wilkens, S., Aggeler, R., Morris, M. B., Howitt, S. M. & Capaldi, R. A. (1997). The subunit delta-subunit *b* domain of the *Escherichia coli* F_1F_0-ATPase. *Journal of Biological Chemistry* **272**, 31058–31064.

Rondelez, Y., Tresset, G., Nakashima, T., Kato-Yamada, Y., Fujita, H., Takeuchi, S. & Noji, H. (2005). Highly coupled ATP synthesis by F_1-ATPase single molecules. *Nature* **433**, 773–777.

Rosenthal, P. B. & Henderson, R. (2003). Optimal determination of particle orientation, absolute hand, and contrast loss in single-particle electron cryomicroscopy. *Journal of Molecular Biology* **333**, 721–745.

Rubinstein, J. L., Walker, J. E. & Henderson, R. (2003). Structure of the mitochondrial ATP synthase by electron cryomicroscopy. *EMBO Journal* **22**, 6182–6192.

Sabbert, D., Engelbrecht, S. & Junge, W. (1996). Intersubunit rotation in active F-ATPase. *Nature* **381**, 623–625.

Sagermann, M., Stevens, T. H. & Matthews, B. W. (2001). Crystal structure of the regulatory subunit H of the V-type ATPase of *Saccharomyces cerevisiae*. *Proceedings of the National Academy of Sciences of the United States of America* **98**, 7134–7139.

Sambade, M. & Kane, P. M. (2004). The yeast vacuolar proton-translocating ATPase contains a subunit homologous to the *Manduca sexta* and bovine e subunits that is essential for function. *Journal of Biological Chemistry* **279**, 17361–17365.

Sambongi, Y., Iko, Y., Tanabe, M., Omote, H., Iwamoto-Kihara, A., Ueda, I., Yanagida, T., Wada, Y. & Futai, M. (1999). Mechanical rotation of the c subunit oligomer in ATP synthase (F_0F_1): direct observation. *Science* **286**, 1722–1724.

Schäfer, I. B., Bailer, S. M., Duser, M. G., Börsch, M., Bernal, R. A., Stock, D. & Grüber, G. (2006). Crystal structure of the archaeal A_1A_0 ATP synthase subunit B from *Methanosarcine mazei* Gö1: implications of nucleotide-binding differences in the major A_1A_0 subunits A and B. *Journal of Molecular Biology* **358**, 725–740.

Scheres, S. H. W., Gao, H., Valle, M., Herman, G. T., Eggermont, P. P. B., Frank, J. & Carazo, J.-M. (2006). Disentangling conformational states of macromolecules in 3D-EM through likelihood optimization. *Nature Methods* **4**, 27–29.

Schwem, B. E. & Fillingame, R. H. (2006). Cross-linking between helices within subunit *a* of *Escherichia coli* ATP synthase defines the transmembrane packing of a four-helix bundle. *Journal of Biological Chemistry* **281**, 37861–37867.

Seelert, H., Poetsch, A., Dencher, N. A., Engel, A., Stahlberg, H. & Müller, D. J. (2000). Structural biology: proton-powered turbine of a plant motor. *Nature* **405**, 418–419.

Sennoune, S. & Martinez-Zaguilan, R. (2007). Plasmalemmal vacuolar H^+-ATPases in angiogenesis, diabetes and cancer. *Journal of Bioenergetics and Biomembranes* **39**, 427–433.

Sennoune, S. R., Bakunts, K., Martinez, G. M., Chua-Tuan, J. L., Kebir, Y., Attaya, M. N. & Martinez-Zaguilan, R. (2004). Vacuolar H^+-ATPase in human breast cancer cells with distinct metastatic potential: distribution and functional activity. *American Journal of Physiology. Cell Physiology* **286**, C1443–C1452.

Shao, E. & Forgac, M. (2004). Involvement of the non-homologous region of subunit A of the yeast V-ATPase in coupling and *in vivo* dissociation. *Journal of Biological Chemistry* **279**, 48663–48670.

Shao, E., Nishi, T., Kawasaki-Nishi, S. & Forgac, M. (2003). Mutational analysis of the non-homologous region of subunit A of the yeast V-ATPase. *Journal of Biological Chemistry* **278**, 12985–12991.

Sielaff, H., Rennekamp, H., Engelbrecht, S. & Junge, W. (2008a). Functional halt positions of rotary F_0F_1-ATPase correlated with crystal structures. *Biophysical Journal* **95**, 4979–4987.

Sielaff, H., Rennekamp, H., Wächter, A., Xie, H., Hilbers, F., Feldbauer, K., Dunn, S. D., Engelbrecht, S. & Junge, W. (2008b). Domain compliance and elastic power transmission in rotary F_0F_1-ATPase. *Proceedings of*

https://doi.org/10.1017/S0033583510000338 Published online by Cambridge University Press

the National Academy of Sciences of the United States of America **105**, 17760–17765.

Slesarev, A. I., Mezhevaya, K. V., Makarova, K. S., Polushin, N. N., Shcherbinina, O. V., Shakhova, V. V., Belova, G. I., Aravind, L., Natale, D. A., Rogozin, I. B., Tatusov, R. L., Wolf, Y. I., Stetter, K. O., Malykh, A., Koonin, E. V. & Kozyavkin, S. A. (2002). The complete genome of hyperthermophile *Methanopyrus kandleri* AV19 and monophyly of archaeal methanogens. *Proceedings of the National Academy of Sciences of the United States of America* **99**, 4644–4649.

Smith, A. N., Skaug, J., Choate, K. A., Nayir, A., Bakkaloglu, A., Ozen, S., Hulton, S. A., Sanjad, S. A., Al-Sabban, E. A., Lifton, R. P., Scherer, S. W. & Karet, F. E. (2000). Mutations in ATP6N1B, encoding a new kidney vacuolar proton pump 116-kD subunit, cause recessive distal renal tubular acidosis with preserved hearing. *Nature Genetics* **26**, 71–75.

Sorgen, P. L., Bubb, M. R. & Cain, B. D. (1999). Lengthening the second stalk of F_1F_0 ATP synthase in *Escherichia coli*. *Journal of Biological Chemistry* **274**, 36261–36266.

Sorgen, P. L., Caviston, T. L., Perry, R. C. & Cain, B. D. (1998). Deletions in the second stalk of F_1F_0-ATP synthase in *Escherichia coli*. *Journal of Biological Chemistry* **273**, 27873–27878.

Soubannier, V., Vaillier, J., Paumard, P., Coulary, B., Schaeffer, J. & Velours, J. (2002). In the absence of the first membrane-spanning segment of subunit 4(b), the yeast ATP synthase is functional but does not dimerize or oligomerize. *Journal of Biological Chemistry* **277**, 10739–10745.

Speelmans, G., Poolman, B., Abee, T. & Konings, W. N. (1993). Energy transduction in the thermophilic anaerobic bacterium *Clostridium fervidus* is exclusively coupled to sodium ions. *Proceedings of the National Academy of Sciences of the United States of America* **90**, 7975–7979.

Steigmiller, S., Turina, P. & Gräber, P. (2008). The thermodynamic H+/ATP ratios of the H^+-ATPsynthases from chloroplasts and *Escherichia coli*. *Proceedings of the National Academy of Sciences of the United States of America* **105**, 3745–3750.

Stock, D., Leslie, A. G. W. & Walker, J. E. (1999). Molecular architecture of the rotary motor in ATP synthase. *Science* **286**, 1700–1705.

Strauss, M., Hofhaus, G., Schröder, R. R. & Kühlbrandt, W. (2008). Dimer ribbons of ATP synthase shape the inner mitochondrial membrane. *EMBO Journal* **27**, 1154–1160.

Stuart, R. (2008). Supercomplex organization of the oxidative phosphorylation enzymes in yeast mitochondria. *Journal of Bioenergetics and Biomembranes* **40**, 411–417.

Su, Y., Zhou, A., Al Lamki, R. S. & Karet, F. E. (2003). The a-subunit of the V-type H^+-ATPase interacts with phosphofructokinase-1 in humans. *Journal of Biological Chemistry* **278**, 20013–20018.

Sumi, M., Sato, M. H., Denda, K., Date, T. & Yoshida, M. (1992). A DNA fragment homologous to F_1-ATPase β subunit was amplified from genomic DNA of *Methanosarcina barkeri*. Indication of an archaebacterial F-type ATPase. *FEBS Letters* **314**, 207–210.

Sumner, J. P., Dow, J. A., Earley, F. G., Klein, U., Jager, D. & Wieczorek, H. (1995). Regulation of plasma membrane V-ATPase activity by dissociation of peripheral subunits. *Journal of Biological Chemistry* **270**, 5649–5653.

Sun, S., Chandler, D., Dinner, A. R. & Oster, G. (2003). Elastic energy storage in beta-sheets with application to F-1-ATPase. *European Biophysics Journal* **32**, 676–683.

Supek, F., Supekova, L., Mandiyan, S., Pan, Y. C., Nelson, H. & Nelson, N. (1994). A novel accessory subunit for vacuolar H(+)-ATPase from chromaffin granules. *Journal of Biological Chemistry* **269**, 24102–24106.

Supekova, L., Sbia, M., Supek, F., Ma, Y. M. & Nelson, N. (1996). A novel subunit of vacuolar H^+-ATPase related to the b-subunit of F-ATPases. *Journal of Experimental Biology* **199**, 1147–1156.

Svergun, D. I., Konrad, S., Huss, M., Koch, M. H. J., Wieczorek, H., Altendorf, K., Volkov, V. V. & Grüber, G. (1998). Quaternary structure of V_1 and F_1 ATPase: significance of structural homologies and diversities. *Biochemistry* **37**, 17659–17663.

Takase, K., Yamato, I. & Kakinuma, Y. (1993). Cloning and sequencing of the genes coding for the A and B subunits of vacuolar-type Na(+)-ATPase from *Enterococcus hirae*. Coexistence of vacuolar- and F_0F_1-type ATPases in one bacterial cell. *Journal of Biological Chemistry* **268**, 11610–11616.

Takeyasu, K., Omote, H., Nettikadan, S., Tokumasu, F., Iwamoto-Kihara, A. & Futai, M. (1996). Molecular imaging of *Escherichia coli* F_0F_1-ATPase in reconstituted membranes using atomic force microscopy. *FEBS Letters* **392**, 110–113.

Thaker, Y., Roessle, M., & Grüber, G. (2007). The boxing glove shape of subunit *d* of the yeast V-ATPase in solution and the importance of disulfide formation for folding of this protein. *Journal of Bioenergetics and Biomembranes* **39**, 275–289.

Toei, M., Gerle, C., Nakano, M., Tani, K., Gyobu, N., Tamakoshi, M., Sone, N., Yoshida, M., Fujiyoshi, Y., Mitsuoka, K. & Yokoyama, K. (2007). Dodecamer rotor ring defines H^+/ATP ratio for ATP synthesis of prokaryotic V-ATPase from *Thermus thermophilus*. *Proceedings of the National Academy of Sciences of the United States of America* **104**, 20256–20261.

Toei, M., Saum, R. & Forgac, M. (2010). Regulation and isoform function of the V-ATPases. *Biochemistry* **49**, 4715–4723.

Tomashek, J. J. & Brusilow, W. S. A. (2000). Stoichiometry of energy coupling by proton-translocating ATPases: a history of variability. *Journal of Bioenergetics and Biomembranes* **32**, 493–500.

https://doi.org/10.1017/S0033583510000338 Published online by Cambridge University Press

Tsunoda, S. P., Rodgers, A. J. W., Aggeler, R., Wilce, M. C. J., Yoshida, M. & Capaldi, R. A. (2001). Large conformational changes of the ε subunit in the bacterial F_1F_0 ATP synthase provide a ratchet action to regulate this rotary motor enzyme. *Proceedings of the National Academy of Sciences of the United States of America* **98**, 6560–6564.

Ueno, H., Suzuki, T., Kinosita, K. & Yoshida, M. (2005). ATP-driven stepwise rotation of F_0F_1-ATP synthase. *Proceedings of the National Academy of Sciences of the United States of America* **102**, 1333–1338.

Uhlin, U., Cox, G. B. & Guss, J. M. (1997). Crystal structure of the ε subunit of the proton-translocating ATP synthase from *Escherichia coli*. *Structure* **5**, 1219–1230.

Väänänen, H. K., Zhao, H., Mulari, M. & Halleen, J. M. (2000). The cell biology of osteoclast function. *Journal of Cell Science* **113**, 377–381.

Valiyaveetil, F. I. & Fillingame, R. H. (1997). On the role of Arg-210 and Glu-219 of subunit *a* in proton translocation by the *Escherichia coli* F_0F_1-ATP synthase. *Journal of Biological Chemistry* **272**, 32635–32641.

Venzke, D., Domgall, I., Kocher, T., Féthière, J., Fischer, S. & Böttcher, B. (2005). Elucidation of the stator organization in the V-ATPase of *Neurospora crassa*. *Journal of Molecular Biology* **349**, 659–669.

Vik, S. B. & Antonio, B. J. (1994). A mechanism of proton translocation by F_1F_0 ATP synthases suggested by double mutants of the *a* subunit. *Journal of Biological Chemistry* **269**, 30364–30369.

Vik, S. B., Long, J. C., Wada, T. & Zhang, D. (2000). A model for the structure of subunit *a* of the *Escherichia coli* ATP synthase and its role in proton translocation. *Biochimica et Biophysica Acta* **1458**, 457–466.

Vik, S. B., Patterson, A. R. & Antonio, B. J. (1998). Insertion scanning mutagenesis of subunit *a* of the F_1F_0 ATP synthase near His245 and implications on gating of the proton channel. *Journal of Biological Chemistry* **273**, 16229–16234.

Vinothkumar, K. R. & Henderson, R. (2010). Structures of membrane proteins. *Quarterly Review of Biophysics* **43**, 65–158.

Vollmar, M., Schlieper, D., Winn, M., Büchner, C. & Groth, G. (2009). Structure of the c(14) rotor ring of the proton translocating chloroplast ATP synthase. *Journal of Biological Chemistry* **284**, 18228–18235.

Von Ballmoos, C., Brunner, J. & Dimroth, P. (2004). The ion channel of F-ATP synthase is the target of toxic organotin compounds. *Proceedings of the National Academy of Sciences of the United States of America* **101**, 11239–11244.

Von Ballmoos, C., Cook, G. M. & Dimroth, P. (2008). Unique rotary ATP synthase and its biological diversity. *Annual Review of Biophysics* **37**, 43–64.

Von Ballmoos, C., Wiedenmann, A. & Dimroth, P. (2009). Essentials for ATP synthesis by F_1F_0 ATP synthases. *Annual Review of Biochemistry* **78**, 649–672.

Vonck, J., Pisa, K. Y., Morgner, N., Brutschy, B. & Müller, V. (2009). Three-dimensional structure of A_1A_0ATP synthase from the hyperthermophilic archeon *Pyrococcus furiosus* by electron microscopy. *Journal of Biological Chemistry* **284**, 10110–10119.

Voss, M., Vitavska, O., Walz, B., Wieczorek, H. & Baumann, O. (2007). Stimulus-induced phosphorylation of vacuolar H^+-ATPase by protein kinase A. *Journal of Biological Chemistry* **282**, 33735–33742.

Wagner, C. A., Finberg, K. E., Breton, S., Marshansky, V., Brown, D. & Geibel, J. P. (2004). Renal vacuolar H^+-ATPase. *Physiological Reviews* **84**, 1263–1314.

Wang, Y., Cipriano, D. J. & Forgac, M. (2007). Arrangement of subunits in the proteolipid ring of the V-ATPase. *Journal of Biological Chemistry* **282**, 34058–34065.

Wang, Y., Inoue, T. & Forgac, M. (2005). Subunit *a* of the yeast V-ATPase participates in binding of bafilomycin. *Journal of Biological Chemistry* **280**, 40481–40488.

Wang, Y., Toei, M. & Forgac, M. (2008). Analysis of the membrane topology of transmembrane segments in the C-terminal hydrophobic domain of the yeast vacuolar ATPase subunit *a* (Vph1p) by chemical modification. *Journal of Biological Chemistry* **283**, 20696–20702.

Watts, S. D., Zhang, Y., Fillingame, R. H. & Capaldi, R. A. (1995). The γ subunit in the *Escherichia coli* ATP synthase complex (ECF_1F_0) extends through the stalk and contacts the c subunits of the F_0 part. *FEBS Letters* **368**, 235–238.

Weber, J., Wilke-Mounts, S., Nadanaciva, S. & Senior, A. E. (2004). Quantitative determination of direct binding of *b* subunit to F_1 in *Escherichia coli* F_1F_0-ATP synthase. *Journal of Biological Chemistry* **279**, 11253–11258.

White, H. D., Thirumurugan, K., Walker, M. L. & Trinick, J. (2003). A second generation apparatus for time resolved electron cryo-microscopy using stepper motors and electrospray. *Journal of Structural Biology* **144**, 246–252.

Whyteside, G., Meek, P. J., Ball, S. K., Dixon, N., Finbow, M. E., Kee, T. P., Findlay, J. B. C. & Harrison, M. A. (2005). Concanamycin and indolyl pentadieneamide inhibitors of the vacuolar H+-ATPase bind with high affinity to the purified proteolipid subunit of the membrane domain. *Biochemistry* **44**, 15024–15031.

Wieczorek, H., Brown, D., Grinstein, S., Ehrenfeld, J. & Harvey, W. R. (1999). Animal plasma membrane energization by proton-motive V-ATPases. *BioEssays* **21**, 637–648.

Wieczorek, H., Putzenlechner, M., Zeiske, W. & Klein, U. (1991). A vacuolar-type proton pump energizes K^+/H^+-antiport in an animal plasma membrane. *Journal of Biological Chemistry* **266**, 15340–15347.

https://doi.org/10.1017/S0033583510000338 Published online by Cambridge University Press

Wilkens, S. & Capaldi, R. (1998). Electron microscopic evidence of two stalks linking the F_1 and F_0 parts of the *Escherichia coli* ATP synthase. *Biochimica et Biophysica Acta* **1365**, 93–97.

Wilkens, S. & Capaldi, R. A. (1994). Asymmetry and structural-changes in EcF(1) examined by cryoelectronmicroscopy. *Biological Chemistry Hoppe-Seyler* **375**, 43–51.

Wilkens, S. & Forgac, M. (2001). Three-dimensional structure of the vacuolar ATPase proton channel by electron microscopy. *Journal of Biological Chemistry* **276**, 44064–44068.

Wilkens, S., Inoue, T. & Forgac, M. (2004). Three-dimensional structure of the vacuolar ATPase: localization of subunit H by difference imaging and chemical cross-linking. *Journal of Biological Chemistry* **279**, 41942–41949.

Wilkens, S., Vasilyeva, E. & Forgac, M. (1999). Structure of the vacuolar ATPase by electron microscopy. *Journal of Biological Chemistry* **274**, 31804–31810.

Wolgemuth, C. W. & Sun, S. X. (2006). Elasticity of α-helical coiled coils. *Physical Review Letters* **97**, 248101.

Xu, T., Vasilyeva, E. & Forgac, M. (1999). Subunit interactions in the clathrin-coated vesicle vacuolar (H+)- ATPase complex. *Journal of Biological Chemistry* **274**, 28909–28915.

Yagi, H., Kajiwara, N., Tanaka, H., Tsukihara, T., Kato-Yamada, Y., Yoshida, M. & Akutsu, H. (2007). Structures of the thermophilic F_1-ATPase ε subunit suggesting ATP-regulated arm motion of its C-terminal domain in F_1. *Proceedings of the National Academy of Sciences of the United States of America* **104**, 11233–11238.

Yamamoto, M., Unzai, S., Saijo, S., Ito, K., Mizutani, K., Suno-Ikeda, C., Yabuki-Miyata, Y., Terada, T., Toyama, M., Shirouzu, M., Kobayashi, T., Kakinuma, Y., Yamato, I., Yokoyama, S., Iwata, S. & Murata, T. (2008). Interaction and stoichiometry of the peripheral stalk subunits NtpE and NtpF and the N-terminal hydrophilic domain of NtpI of *Enterococcus hirae* V-ATPase. *Journal of Biological Chemistry* **283**, 19422–19431.

Yang, W., Gao, Y. Q., Cui, Q., Ma, J. & Karplus, M. (2003). The missing link between thermodynamics and structure in F_1-ATPase. *Proceedings of the National Academy of Sciences of the United States of America* **100**, 874–879.

Yasuda, R., Masaike, T., Adachi, K., Noji, H., Itoh, H. & Kinosita Jr., K. (2003). The ATP-waiting conformation of rotating F_1-ATPase revealed by single-pair fluorescence resonance energy transfer. *Proceedings of the National Academy of Sciences of the United States of America* **100**, 9314–9318.

Yasuda, R., Noji, H., Yoshida, M., Kinosita, K. & Itoh, H. (2001). Resolution of distinct rotational substeps by submillisecond kinetic analysis of F_1-ATPase. *Nature* **410**, 898–904.

Yokoyama, K., Akabane, Y., Ishii, N. & Yoshida, M. (1994). Isolation of prokaryotic V_0V_1-ATPase from a thermophilic eubacterium *Thermus thermophilus*. *Journal of Biological Chemistry* **269**, 12248–12253.

Yokoyama, K., Nagata, K., Imamura, H., Ohkuma, S., Yoshida, M. & Tamakoshi, M. (2003a). Subunit arrangement in V-ATPase from *Thermus thermophilus*. *Journal of Biological Chemistry* **278**, 42686–42691.

Yokoyama, K., Nakano, M., Imamura, H., Yoshida, M. & Tamakoshi, M. (2003b). Rotation of the proteolipid ring in the V-ATPase. *Journal of Biological Chemistry* **278**, 24255.

Yoshida, M., Muneyuki, E. & Hisabori, T. (2001). ATP synthase- a marvellous rotary engine of the cell. *Nature Reviews Molecular and Cellular Biology* **2**, 669–677.

Zhang, J., Myers, M. & Forgac, M. (1992). Characterization of the V_0 domain of the coated vesicle (H+)- ATPase. *Journal of Biological Chemistry* **267**, 9773–9778.

Zhang, J. W., Parra, K. J., Liu, J. & Kane, P. M. (1998). Characterization of a temperature-sensitive yeast vacuolar ATPase mutant with defects in actin distribution and bud morphology. *Journal of Biological Chemistry* **273**, 18470–18480.

Zhang, Z., Charsky, C., Kane, P. M. & Wilkens, S. (2003). Yeast V_1-ATPase: affinity purification and structural features by electron microscopy. *Journal of Biological Chemistry* **278**, 47299–47306.

Zhang, Z., Zheng, Y., Mazon, H., Milgrom, E., Kitagawa, N., Kish-Trier, E., Heck, A. J. R., Kane, P. M. & Wilkens, S. (2008). Structure of the yeast vacuolar ATPase. *Journal of Biological Chemistry* **283**, 35983–35995.

Zimmermann, B., Diez, M., Zarrabi, N., Gräber, P. & Börsch, M. (2005). Movements of the e-subunit during catalysis and activation in single membrane-bound H^+-ATP synthase. *EMBO Journal* **24**, 2053–2063.

https://doi.org/10.1017/S0033583510000338 Published online by Cambridge University Press